



ADDIS ABABA UNIVERSITY
ADDIS ABABA INSTITUTE OF TECHNOLOGY
SCHOOL OF MECHANICAL AND INDUSTRIAL
ENGINEERING

Design, Simulation, Manufacturing and
Testing of Forced Draft Microgasifier

A Thesis submitted to School of Mechanical and Industrial Engineering
in Partial Fulfillment of Degree of Masters of Science in Mechanical
Engineering (Thermal Stream)

Samuel Kelbesa Ligdi

Advisor: Kamil Dino Adem (PhD)

December 2020, Addis Ababa, Ethiopia



School of Mechanical and Industrial Engineering

Design, Simulation, Manufacturing, and Testing of Forced Draft

Microgasifier

(Addis Ababa, Ethiopia)

APPROVAL BY BOARD OF EXAMINERS

Kamil Dino Adem (PhD)

Advisor

Signature

Dr. Abdulkadir Aman

Internal Examiner

Signature

Dr. Wondwosen Bogale

External Examiner

Signature

Dr. Yilma Tadesse

Chairman

Signature

Dr. Ermias Tesfaye

Associate Graduate,
program Director

Signature

DECLARATION

I, the undersigned, declare that the work which is being presented in this thesis is my original work and has not been presented for a degree in any University, and that all the source of materials used for the thesis has been duly acknowledged.

Declared by:

Name: Samuel Kelbesa Ligdi

Signature: _____

Date: _____

ACKNOWLEDGMENTS

First I would like to thank God for giving me the health, the patience and the blessing that I have received from the beginning to the end of the Master's study.

Next, I would like to express my deeply thankful to my advisor Kamil Dino Adem (PhD). It is impossible to accomplish this thesis work without his sincere help, guidance, and support.

I extend my gratitude to all my friends for their unforgettable moral support during my thesis work.

Finally, I would like to show my love and gratitude to all my family members who has always there to give me fresh inputes along all my journeys to reach the goal I have been aiming for.

ABSTRACT

This research has been carried out to develop a forced draft microgasifier cookstove from locally available materials. To achieve the objective of the research, an Analytical method was used for designing different parts of the gasifier. SOLID WORK 2020 was used to model various geometries of the microgasifier stove and COMSOL Multiphysics 5.5 was used for CFD analysis of the cookstove to analyze the thermal behavior of the stove and, International Standards Organizations ISO 19867-1:2018 guideline was used for testing the performance of a forced draft microgasifier stove. Finally, by using surface temperature measured during the experiment, the contribution of each mode of heat transfer was calculated.

The developed forced draft microgasifier cookstove has a combustion chamber diameter of 200mm and height of 260mm. In order to minimize the heat loss from the combustion chamber to the stoves outside body the combustion chamber of the stove was covered with clay of 20mm thickness. Also the gap between the insulation clay and the outside cylinder of the stove was 20mm and it used for secondary air supply as well as used as additional insulator. The air was supplied with the help of 12V, 92mm computer fan. The fan supply air at the speed of 5m/s.

The CFD result shows the effects of pot support height on the thermal efficiency of the stove and the study found that a lower pot support height has high thermal efficiency than the higher ones. The result of CFD was compared and validated with the experimental data. From the result obtained, the thermal efficiency of CFD, Experiment, and heat transfer analysis was 49.72, 44.70, and 40.12% respectively. The specific fuel consumption of the developed stove was 56g/liter.

Generally, the developed forced draft microgasifier stove provides better performance when compared to the previous design proposed by other researchers. Thus disseminating the developed microgasifier stove at a larger scale in developing countries like Ethiopia will be beneficial in reducing deforestation and emission that will be brought about by using open-fire stoves and thus, helps to obtain carbon credit.

Keywords: Forced draft Microgasifier, Microgasifier, COMSOL, CFD, SOLIDWORK

TABLE OF CONTENTS

DECLARATION	ii
ACKNOWLEDGMENTS.....	iii
ABSTRACT.....	iv
TABLE OF CONTENTS	v
TABLE OF FIGURE	viii
LIST OF TABLE	ix
CHAPTER 1 INTRODUCTION	1
1.1. Background	1
1.2. Statement of the Problem	2
1.3. Objective	4
1.4. Significance of the Research	4
1.5. Limitation.....	5
1.6. Organization of the research	5
CHAPTER 2 LITERATURE REVIEW	6
2.1. Biomass Energy	6
2.2. Biomass Energy Utilization and Environmental Impact	6
2.2.1. Deforestation	6
2.2.2. Indoor Air Pollution and Health.....	7
2.3. Biomass Cookstoves	7
2.4. Improved Biomass Cookstoves	8
2.5. Biomass Gasification Process and Technologies	9
2.5.1. Process Overview	9
2.5.2. Types of Biomass Gasifier	10
2.6. Microgasifier	12
2.6.1. Basic Principles of Microgasifier Design.....	15
2.6.2. Manufacture of microgasifier stove.....	16
2.6.3. Computational Modeling and Simulation of Microgasifier Stove	17

2.6.4. Theoretical Consideration on CFD.....	18
2.6.5. Testing the performance of gasifier cookstove.....	19
2.7. Biomass Cookstove Development in Ethiopia.....	20
2.7.1. Traditional Three-Stone Cooking Stove.....	21
2.7.2. Wood Stoves.....	21
2.7.3. Gasifier stove.....	23
CHAPTER 3 MATERIALS AND METHODS.....	24
3.1. Material and Equipment Required	24
3.2. Design of Microgasifier	25
3.3. CFD analysis by using COMSOL Multiphysics	29
3.3.1. Model Structure.....	29
3.3.2. Geometry.....	30
3.3.3. Governing Equation	33
3.3.4. Boundary Conditions.....	37
3.3.5. Meshing.....	37
3.3.6. Solution Technique.....	37
3.4. The stove performance analysis resulting from simulation.....	38
3.5. Testing of the performance of the Gasifier	40
3.6. Experimental set-up.....	41
3.6.1. Procedure of Water Boiling Test.....	44
3.6.2. The stove performance analysis resulting from the experiment.....	44
CHAPTER 4 ANALYTICAL ANALYSIS OF FORCED DRAFT MICROGASIFIER STOVE ..	46
4.1. Mode of Heat Transfer of The FDM stove.....	46
4.2. Heat Transfer and Energy Balance.....	46
4.2.1. Heat Transfer Analysis of Zone 1 (fuel bed zone)	47
4.2.2. Heat Transfer Analysis of Zone 2 (flame zone)	49
4.2.3. Heat Transfer Analysis of Zone 3 (convective heat transfer zone)	51
CHAPTER 5 RESULT AND DISCUSSION	56

5.1. Constructed Stove	56
5.2. Water Boiling Test Result	58
5.2.2. Comparisons of different cookstoves	59
5.3. CFD Analysis Result.....	60
5.3.1. Velocity Profile	60
5.3.2. Temperature Profile.....	62
5.3.3. Effect of pot support height on thermal efficiency	62
CHAPTER 6 CONCLUSION AND RECOMMENDATION	68
6.1. Conclusion.....	68
6.2. Recommendation.....	69
REFERENCES.....	70

TABLE OF FIGURE

<i>Figure 2.1 Gasification process steps (Safarian et al, 2019)</i>	9
<i>Figure 2.2 Updraft gasifier(biofuelsacademy.org)</i>	10
<i>Figure 2.3 Downdraft gasifier (biofuelsacademy.org)</i>	11
<i>Figure 2.4 Fluidized-bed gasifier (fao.org (1987))</i>	12
<i>Figure 2.5 TEG powered forced draft cookstove with the details of its components</i>	14
<i>Figure 3.1(a) Eucalyptus wood sized for usage, (b) sun-drying of the wood fuel</i>	24
<i>Figure 3.2 Equipment used: (a) platform balance, (b) wood moisture meter, (c) environmental meter, (d) infrared thermometer</i>	25
<i>Figure 3.3 Insulating clay</i>	28
<i>Figure 3.4 12V, 92mm fan</i>	28
<i>Figure 3.5 3D view of forced draft microgasifier</i>	29
<i>Figure 3.6 Model Geometry</i>	31
<i>Figure 3.7 Boundary conditions</i>	37
<i>Figure 3.8 Screenshot of COMSOL model Structure</i>	38
<i>Figure 3.9 Manufacturing processes</i>	39
<i>Figure 3.10 Diagram of the standard test sequence of cookstove with ranging cooking power (ESA, 2018)</i>	41
<i>Figure 3.11 (a) schematic of the experimental setup (b) actual experimental set up of microgasifier stove</i>	43
<i>Figure 4.1 Schematic diagram of axis-symmetry of different mode of heat transfer</i>	46
<i>Figure 4.2 Axis-symmetry of different heat zones within FDM stove</i>	47
<i>Figure 4.3 Schematic diagram of heat transfer in zone 1 with thermal resistance circuit</i>	48
<i>Figure 4.4 Schematic diagram of heat transfer in zone 2 with thermal resistance circuit</i>	50
<i>Figure 5.1 The manufactured stove during operation</i>	57
<i>Figure 5.2 Water Temperature during WBT</i>	59
<i>Figure 5.3 Velocity distribution</i>	61
<i>Figure 5.4 Temperature distribution</i>	62
<i>Figure 5.5 Comparison of temperature distribution at the top of the stove</i>	63
<i>Figure 5.6 Convective heat flux of wall of pot bottom for A, B, and C configurations</i>	65
<i>Figure 5.7 Thermal efficiency of three different pot support height</i>	66

LIST OF TABLE

<i>Table 2-1 Summary of literature review of microgasifier cookstove</i>	<i>15</i>
<i>Table 3-1 Energy requirement for cooking food and for boiling water (Alexis, 2005).....</i>	<i>25</i>
<i>Table 3-2 Ultimate analysis of woodchips done by (Varunkumar et al, 2011).....</i>	<i>32</i>
<i>Table 3-3 Producer gas composition (Varunkumar et al, 2011)</i>	<i>32</i>
<i>Table 3-4 Distribution of volatile assumed for fuel</i>	<i>33</i>
<i>Table 3-5 Basic geometrical parameters</i>	<i>33</i>
<i>Table 5-1 Physical observation of the stove.....</i>	<i>58</i>
<i>Table 5-2 Performance result of forced draft microgasifier cookstove</i>	<i>58</i>
<i>Table 5-3 Comparisons of performance of various cookstoves</i>	<i>60</i>
<i>Table 5-4 Production cost of the developed forced draft microgasifier cookstove.....</i>	<i>67</i>

CHAPTER 1

INTRODUCTION

1.1. Background

Globally, around three billion people mainly dependents on biomass including wood, charcoal, tree leaves, crop residues, and animal dung for cooking (WBA, 2016). Like other citizens of other developing countries, Ethiopians are highly dependent on biomass energy sources. This is due to socioeconomic factors such as poverty. Around 91% of energy consumption comes from biomass and it accounts for 98% energy supply of the residential sector (Alam et al, 2018). This high level of dependence on biomass resources will continue to dominate energy demand for the future (Beyene & Koch, 2013).

In developing countries, the three-stone cooking stove is used for cooking in many households. This three-stone cooking stove was a very low thermal efficiency of about 10 - 15% (Adria & Bethge, 2013) and emits a high smoke which leads to respiratory as well as other health problems. In addition to this, the indoor air released from the three-stone cooking stove contributes to the building up of greenhouse gases (Kshirsagara & Kalamkar, 2014). Greenhouse gases cause pollution which resulted in damage to the environment and serious health-related problems. Woodring & Reed (1996), estimates that around 1.6 million peoples (mostly women and children) die in developing countries every year due to indoor air released from the biomass cookstoves. Therefore, changing the three-stone biomass cookstoves; with high pollutant emissions; to clean and high efficiency was urgent for sustainable uses of the biomass resources. This could also lead to significant environmental and health benefits (Deng et al, 2019).

To overcome the problem, several kinds of research and studies were conducted to improve the performance of the three-stone biomass cookstoves. The developed improved cookstove is classified in a various ways based on configuration, material, and mode of biomass combustions. In recent years, the need for cleaner combustion lead researchers to focus on biomass gasification technology (Sutar et al, 2015). Biomass gasification is the thermochemical conversion of solid biomass fuel into combustible fuel in the presence of oxygen less than what is required for stoichiometric combustion (Sansaniwal et al, 2017). The gasification process is the process of converting biomass materials into combustible

fuel gas called producer gas. A gasifier stove is essentially a small gasifier-gas burner system.

Microgasifier is the gasifier small enough in size to fit under a cooking pot at a convenient height. Microgasifier stove is an instrument which is used for gasification in small scale and, fall into two categories based on having forced air or natural draft. Natural draft microgasifier stove can work in case of chunky fuels. In case of small fuel size, air needed to be forced through fuel bed which is easiest to provide with the help of small power fan or blower. The source used for fan to operate was from DC power, PV panel or, thermoelectric generator (Roth, 2011b). Different types of forced draft microgasifier cookstoves have been made in different countries: Oorja in India, Daxu in India, Champion TLUD in India, Vesto in Switzerland, Lucia in Italy, Rise husk in Philippines, Turbo stove in USA and many more (Roth, 2011b).

Due to their socio-economic factor, most of the households of the developing countries cannot afford to the these gasification cookstove technology. Therefore, it is important to develop the stove in such a way that, it is manufactured from locally available material, cost-effective and environmental friend so that they are safe to uses, so that, affordable by most of the householders.

This research aims to design and manufacture a forced draft microgasifier from locally available material. The performance of the developed forced draft microgasifier is simulated and it is reliability for cooking is experimentally investigated.

1.2. Statement of the Problem

In most developing countries, due to the limited access to electricity, peoples who live in rural areas, as well as the majority of peoples who live in the urban area, uses biomass as their only energy source for cooking their foods. Most developing countries experienced a rural energy crisis where demand for household energy was much high. Due to their low economic ability, there is a limitation of technology and infrastructure which facilitates the way of cooking, peoples who live in rural areas of these countries mostly use three-stone cookstoves which is inefficient and releases high smoke Those who live in an urban area of the countries were mostly uses improved cookstoves, but these improved cookstoves

improve mostly thermal efficiency and reduce biomass fuel usages. However, both a three-stone cook stove as well as improved cookstoves releases smoke significantly which contains different gases and particulate matters; resulted in causing serious health-related problems.

To overcome the problem, in recent years, researches mainly focused on reducing the emission from the stove and, gasification of biomass gets attention and gasifier stoves are preferred. Many gasifier stoves with very high efficiency and negligible emissions were developed and currently in use in different countries. These developed improved cookstove categorized into both natural convective as well as forced draft gasifier cookstoves. Forced draft Microgasifier is the most promising gasifier stoves; because, it creates high-velocity air mix fuel, air, and flame; because it is integrated with a fan; reduce emissions through improved combustion and, improve heat transfer to the cooking vessel. Few of forced draft gasifier cookstove introduced and distributed globally. Turbo stove, Philips Stove, Oorja stove, Rise hask stove are few of them. These gasifier cookstoves provides advantages such as high thermal efficiency ranging from 35% to 50%, very low level of emissions of CO and particulate matter (Sutar et al, 2015).

Like in other developing countries, in Ethiopia biomass fuel is the main energy source used for a different activity like cooking and heating. The heavy dependence on biomass resources; traditional and inefficient uses can be a source of significant problems like deforestation as well as the negative health effects associated with indoor air pollution resulted in the case of thousands of death every year. To solve the problem, different types of improved biomass stoves were introduced and distributed for households by different governmental organizations and non-governmental organizations aiming at reducing fuel consumption and emission released from the stove as well as increasing the thermal energy efficiency (GIZ, 2013; SNV, 2018).

Mirchaye, Lakech, Tikikil stove is few of the improved cookstoves adopted in the country. *Mirchaye* and *Lakech* are charcoal stoves and they reduce the emission of Carbon monoxide, Carbon dioxide, and PM_{2.5} by 28, 22, and 27%; and 15, 8, and 13% respectively when compared to the traditional metal charcoal stove (Fikadu et al, 2018). *Tikikil* stove is a biomass cookstove that has a thermal efficiency of 27% (Daniel, 2016). Natural draft

microgasifier stove is developed by Adem & Ambie (2017) at the laboratory level and has a thermal efficiency of 39.6% and specific fuel consumption of 57 g of fuel/ liter of water. But the forced draft microgasifier stove is not introduced yet. This research aims to design, simulate, and develop a prototype from locally available material and conduct a test on a forced draft microgasifier.

1.3. Objective

The general objective of this research is to design, simulate, manufacture a prototype, and conduct test on a forced draft Microgasifier stove made from locally available materials. The specific objectives are:

- Design of forced draft Microgasifier
- Simulation of forced draft Microgasifier by using COMSOL Multiphysics to analyze the effect of pot support height on the thermal efficiency of the stove.
- Manufacturing of a prototype forced draft Microgasifier from locally available materials.
- Conducting a test on the prototype of forced draft Microgasifier to analyze the thermal performance of the developed stove.

1.4. Significance of the Research

Due to the economic ability, citizens of most developing countries are limited to technology and infrastructure which facilitates the ways of cooking. As a result, they use the traditional ways of cooking which resulted in causing serious health-related problems. The improved cookstoves concept has recognized the enormous potential in reducing the health-related problems arise due to the usage of traditional cookstoves. A gasifier stove technology is one of the improved cookstoves; and developing a forced draft microgasifier stove from locally available materials has great benefit than other improved cookstoves since; it emits less CO and PM_{2.5}.

In addition to its benefit by providing basic information on designing, simulation, manufacturing, and testing of forced draft microgasifier stove, the study also believed to significantly contribute to the countries for most in reducing deforestation and emission that will be brought about by using open-fire stoves.

This paper also provides basic information and ideas to the design forced draft microgasifier stove and it will be used as a source for future studies carried out in this area.

1.5. Limitation

- Due to the unavailability of indoor air pollution measuring instrument, the content of indoor air reduction of the microgasifier is not included in this study.

- The CFD simulation of biomass drying, devolatization and char reduction was not included in this study. This is because of the CFD simulation of gasifier stove needs high performing computers.

1.6. Organization of the research

The structure of the research work is categorized into six chapters. The first chapter introduces the research paper by describing the background of the work, defining statement of the problem, objective of the research, significance of the research, and finally limitation of the study. The second chapter reviews different related literature from different sources like; books, journal articles, different websites, and others. Biomass energy utilization and impact, traditional biomass cookstoves, improved biomass cookstoves, biomass gasification, gasifier stoves, different types of gasifier stoves, and finally stove development in Ethiopia are discussed. The third chapter describes material and methods and, explains in detail the materials and methods used in this study. The fourth chapter is about heat transfer analysis of the stove by using the analytical method. Detailed analysis of heat transfer from the stove to the pot as well as different heat losses is discussed in this chapter. The fifth chapter is the result and discussion. The result from CFD as well as the experiment was discussed in this chapter. Also, the result obtained is validated by using data from other researches. Also based on the final result obtained, discussion and judgments are discussed. The final chapter of this research is a conclusion and recommendation. The basic finding of this research is summarized in the form of a conclusion. The recommendation for further work is also stated.

CHAPTER 2

LITERATURE REVIEW

2.1. Biomass Energy

Biomass is the oldest source of energy that covers broad ranges of materials that can be used as fuel or raw materials. Next to fossil fuels biomass is the second-highest energy sources account around 10% of the total energy supply of the world (Safarian et al, 2019). Sources of biomass energy include various natural and derived materials, such as woody and herbaceous species, woody wastes, agricultural and industrial residues, waste paper, municipal solid waste, sawdust, grass, waste from food processing, animal wastes, aquatic plants, and industrial and energy crops are grown for biomass (Arnavat, 2011). Unlike fossil fuel, biomass energy is renewable energy which is considered to be environmentally beneficial by providing clean energy from resources that are continually replaced. Compared to other energy sources like fossil fuels and other non-renewable energies, using biomass energy has some advantages according to energy-matter.

2.2. Biomass Energy Utilization and Environmental Impact

Biomass energy is mainly used as fuel in most developing countries. Still, over one billion people use biomass fuel as their only energy source for heating and cooking. In developed and industrialized countries, biomass energy conversion technology is used to extract energy from biomass and convert it into a different form of useful energy. Due to their socioeconomic factors, most of the developing countries have limited access to technologies and infrastructures as a result they use traditional direct combustion. Direct combustion gives energy in a very inefficient way. Also consume too much biomass fuel as well as release serious gases which resulted in a contribution to GHGs as well as causes serious health-related problems.

2.2.1. Deforestation

Most of the citizens of the developing countries particularly those who live in rural areas use open fire, a three-stone cooking stove. Open fire cookstoves has a very low energy conversion rate. As a result, they consume too much wood fuel. Most of these developing countries have a high population as well as a high population growth rate as a result the use of inefficient cooking methods coupled with population resulted in extensive

deforestation which has serious consequences. Global warming, climate change, loss of biodiversity, soil erosion, landslide are a few of the consequences.

2.2.2. Indoor Air Pollution and Health

The three-stone cookstove is the most common method of cooking and heating in developing countries. During the combustion process, biomass fuels release high smoke. This is mainly due to the incomplete combustion process or partly oxidized compounds in the combustion process. The most common pollutant released from the combustion of biomass fuels is PM_{2.5}, carbon monoxide, hydrocarbons, nitrogen oxides and, sulfur oxides. The composition of the pollutants depends on several factors: original compositions of the fuel, ambient and combustion temperatures, airflow into the fire, mode of burning, and type of stove. This pollutant leads to a serious problem which disturbs the atmosphere as well as causes serious health problems.

2.3. Biomass Cookstoves

Biomass cookstove is the biomass burning device which is used for cooking. The history of Cookstove started with the invention of fire and it is estimated that fire has been used for meals and protection from wild animals for about 100,000 years (Kumar et al, 2013). During the earliest ages, the cooking was done over an open fire. Then after the human civilization continued and modification had been started by making different shaped pots and sizes led down to the development of shielded fire from open fires. The most common type of shielded-fire was the three-stone fire arrangement. Since then, a three-stone fire arrangement is used for cooking and heating purposes. Since they are easy and simple they are more convenient for the users. From the open fires of prehistoric times and three-stone fires, cookstove designs evolved into shielded fires, that paved way to the development of improved cookstoves (De Lepeleire et al, 1981). There are more sophisticated types of traditional stoves ranging from mud stoves to heavy brick stoves to metal ones (Kshirsagara & Kalamkar, 2014). Most sources cite the fuel-efficiency of traditional stoves as 10-15% (Adria & Bethge, 2013). All the cookstoves developed during early time i.e. before the 17th century were called 'traditional cookstoves' because their thermal efficiencies were very low and the material of construction was also very poor besides, they emitted a very high level of smoke (Kumar et al, 2013).

2.4. Improved Biomass Cookstoves

In developing countries, biomass is still the predominant cooking fuel and three-stone cookstoves are still the most prevalent way of cooking (Fikadu et al, 2018). The three-stone cookstoves have very low thermal efficiency and have a very high level of smoke which resulted in risks associated with humans as well as the environment (Daniel, 2016; Fikadu et al, 2018). To overcome these problems, and improved cookstoves concepts were raised. These improved cookstoves concept aiming at reducing the emission of healthy risky pollutants, reducing fuel consumption as well as reducing the pressure on biomass resources and also, helps to avoid rural health problems arising from smoke and heat during food preparation.

Starting from the 1950s the design and development of improved cookstoves with better efficiency and lower emission have been introduced (Kshirsagara & Kalamkar, 2014). In developing countries, improved cookstoves with improved efficiency started to be introduced in the late 1960s (Kshirsagara & Kalamkar, 2014). Improved cookstoves are cookstoves that use different biomass energy sources such as wood, charcoal, animal dung, paper, or vegetable matter and designed to improve the thermal efficiency, reduce fuel consumption, reduce emission released from the stove, and safely operates. In the 1980s, various types of improved cookstoves were introduced in most developing countries in Asia and East Africa (Sutar et al, 2015).

There were no guidelines until Chaplin (1983) present guidelines on the selection of materials for fabrication of the cookstoves, considering economic factors as well as material properties such as strength, stiffness, impact resistance, resistance to thermal stress and shock, formability, etc. due to different cooking practice across the world. Then after, different engineering design for improved cookstoves is carried out. The focus was on improving specific parts of the stove such as the grate, skirt, and insulation to increase the thermal efficiency of the stove as well as reducing fuel consumption (Adem et al, 2019). Then, several biomass cookstove designs are available in different countries such as Guatemala (Beiliecki & Wingenbach, 2014), China (De et al, 2013), Mexico (Masera et al, 2007), Gambia (Jacob, 2013), and many more. These developed improved cookstoves can be classified based on their construction material, the number of pots, type of fuel, etc. These improved cookstoves were able to reduce emissions by 40–75%, increase fuel

efficiency by almost 30% (Still et al, 2011) and reduce global warming potential up to 40–60% (MacCarty et al, 2008). Nowadays, new efforts now focus on further improving existing improved cookstoves in burning solid biomass fuels efficiently as well as making them cleaner. For this reason, ‘gasifier’ stoves are receiving more attention (Adem et al, 2019; Wanga et al, 2014).

2.5. Biomass Gasification Process and Technologies

2.5.1. Process Overview

Biomass gasification is the thermochemical conversion of solid biomass fuel into combustible fuel with a limited amount of oxygen. A *gasifier* is an equipment required to facilitate the gasification process. The gasification process is the process of converting biomass materials into combustible fuel gas called producer gas. Detail gasification processes were discussed in Figure 2.1. Producer gases are combustible fuels containing mainly carbon monoxide (CO), hydrogen (H₂), carbon dioxide (CO₂), methane (CH₄) and nitrogen (N₂) (Yu & Smith, 2018).

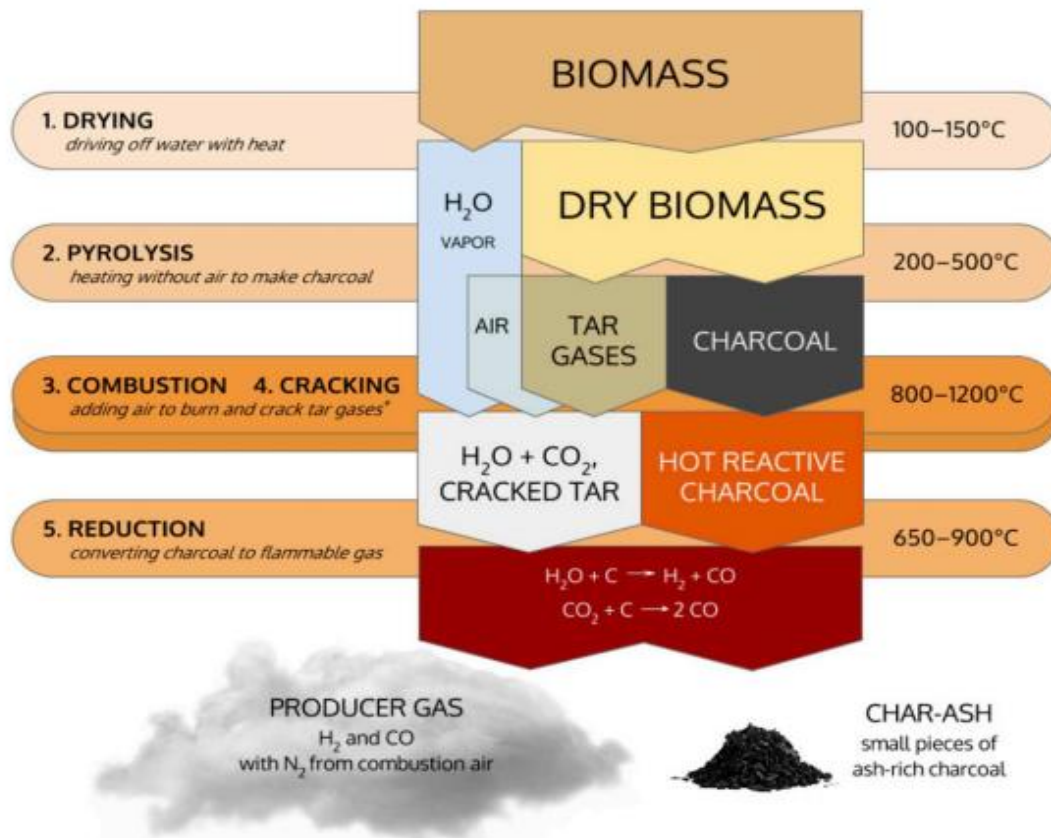


Figure 2.1 Gasification process steps (Safarian et al, 2019)

The gasification process also produces liquids (tars, oils, and other condensates) and solids (char, ash) from solid feed-stocks (Robert & Kaffka, 2015). Producer gas is a mixture of gases; However, the actual gas composition may vary considerably depending on fuel type and gasifier design (Bhattacharya & Leon, 2005). The gasification process consists of the following stages: drying, pyrolysis, oxidation (combustion), reduction (char gasification), and cracking (Safarian et al, 2019).

2.5.2. Types of Biomass Gasifier

Based on the way fuel flows and supported and, the way air/oxygen flows to the fuel we can classify gasifier as updraft, downdraft, fluidized bed, and entrained flow.

Updraft gasifier is a fixed type in which air inlet is at the bottom, and the gas output is at the top. Figure 2.2 illustrates the motion of biomass, gas, and tar. Biomass is dried in drying zone and biomass decomposition to volatile gas and solid char is takes place in the pyrolysis zone. The heat for pyrolyzation and drying is delivered by upward flowing producer gas and by radiation from the combustion zone (Reed & A, 1988).

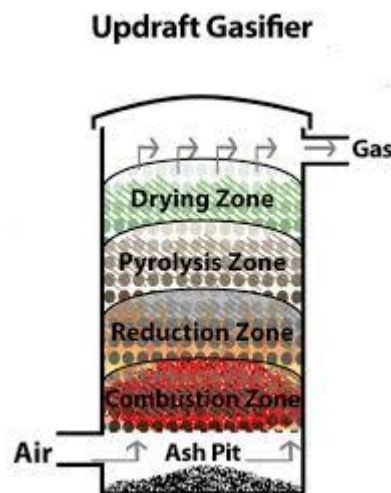


Figure 2.2 Updraft gasifier(biofuelsacademy.org)

Downdraft gasifier shown in Figure 2.3 is another type of gasifier in which, biomass is fed at the top and air enters at the top of the combustion zone. The gas leaves at the bottom of the reactor. The zones of downdraft gasifier are similar to updraft gasifier, but the order is different. The biomass is dried in the drying zone, and then pyrolyzed in pyrolyzation zone. These zones are mainly heated by radiation heat from the combustion zone, where a

part of the char is burned. The main advantage of a downdraft gasifier is the production of gas with low tar content suitable for engines (Reed & A, 1988).

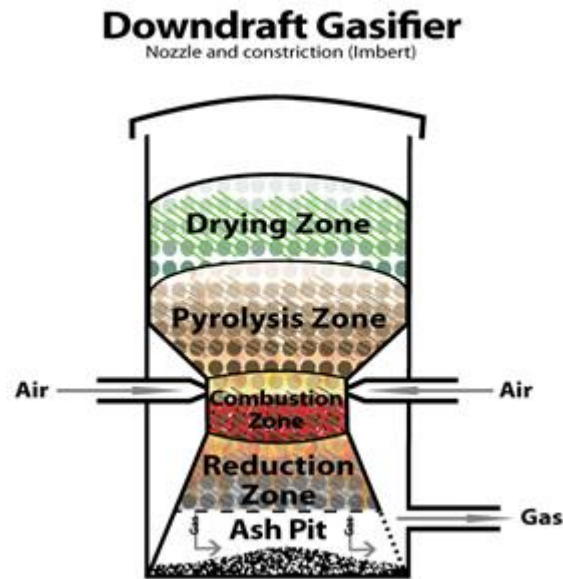


Figure 2.3 Downdraft gasifier (biofuelsacademy.org)

The fluidized bed gasifier shown in figure 2.4 has been the latest development. It has been designed to overcome problems commonly rises with the operation of both up and downdraft gasifier; i.e. luck of bunker flow, slagging, and extreme pressure drop over gasifier. The fuel is fed into a bubbling fluidized bed or circulating fluidized bed. The bed behaves like a fluid and is characterized by high turbulence (Reed & Das, 1988). The advantage of fluidized bed gasifiers is compact construction because of high heat exchange and flexibility to changes in moisture and ash contents (Reed & A, 1988).

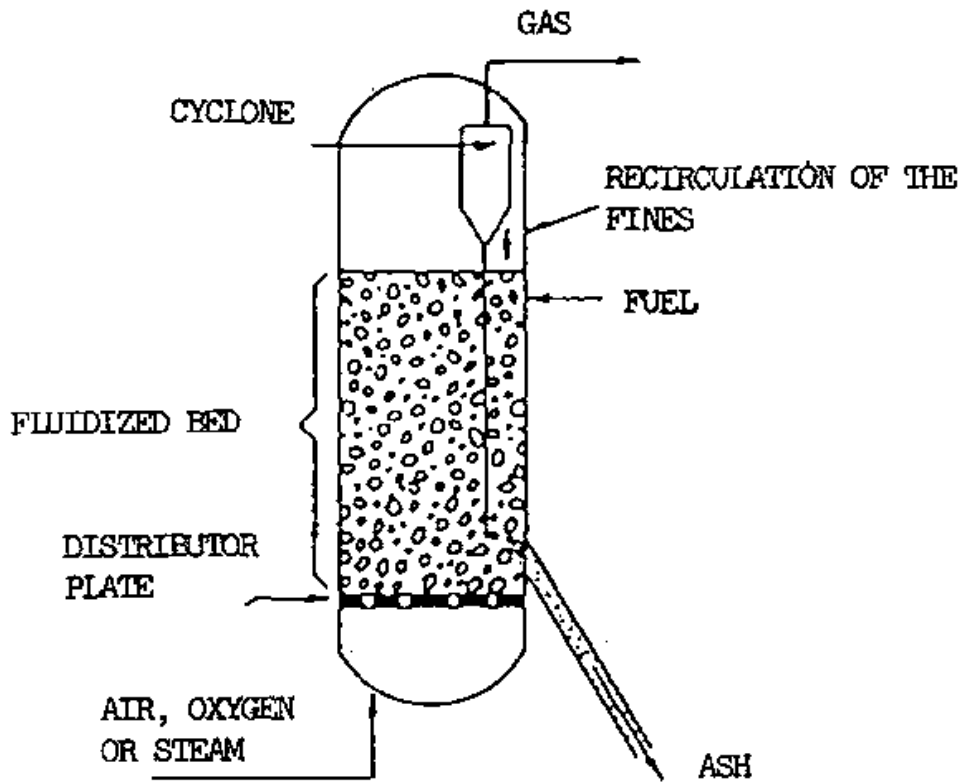


Figure 2.4 Fluidized-bed gasifier (fao.org (1987))

2.6. Microgasifier

Micro-gasification is a process of producing gas from fuel in a gasifier and small in size to fit under a cooking pot and used for domestic use as heat-generating combustion units in cook-stoves (Patrick, 2017; Roth, 2011a). Microgasifier concept was first invented as a top-lit up-draft; the TLUD process in 1985 and developed to laboratory prototype stages by Reed in the USA (Reed & Das, 1988; Roth, 2011a). Reed & Larson (1996b) Developed a new “inverted downdraft gasifier” stove which is operated using only natural convection. The first commercialized microgasifier was available in 2003(Roth, 2011a).

Microgasifier cookstove was classified into two based on forced air or natural draft. Natural draft is preferable in case of large size of fuel. As the size of the fuel minimized, it is affect the combustion process because it affect the air flow which is used for combustion process. As a result air is supplied with the help of low power fan or blower to force air through. Different power sources was used to run the fan like DC power, PV, and Thermo-electric generators.

2.6.1. Forced Draft Microgasifier cookstove

Forced draft microgasifier cookstove one of the improved cookstove in which air used for combustion process was supplied with the help of external fan. Also, it operates at high thermal efficiency ranging from 35 – 50% as well as releases very low emissions (Safarian et al, 2019).

The first study related to forced draft microgasifier as done by Reed & Larson (1996a). The developed was difficult to control and manufacture. By using these concept the first commercialized forced draft microgasifier cookstove named Turbo stove was developed Reed et al (2001). The developed stove operates at thermal efficiency of 31% Reed et al (2001). Later different types of forced draft microgasifier cookstove developed in different parts of the world: Oorja stove developed in India, Rise husk stove in Philippines, Daxu in China, Vesto in Switzerland, Lucio stove in Italy and many more. These developed cookstoves uses different types of fuels like different types of wood chips and rice husks.

Also, different scientific studies related to these forced draft microgasifier cookstove was carried out in order to analyze the performance of the stoves. Varunkumar et al (2011) Studied a computational investigation into the gasification and combustion by taking the assumption of premixed combustion and mixed control chemical reaction, of a forced draft gasifier stove. From the result, the overall flaming mode efficiency of the stove is 50–54%; the convective and radiative components of heat transfer are established to be 45–47 and 5–7% respectively. Raman et al (2014) studied the design and development of a Thermal Energy Generator powered clean combustion forced draft cookstove that works with higher efficiency. The study was mainly focused on optimizing the material and geometry of the cookstove to reduce cost in fabrication and, design and development of Thermal Energy Generator powered cookstoves with multi-options like mobile phone charging, LED light and also conducted economic viability and adaptability of the stove and concluded that the Thermal Energy Generator powered forced draft cookstove performed with an efficiency of 44%.

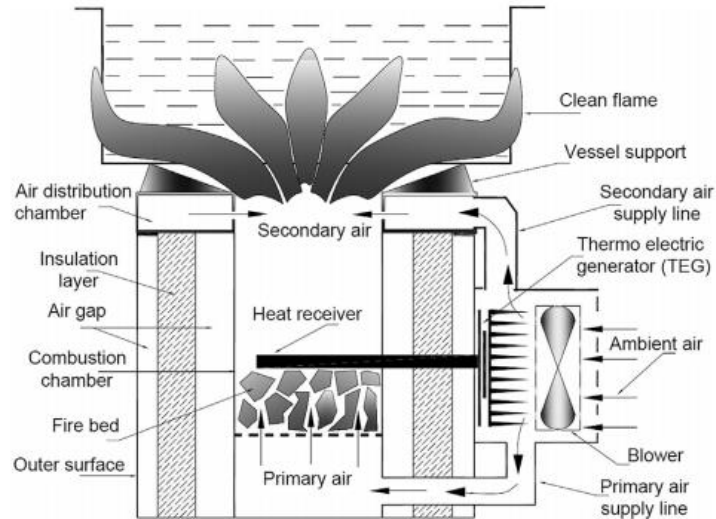


Figure 2.5 TEG powered forced draft cookstove with the details of its components

Mal et al (2015) Studied the development of forced draft biomass cookstoves integrated with a thermoelectric generator for off-grid rural areas where the technology of thermoelectric generator has been implemented for electricity generation. DC fan is integrated into the cookstove to supply air inside the combustion chamber to increase fuel-to-air ratio and to achieve a cleaner fuel burning by reducing harmful emissions and the electricity generated from the thermoelectric generator is used to run a DC fan. The study was evaluated based on the performances of the 25 stove and the basis of feedback from the stove users. De La Hoz et al (2017) studied the thermo-mechanical design of a biomass TLUD cookstove based on mass and energy balance and simulates the geometric relations among main dimension of the cookstoves by using fluent and, concluded that the operation with axial fan allows obtaining a good standard deviation of air velocity through grate holes and through the secondary air ring holes which entails a better cookstove performance (higher thermal efficiency, lower biomass fuel consumption, and lower emissions). (Deng et al (2019)) carried out a study based on a dynamic measurement system to test a typical forced-draft gasifier stove consuming wood pellets and maize straw pellets. The study analyzed the relationship between combustion and emission and concluded that the identified relationships could potentially help to estimate emission performance of forced-draft biomass gasifier stoves based on combustion indicators and guide improvements in stove design with relevant effects on the reduction of gaseous air pollutant emissions.

Different literature related to microgasifier cookstove was summarized in the table below.

Table 2-1 Summary of literature review of microgasifier cookstove

Title	Research output	Author
Application of numerical simulation on biomass gasification	numerical simulation on biomass gasification technology are reviewed by using Aspen and fluent	Deyong Che, Shaohua Li et al. 2012
Experimental and computational studies on gasifier based stove	Reactive flow computational studies are used to simulate the thermochemical flow field and heat transfer to the vessel	Varunkumar, Rajan et al. 2011
Performance evaluation of three forced draft cookstove	The performance of the three cookstove was analyzed experimentally by using two different fuel types	Raman et al, 2013
Energetic performance of TLUD cookstove	The performance of TLUD was analyzed by using three different wood types. The analysis was done by using WBT and CCT cookstove testing protocol	Okey et al, 2016
Performance and emission reduction potential of microgasifier through better design	The performance of the microgasifier using woody biomass was analyzed and compare its advantage in-terms of IAP	Adem & Ambie, 2017
Design of TLUD microgasifier biomass cookstove	The complete thermo-mechanical design of TLUD cookstove is presented	De La Hoz, et al. 2017

2.6.2. Basic Principles of Microgasifier Design

There is a wide range of consumer needs and considerations to build improved cookstoves. Each particularly improved cookstoves commonly represents a compromise to address the consumer needs, local resources, safety, and economic consideration (Febriansyah et al, 2014). Microgasifier is one of the improved cookstoves which aims to make biomass cooking comfortable as much as possible.

The aim of developing improved biomass cookstoves is to increase thermal efficiency, increase fuel efficiency, and reduce emissions. Generally, basic principle designs to achieve these aims are to enhance heat transfer and combustion efficiency. Heat transfer efficiency is a ratio of energy that is delivered to the cooking pot to the total heat energy produced by the combustion of fuel (Kumar et al, 2013). Similarly, combustion efficiency is the ratio of energy released during combustion to the total combustible energy potential of the fuel. The overall efficiency of the cookstove is a combination of the two. Perfect combustion prevents negative effects on emission. Incomplete combustion produces harmful emissions such as carbon monoxide (CO), unburned hydrocarbons (UHC), nitrogen oxides (NO_x), smoke, etc... (Febriansyah et al, 2014).

To develop the gasifier stove first we have to design major parameters. This parameter includes Energy Input, Reactor Diameter, and Height of reactor (Alexis, 2005). To design these major parameters of the microgasifier stove, we have to first calculate the required energy for cooking and identify fuel type because the dimensioning of cookstoves mainly depends on them (De La Hoz et al, 2017). The required energy for cooking is the rate of energy due to the combustion of biomass fuel which is determined by multiplying the consumption rate of biomass (kg/s) with its lower calorific value (LCV) (kJ/kg) (Sutar et al, 2017). Based on the energy required to cook food for a specific period, determining the energy required for cooking is important. The energy demand is the main parameter that helps us to design other important parameters like energy input, reactor diameter, and reactor height (Alexis, 2005).

The energy required for cooking or energy input is the amount of energy required for cooking and to be supplied for the heating application. To calculate the energy required we have to identify fuel type as well as determine the physical, chemical as well as thermal properties of the fuel (Adem & Ambie, 2017). Based on the required energy for cooking activity, we can design reactor diameter and reactor height which help us to develop the stove.

2.6.3. Manufacture of microgasifier stove

Size, as well as thickness of the material, and availability of material is the main thing to be considered during the manufacturing of the microgasifier stove; because the cost and the life span of the stove unit are mainly affected by the type, size and thickness of

materials. User satisfaction is another parameter used to evaluate stove acceptability at the community level. To manufacture the microgasifier it requires locally available materials. Materials needed to produce the stove are mild-steel sheet metal.

2.6.4. Computational Modeling and Simulation of Microgasifier Stove

Biomass gasification is a very complex process involving drying, devolatilization, combustion, and gasification of volatiles and char particles. A detailed understanding of the biomass gasification mechanism requires the investigation of gasification performances under different operating conditions and structural parameters (Gao et al, 2019). When we deal with modeling and simulation of the biomass gasification process, it can mainly be simulated by using three different approaches: kinetic models, equilibrium model, and CFD models (Gambarotta et al, 2018):

Kinetic models can give accurate results, in particular regarding the time evolution of the process. The kinetic model implemented though accounted for the reaction kinetics and temperature of the gasifier, still lacks a comprehensive understanding of the biomass Gasification process (Gonzalez-Vazquez et al, 2018; Sharma, 2008; Yu & Smith, 2018). Furthermore, this model is unable to investigate the effects of varying operating and design parameters on the production of synthesis gas.

Equilibrium models are simple and fast. The equilibrium condition is essentially never reached within the gasifier, although these models can describe gasification processes with good approximation (Gambarotta et al, 2018). An equilibrium model, which is also known as the 0D model of gasification widely used by different researchers (Chaurasia, 2018; Li & Yin, 2019; Luo et al, 2020; Park & Choi, 2019) lacks a clear understanding of the interface between the gas and solid phase reactions during gasification, and also of the temperature and concentration profiles inside a gasifier. The model calculations are independent of gasifier design and hence helpful for studying the influence of fuel and process parameters only (Patra & Sheth, 2015).

A computational Fluid Dynamic model is used to predict the performance of the actual stove, and obtain the model equations that relate design and performance parameters. These equations would help in the analysis and prediction of the performance of the stove under various operating conditions, and would also be useful in carrying out design

optimization of a given type of biomass stove for a given fuel. CFD appears to be a cost-effective option to explore the various configurations and operating conditions at any scale to identify the optimal configuration depending on the project specification (Patra & Sheth, 2015).

Quite a few works have been carried out in numerical studies on the gasification process using the CFD technique. Detailed CFD simulation of the flow, heat transfer, pyrolysis, and combustion is studied by Ravi et al (2002), and by using a simple algebraic equation, the performance analysis, and prediction, optimization of the stove geometry and performance of the stove is studied. MacCarty & Bryden (2016) studied a generalized heat-transfer model for shielded-fire household cookstoves to improve the understanding of the cookstove system and support the design. In the study, temperature profile, pressure profile, location, and magnitude of losses and heat transfer contribution through various models and regions of the pot are analyzed by using CFD. The thermo-mechanical design of biomass TLUD cookstoves based on mass and energy balance is studied analytically and simulated using FLUENT by De La Hoz et al (2017). The study showed that the geometric relations among the main dimension of cookstoves affect the cookstove performances (higher thermal efficiency, lower biomass fuel consumption, and lower emissions). Numerical simulation of the gasifier using the species transport model in CFD by incorporating all zones of the gasifier, drying, pyrolysis, oxidation, and reduction is studied by Murugan & Sekhar (2017). In the study, the factors which affect the producer gas like equivalent ratio, gas composition, high heating value; temperature distribution inside the reactor are analyzed. Similarly, the gasification of thermochemical processes of biomass in a 20kW downdraft gasifier is investigated by Kumar & Paul (2019) using CFD. In the study all zones of gasifier are included and, step by step approach is used to evaluate the composition of different gases as a result of volatile break-up approach and the air equivalent ratio which affect the gasifier temperature and composition of producer gas. In this study, CFD modeling of the forced draft gasifier is developed to analyze the effect of pot support height on the thermal efficiency of the stove.

2.6.5. Theoretical Consideration on CFD

CFD codes are arranged by the numerical algorithm accordingly so that the fluid flow problem can be tackled. There are three main elements of CFD codes in the CFD packages which consist of pre-processor, solver, and post-processor.

The pre-processor contains all the fluid flow inputs for a flow problem. It can be seen as a user-friendly interface and a conversion of all the input into the solver in the CFD program. In this stage, quite a lot of activities are carried out before the problem is being solved. These stages are listed as below: Definition of the geometry, Grid generation, Selection of the physical and chemical properties, Definition of the fluid properties, and Specifications of correct boundary conditions.

In the numerical solution technique, three different streams form the basis of the solver: finite differences, finite element, and finite volume methods. The differences between them are how the flow variables are approximated and the discretization processes are done.

The finite difference element describes the unknown flow variables of the flow problem through point samples at node points of a grid coordinate. By FDM, Taylor's expansion is usually used to generate finite differences approximation.

The finite volume method was originally developed as a special finite difference formulation. The main computational commercial CFD codes packages using the FVM approaches involve PHOENICS, FLUENT, FLOW 3D, and STAR-CD.

Finite element method uses the simple piecewise functions valid on elements to describe the local variations of unknown flow variables. Governing equation is precisely satisfied by the exact solution of flow variables. In FEM, residuals are used to measure the errors. The main computational commercial CFD code package using the FEM approaches is COMSOL Multiphysics, ANSYS, Autodesk simulation, etc.

In the case of post-processor, the COMSOL Multiphysics package provides data visualization tools to visualize the flow problem. This includes – vectors plots, domain geometry, and grid display, line and shaded counterplots, particle tracking, etc.

2.6.6. Testing the performance of gasifier cookstove

Testing is an important tool to predict the performance of cookstoves. It is difficult to predict the performance of the cookstove without measurements. Therefore, testing is an important tool that should be used to develop a solution and estimate potential

environmental, health, social, and economic impacts. Cookstove testing is usually done using standard methods, which include tests performed in the laboratory i.e. WBT, and the field i.e. CCT and KPT. Laboratory testing is useful for gathering detailed measurements, including fuel efficiency and emissions, in a controlled environment. Field testing is used to understand how the product performs during use in a kitchen with real cooks.

The performance of the cookstove can be characterized into two categories: thermal performance and emission performance. Thermal performance is measured in terms of firepower or input power of the cookstove, specific fuel consumption, efficiency and turns down ratio, while emission performance is measured mainly in terms of emission ratios or emission factors of pollutants. Performance of biomass stoves shows a strong dependence on operation parameters viz., characteristics of the fuel used, sizes and types of pots used, the type of cooking process, the ambient conditions, the ventilation levels, etc. This gives rise to the need for a precise definition of the various performance parameters on one hand, and on the other, it necessitates reporting of the operating conditions precisely, while presenting the experimental results. This is accomplished by standardization of testing protocols

2.7. Biomass Cookstove Development in Ethiopia

Ethiopia is mostly dependent on biomass energy sources. Around 91% of energy consumption comes from biomass and it accounts for 98% energy supply of the residential sector (Alam et al, 2018). Most of the citizens of Ethiopia use the traditional biomass conversion technique (direct burning) which is inefficient and releases high smoke. To overcome the problem, in Ethiopia starting in the 1980s various energy sector studies conducted and identified the rising cost of domestic energy supplies on household consumers, unsustainable consumption of fuelwood, increasing deforestation, and soil erosion as major environmental and economic problems facing Ethiopia (GTZ, 2007). To reduce household demand and reduces the pressure on biomass resources the Ethiopian government introduced the Ethiopian improved stoves program, whose objective was to reduce cost and improve the supply of biomass fuels for domestic consumers. Since then different types of improved cookstoves were introduced and widely used by the people living in urban and rural areas of Ethiopia.

2.7.1. Traditional Three-Stone Cooking Stove

In an open fire stove, three medium-sized stones are used to put the *Mitad* or the cooking pot. It is open except for the spaces occupied by the stones. This kind of traditional household stove widely used throughout the country and a high amount of Firewood use leads to deforestation and erosion, while smoke from a traditional cooking causes health problem.

2.7.2. Wood Stoves

Tikikil Stove is shown in figure 2.4 and it is a portable household cookstove made of galvanized sheet metal with a ceramic liner. It is used for cooking. It uses firewood as fuel which is continuously fed into the combustion chamber. Scrap galvanized sheet metal is made into the cladding while the ceramic liner is made of clay mixture. It saves up to 50% of fuel compared to the three-stone open fire; its thermal efficiency is 27% (Daniel, 2016).



Figure2.4 Tikikil stove (GIZ, 2009)

Charcoal stoves are improved cookstove which widely used for different activities: *Woat* cooking, water boiling, coffee making, and other related activities in urban and semi-urban areas of Ethiopia. The use of these stoves increases with the rapid growth of the urban

population of the country. The major types of charcoal stoves are *Lakech*, *mirchaye*, and metal charcoal stove. There are various versions of the above two.

Lakech stove was adopted from the Kenyan Ceramic Jocko (KCJ), by the Ethiopian Energy studies and Research center of the Ministry of Mines and Energy in 1990 under the Cooking Efficiency Improvement and New Fuels Marketing Project (Gashie, 2005). The stove was optimized by thinning the metal cladding of KCJ to suit the Ethiopian cooking habits & reduces construction cost. It has the shape double conic fitted with ceramic liner above its waist. A half liner combined with the bell-bottom shape provides stability to the stove, with a low cost and low weight as compared to full liners. Materials needed to produce the stove are metal, clay, cement, sand, and water. Metal and clay are the major raw materials to produce the stove. All the joints in the casing are either riveted folded and no welding, soldering, or brazing is required (Daniel, 2016). Each *Lakech* stove is expected to save an average of 75 kg of charcoal per household per year and *Lakech* stove yields a 25% energy savings over the traditional open fire stove (Beyene & Koch, 2013).



Figure2.5. lakech stove(Gashie, 2005)

The “*Lakech*” stove has a thermal efficiency of 32-35% and a fuel-saving of 39% compared with traditional stoves (Gashie, 2005).

Metal charcoal stove is other types of improved cookstove. The charcoal stove of different types and shapes are available in market: square, funnel, and circular shapes. The most widely used are the square and funnel-shaped stoves. These stoves are taken as traditional

charcoal stoves. The Grates of the metal charcoal stoves are removable (Figure 2.6 shows the metal charcoal stove).

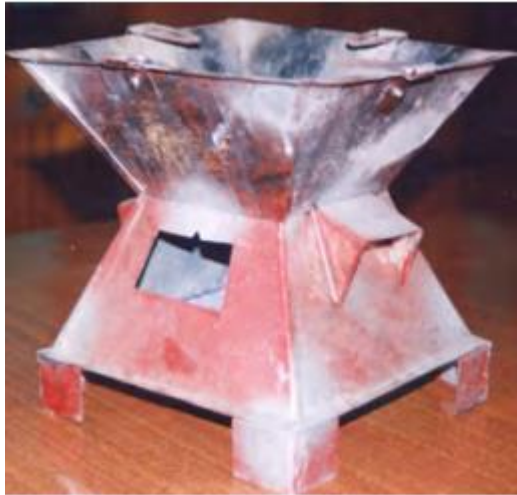


Figure 2.6 Metal charcoal stove (Gashie, 2005)

2.7.3. Gasifier stove

Gasifier stove is the latest and modified technology compared to previously introduced stoves. Gasifier stove technology is known in few countries like China and India. But in Ethiopia, the technology is yet to be introduced to society. Very few researches are conducted by different Ethiopians but the study is limited to a laboratory test. Shiferaw (2011), design and manufacture an applicable type of biomass gasifier stove which used for the production of producer gas using locally available biomass fuels like bamboo, eucalyptus, and Prosopis Juliflora. Adem & Ambie (2017), developed a natural draft microgasifier stove from locally available materials, and the developed gasifier stove has a thermal efficiency of 39.6%.

CHAPTER 3

MATERIALS AND METHODS

3.1. Material and Equipment Required

The type of fuel used for conducting the laboratory test was Eucalyptus tree wood and shown in Figure 3.1. This type of wood is commonly used in most of Ethiopia. The woodcut from the eucalyptus logs and sun-dried for days with sizes ranging from 30 to 35mm. Sun drying is used for reducing the moisture content of the wood to the required value which is below 10 - 15% (Yuntenwi et al, 2008).



Figure 3.1(a) Eucalyptus wood sized for usage, (b) sun-drying of the wood fuel

The material used to manufacture the micro-gasifier was mild steel sheet metal with a thickness of 1.5 mm. The micro-gasifier was manufactured in a convenient way for the users.

Different types of equipment were required for testing the forced draft microgasifier stove. This equipment is: digital stopwatch used to record the time during the tests, Thermocouple integrated with an environmental meter is used for measuring the ambient or surface temperature, boiling water temperature, wind condition, and relative humidity, an infrared thermometer is used for measuring stove body temperature, platform balance was used for measuring the weight of fuel and water, and also the remaining char, a moisture meter is used to measure the moisture content of the biomass fuel, a standard pot is used to evaluate the performance of the microgasifier which is 7-liter capacity stainless steel pot with 5 liters of water, test room is selected in such a way that simulates a typical

rural household kitchen; 2m × 2m area and 2.5m height (Figure 3.2). DC is used as the power source for the fan for conducting a test, in the actual case; solar panel is used as the power source for the fan.



Figure 3.2 Equipment used: (a) platform balance, (b) wood moisture meter, (c) environmental meter, (d) infrared thermometer

3.2. Design of Microgasifier

The main components to design a forced draft biomass microgasifier are energy demand, power output, total operating time, reactor diameter, reactor height, material for the reactor (size and thickness)(Patrick, 2017) with the major parameters required for drafting and manufacturing the gasifier stove.

Knowing the type of fuel used as well as the type of food to be cooked, the amount of energy required for the cooking process is calculated by using equation 3: (Alexis, 2005).

Table 3-1 Energy requirement for cooking food and for boiling water (Alexis, 2005)

Food	Specific Heat (kJ/kg °C)	Total Energy Needed (kJ/kg)
Rice	1.75 – 1.83	331.80
Meat	2.0 – 3.88	235.42
Vegetable	3.88	310.43
Water	4.17	300.00

- Assuming most cooking food in Ethiopia resembles rice, let 1Kg of rice to be cooked within 15minutes, the energy required to cook the rice is:

$$Q_n = \frac{M_f \times E_s}{T}$$

Equation Chapter (Next) Section 1
Equation Chapter (Next) Section 1 (3.1)

- The energy input to the stove is required to calculate the diameter as well as the height of the reactor (Alexis, 2005). The calorific value of the fuel is 18.64MJ/kg (Adem & Ambie, 2017). Assuming a stove efficiency of 17% the fuel consumption rate can be computed by using equation (Alexis, 2005)(3.2):

$$FCR = \frac{Q_n}{\eta \times HV_f} \quad (3.2)$$

- Reactor Diameter refers to the size of the reactor in terms of the diameter of the cross-section of the cylinder where biomass is being burned. Reactor diameter is the function of the amount of fuel consumed per unit time to specific gasification rate of biomass material, which is in the range of 110 – 120kg/m²hr or 5 -130 as revealed by several the result of several tests on biomass material gas stove (Alexis, 2005). For a gasifier stove with a required FCR of 3kg/hr and SGR of 120 kg/m²hr, the reactor diameter is calculated by the following formula (Alexis, 2005):

$$D = \sqrt{\frac{1.27 \times FCR}{SGR}} \quad (3.3)$$

- Reactor Height refers to the overall height of the combustion chamber. It is a function of several variables such as the required time to operate the gasifier, the specific gasification rate, and the density of biomass material, $\rho_a = 450\text{kg/m}^3$. The height of the reactor can be computed using the following formula (Alexis, 2005):

$$H = \frac{SGR \times T}{\rho_a} \quad (3.4)$$

- Time to consume fuel refers to the total time required for fuel inside the reactor to completely gasify. This includes the time to ignite the fuel and the time to generate gas, plus the time to completely burn all the fuel in the reactor. The time required by the stove will be (Alexis, 2005):

$$T = \frac{\rho a \times Vr}{FCR} \quad (3.5)$$

- Amount of Air Needed for Gasification refers to the rate of flow of air needed to gasify fuel. This can be simply determined using the rate of consumption of fuel, the stoichiometric air, and the recommended equivalence ratio for gasifying wood fuel of 0.4 (De La Hoz et al, 2017). It is estimated that during the gasification process around 20% - 40% from the stoichiometric air is used, to reach partial oxidation. Stoichiometric air is in the range of 6:1 to 6.5:1 i.e. 6 – 6.5kg of air is required for 1kg of biomass fuel (Keily De La Hoz et al, 2017). The amount of air required for gasification is calculated by using equation (3.6):

$$AFR = \frac{\varepsilon \times FCR \times SA}{\rho_{air}} \quad (3.6)$$

- Superficial Velocity refers to the speed of the airflow in the fuel bed. The velocity of air in the bed of the gasifier will cause channel formation, which may greatly affect gasification. The diameter of the reactor (D) and the airflow rate (AFR) determine the superficial velocity of air in the gasifier. As shown, this can be computed using the formula,

$$V_s = \frac{4AFR}{\pi D^2} \quad (3.7)$$

- For better conversion of biomass fuel into gas as well as preventing burning of skin when accidentally touching the combustion chambers body, the combustion chamber should be properly insulated. For the developed microgasifier stove clay is shown in the Figure 3.3 used since it was found to be cheaper when compared to ceramic/concrete; since it is manufactured by traditional pottery as well as has effective insulating material insulator for the microgasifier stove. The hole found in the clay was used for air inlet and sized based on primary and secondary air inlet hole found on the combustion chamber.



Figure 3.3 Insulating clay

- To overcome the pressure exerted by biomass fuel and by char, a fan used should be a high-pressure fan. For the TLUD reactor, the amount of airflow per unit mass is about 0.3 to 0.4 of the stoichiometric air requirement of the fuel. In case of availability and cost-effectiveness, a 92mm, 12V computer fan is used, and the fan proved that, it is effective in increasing the pressure for the available airflow. The power required to run the fan was 3Watt.



Figure 3.4 12V, 92mm fan

- The geometry of a forced draft microgasifier was drawn by using SOLIDWORK 2020. The 3D view of the developed geometry was shown in figure 3.4. For a detailed drawing see Appendix D.

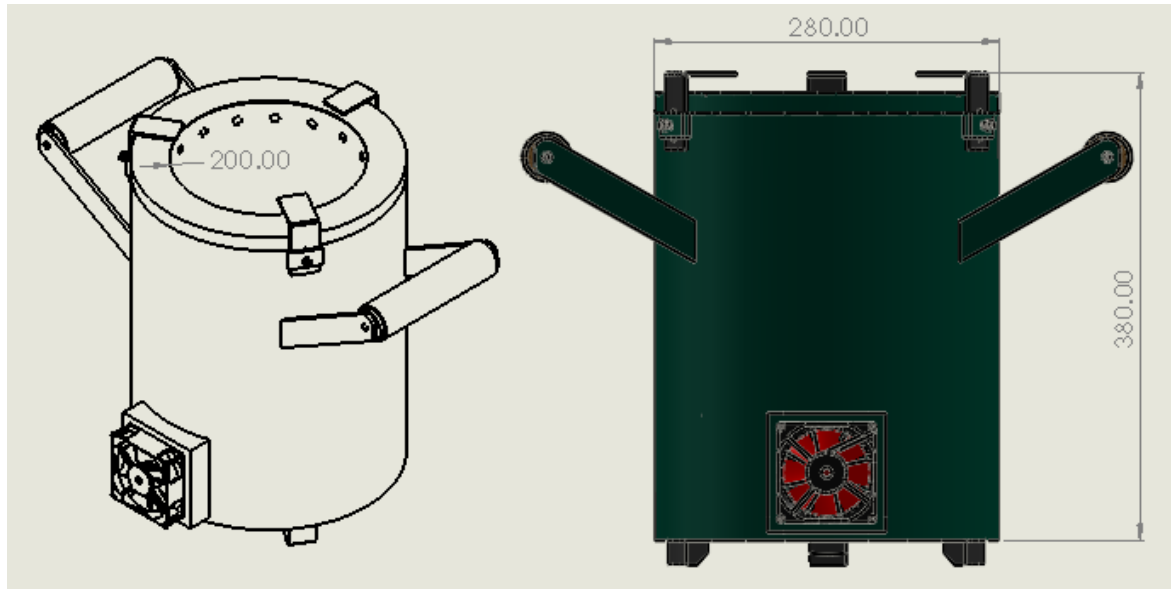


Figure 3.5 3D view of forced draft microgasifier

3.3. CFD analysis by using COMSOL Multiphysics

CFD Module in COMSOL Multiphysics is used to provide an opportunity to couple fluid flow to a wide range of physical processes with detailed simulation. It is used to predict the actual performance of the analysis, obtain the model equation that relates the design and performance parameter, also useful in carrying out design optimizations. It provides the capability to use different physical models such as incompressible or compressible, inviscid or viscous, laminar or turbulent, etc. Generally, the following steps are followed in modeling and simulating a Multiphysics system in COMSOL Multiphysics.

3.3.1. Model Structure

The model studied in this research only focused on the secondary combustion zone of the stove. Half of the stove chamber is loaded with fuel. The fuel gas generated from the primary combustion zone moves upward toward the top of the stove. The secondary air inlet is supplied with the help of an external fan. At the secondary air exit, the gas resulting from the pyrolysis of biomass is mixed with the volatile gas generated from the pyrolysis and gasification process and creates an unconfined circular jet. The volatile gas generated react with air at the exit of the secondary air inlet and resulted in producing producer gas. The gas produced mainly consists of three compounds: carbon monoxide (CO), hydrogen (H₂), and nitrogen (N₂). The gas generated is at high temperature, as they move upward to the chamber top, at the exit of secondary airflow, when reacting with the supplied air, the fuel ignites. Since the fuel and oxidizer enter the reaction zone separately, the resulting

combustion is a non-premixed type. A continuous reaction requires that the reactants and the oxidizer are mixed to stoichiometric conditions. The study is carried out by using COMSOL Multiphysics.

3.3.2. Geometry

The microgasifier used for CFD analysis is shown in figure 3.6(b). The stove has 22 circular holes on the circumference of the chamber; through which secondary air enters the combustion chamber. The secondary air is supplied with the help of an external 12V, 92mm fan. The flow properties of the entering air specifically air flow rate is needed to be established. To identify the type of flow at the exit of the secondary air inlet Reynolds number has been calculated.

$$Re = \frac{\rho^* u^* L}{\mu} \quad (3.8)$$

where:

ρ - 1.09kg/m³ [density of air]

U - 5m/s [air speed]

μ - 2.075e-5 [dynamic viscosity of air]

L - 0.02 [characteristic length]

The flow Reynolds number is 1,724. For the flow which has Reynolds number between 1,800 up to 2,100 has transitioned to turbulent or turbulent flow. Therefore, the flow at the exit of the secondary air hole can make the transition to turbulence or transitional flow. The flows Reynolds number is small too close to be transition flow. But, since there are 22 holes are coming to cross-flow, the flow at the exit of secondary air could be turbulent. But, the net behavior of the fluid is close to laminar flow. As a result, turbulence vitally affects the diffusion process. Therefore the k- ω model is used by taking into account the turbulence effect.

In this study, by taking the assumption of complete oxidation of fuel to produce producer gas, two global irreversible chemical reactions were used:



Using this assumption as a starting point, and perform the simulation by using the modified approach used in (Asranna, 2015; Varunkumar et al, 2011).

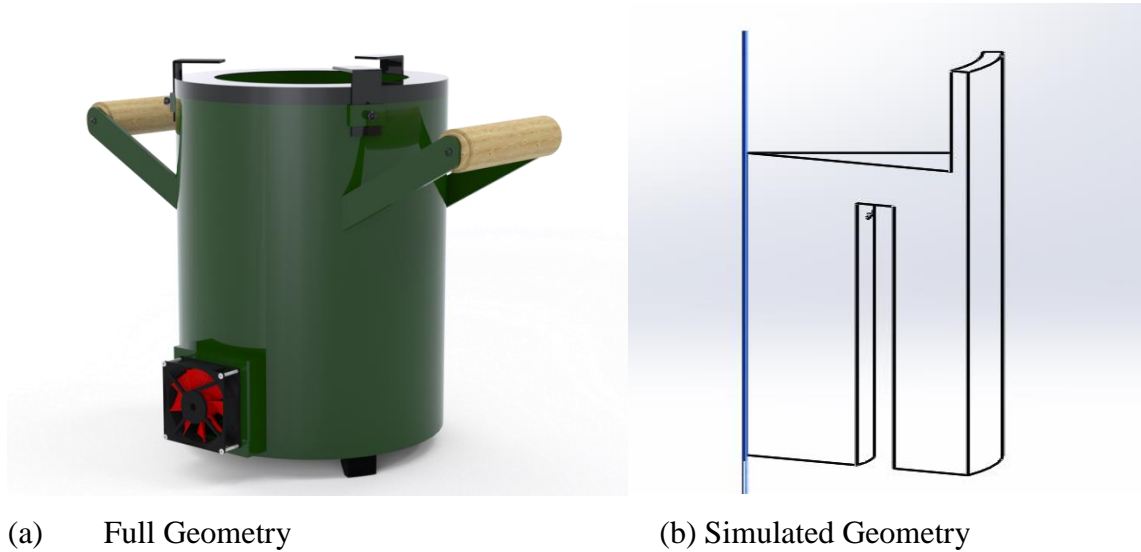


Figure 3.6 *Model Geometry*

Since large and complex geometries require a huge amount of memory and bigger computational re-sources, hence longer solution time than smaller and simpler ones. Thus, during the CFD simulation, it is customary to simplify and reduce the model using different approaches without sacrificing accuracy. One such approach is the use of symmetry. From the symmetric behavior of the model, one can see that simulating only one-twelfth of the total model can provide the necessary information to predict the characteristic of the whole model.

The gasifier stove used for the COMSOL Multiphysics analysis is shown in Figure 3.6(b). Secondary air is supplied with the help of an external fan which has the ability to supply atleast 5m/s. The composition of producer gas produced from biomass combustion was depend on the type of biomass used and wooden chips are typically used in the developed gasifier cookstove. The ultimate analysis of woodchips is given in table below. The composition is calculated on a moisture and ash free basis and taken as a reference based on previously studied literatures discussed in Table 3.2 (Series, 2016; Varunkumar et al, 2011).

Table 3-2 Ultimate analysis of woodchips done by (Varunkumar et al, 2011)

Element	Weight (%)
C	44.4
H	6.3
O	48.8
N	0.6

The flaming mode of biomass initially undergoes drying and devolatilization. The volatile react with primary air supply at bottom part of the combustion chamber and undergoes sub-stochiometric combustion. The product gas produced as CO, CO₂, H₂, CH₄ and H₂O as constituent. These gases passes through the hot char bed on the top of the fuel bed forming a producer gas rich in CO and H₂ (Varunkumar et al, 2011). The composition of producer gas formed was shown in table 3.3.

Table 3-3 Producer gas composition (Varunkumar et al, 2011)

Element	Mass fraction (%)	Mole fraction (%)
CO	27.3	9.6
CO ₂	6.8	13.3
CH ₄	0.5	3.9
H	17.6	10.0
H ₂ O	0.8	21.6
O	0.8	0.6
N ₂	46.2	41.0

The producer gas formed is oxidized by secondary air releasing heat in the process. The main process involved in the gasifier includes heat transfer, mass transfer and chemical reaction. To simplify and more track able the physical problems during the simulation study, some assumptions are made: The flow field was assumed as incompressible, turbulent, axisymmetric, and steady flow; Nitrogen (N₂) species was considered an inert species and did not participate in any reaction; furthermore, the formation of other air

pollutants like COS, CS₂, HCN, NH₃, H₂S, SO₂ during the gasification process was ignored; The walls of the entrained-flow gasifier are considered as adiabatic; In producer gas composition, the primary components are CO and H₂ and the contribution of CH₄ in heating value of the producer gas is usually negligible hence methane formation is not included in present simulations. Based on these assumptions, Table 3.4 shows the composition of producer gas assumed from previously studied related literatures by Varunkumar et al (2011) and Series (2016).

Table 3-4 Distribution of volatile assumed for fuel

Species	Mass fraction
N ₂	0.5
H ₂	0.2
CO	0.3

Two irreversible chemical reactions expressed in equation (3.26) were used as a heat source for the simulation. Using those values as a starting point the simulation was performed (see Appendix C); the geometrical parameters needed for the simulation can be generated, see Table 3.5.

Table 3-5 Basic geometrical parameters

Parameter	Value	Unit
Inner cylinder diameter	200	Mm
Outer cylinder diameter	280	Mm
Combustion chamber insulator	20	Mm
Primary air inlet	7	mm
Secondary air inlet	5	mm
Pot diameter	240	mm
Pot height	120	mm
Air gap	20	mm

3.3.3. Governing Equation

The law of conservation of mass states that “the rate of increase of mass flow through a control volume is equal to the rate of inflow through the boundaries.” In other words, the mass flow entering and leaving the control volume must balance exactly(White, 2001).

$$\frac{\partial \rho}{\partial t} + \nabla \cdot (\rho u) = 0 \quad (3.10)$$

In the case of steady-state analysis, $\frac{\partial \rho}{\partial t} = 0$; as a result, the equation reduced to

$$\nabla \cdot \rho u = 0 \quad (3.11)$$

The momentum conservation equation is obtained by balancing the forces acting on the fluid element i.e. conservation of momentum generalize the newton's second law to define the motion of the fluid(White).

$$F_i = \sum F = \rho \frac{\partial V}{\partial t} dx dy dz \quad (3.12)$$

The net force on control volume must be a differential size and proportional to the element volume. Also, F_i represents all resultant force acting on a fluid element: body force and surface forces.

Body force is due to external fields, gravity, magnetism, and electric potential which act on entire mass within the element (White, 2001). The only body force considered in this study was gravity. The gravity force on the differential mass ($\rho g dx dy dz$) with the controlled volume is:

$$dF_{grav} = \rho g dx dy dz \quad (3.13)$$

Surface forces are forces due to the stresses on the sides of the control surface.

$$\left(\frac{\partial F}{\partial V} \right)_{viscous} = \nabla P + \tau_{ij} \quad (3.14)$$

Substituting the body and surface force in equation 3.2, we obtain;

$$\rho g - \nabla P + \nabla \cdot \tau_{ij} = \rho \frac{\partial V}{\partial t} \quad (3.15)$$

Expressing stress tensor in terms of the deformation of the element and by using the divergence formula to reduce the equation (Asranna, 2015):

$$\tau_{ij} = \mu(\nabla u) - \frac{2}{3} \nabla \cdot u_{ij} I \quad (3.16)$$

For stationary case,

$$\rho u \cdot \nabla u = \rho g - \nabla P + \nabla \cdot (\nabla u + (\nabla u)^T) - \mu(\nabla u) - \frac{2}{3} \nabla \cdot u_{ij} I \quad (3.17)$$

The k- ω turbulent flow model is the governing equation of fluid flow is average Navier-stokes equation and conservation.

Since the fluid properties become invariant in space and time when the flow makes a transition to turbulence, plus Turbulent flow is chaotic, characterized by the presence of a diverse range of length and time scales. As a result, it is difficult to diverse the scale of the flow which makes the solving process difficult.

An alternative is to use the Reynolds Averaged Navier-Stokes equation which incorporates additional equations to account for the mixing and transport by the turbulent eddies. In this method, the fluid properties are divided into an averaged value and a fluctuating part. Any scalar quantity of flow ϕ is decomposed and expressed as

$$\phi = \bar{\phi} + \phi'' \quad (3.18)$$

Where $\bar{\phi}$ represents the averaged component and ϕ'' represents the fluctuating component. Expressing the terms in the Navier-Stokes equations in this form leads to the Reynolds averaged Navier-Stokes equation.

$$\rho u \cdot \nabla u = \rho g - \nabla P + \nabla \cdot (\mu(\nabla u + (\nabla u)^T)) - \frac{2}{3} \mu(\nabla \cdot u) I - (\overline{\rho u_i'' u_i''}) \quad (3.19)$$

Species Transport Equation is the transport of concentrated species interface solves for an arbitrary number of mass fractions. The species equations include transport by convection and diffusion. Mass transport close to solid walls is modeled using wall functions, and reactions within the turbulent flow are modeled using the eddy dissipation model (COMSOL, 2018). The combustion model based on the eddy dissipation model postulates that the reaction only occurs if the breakup of the turbulent structure reaches the finest turbulent scales. Therefore, the reaction rate can be described by common parameters of

two-equation models (equation 3:13): the turbulent dissipation model and the turbulent kinetic energy.

Using the Fick's law diffusion model the relative mass flux derived from the reaction:

$$\nabla \cdot j_i + \rho(u \cdot \nabla) \omega_i = \phi_f R_i$$

where :

$$j_i = \left(\rho \left(D_i^F + \frac{u_T}{Sc_i} \right) \nabla \omega_i + \rho \omega_i D_i^F \nabla \frac{\nabla M_n}{M_n} + D_i^F \frac{\nabla T}{T} \right) \quad (3.20)$$

When using a turbulence model in a reacting flow interface, the production rate (SI unit: kg/(m³•s)) of species i resulting from reaction j is modeled as the minimum of the mean value-closure reaction rate and the eddy-dissipation-model rate (COMSOL, 2018):

$$R_{ij} = V_{ij} M_{ij} \cdot \min[r_{MVC,j}, r_{ED,j}] \quad (3.21)$$

The reaction rate defined by the eddy-dissipation model is (COMSOL, 2018):

$$r_{ED,j} = \frac{\alpha_j}{\tau_T} \rho \cdot \min \left[\min \left(\frac{\omega_r}{v_{rj} M_r} \right), \beta \sum_p \frac{\omega_p}{v_{pj} M_p} \right] \quad (3.22)$$

NB: Properties of reactants of the reaction are indicated using a subscript r, while product properties are denoted by a subscript p.

The heat of reaction, or change in enthalpy, following each reaction is defined from the heat of formation of the products and reactants:

$$\sum \Delta H_r = \sum \Delta H_p - \sum \Delta H_r \quad (3.23)$$

Since the heat of formation of the products is lower than that of the reactants, both reactions are exothermic and release heat. The heat release is included in the model by adding a Heat Source feature to the Heat Transfer in Fluids interface.

The heat source (SI unit: W/m³) applied is defined as:

$$q = r_{ED,1} H_{r1} + r_{ED,2} H_{r2} \quad (3.24)$$

3.3.4. Boundary Conditions

It is important to take the right boundary conditions that are most appropriate to the practical problem. In this study, four types of boundary conditions have been used for the simulation while getting a practical in-touch with the gasifier cookstove: Inlets, outlet, symmetry and stove walls. The computational domain with a detailed boundary condition is described in Figure 3.7.

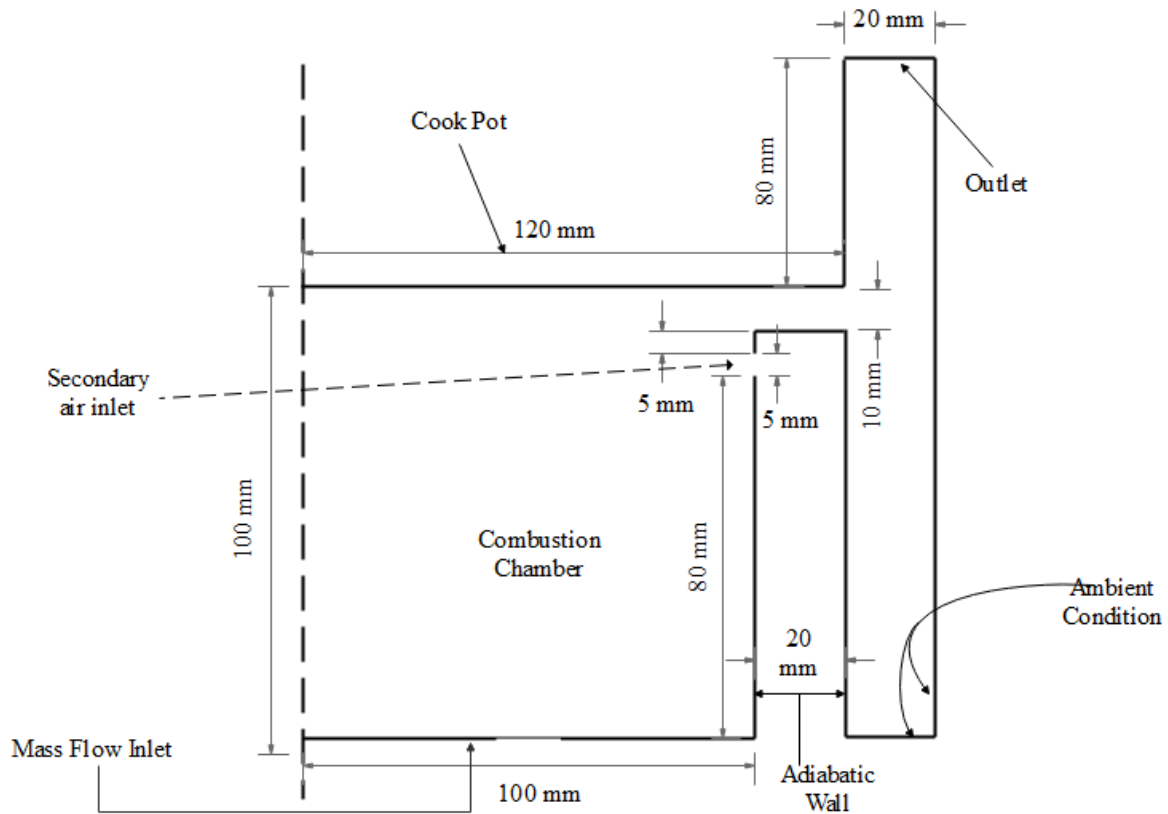


Figure 3.7 boundary conditions

3.3.5. Meshing

Solutions by numerical methods require physical discretization/meshing of the domain. A good solution is obtained if good meshes for the models are generated. The accuracy of the solutions depends on the sizes of the meshes. An unstructured mesh composed mostly of triangular and tetrahedral elements is used for in the simulations.

3.3.6. Solution Technique

Solution procedure contains three steps:

1. Turbulent flow and reacting flow are solved.
2. The flow at the secondary air exit is set as an inlet

3. Finally, heat transfer is included and coupled with reacting flow and solved based on the previous iteration (see figure 3.8).

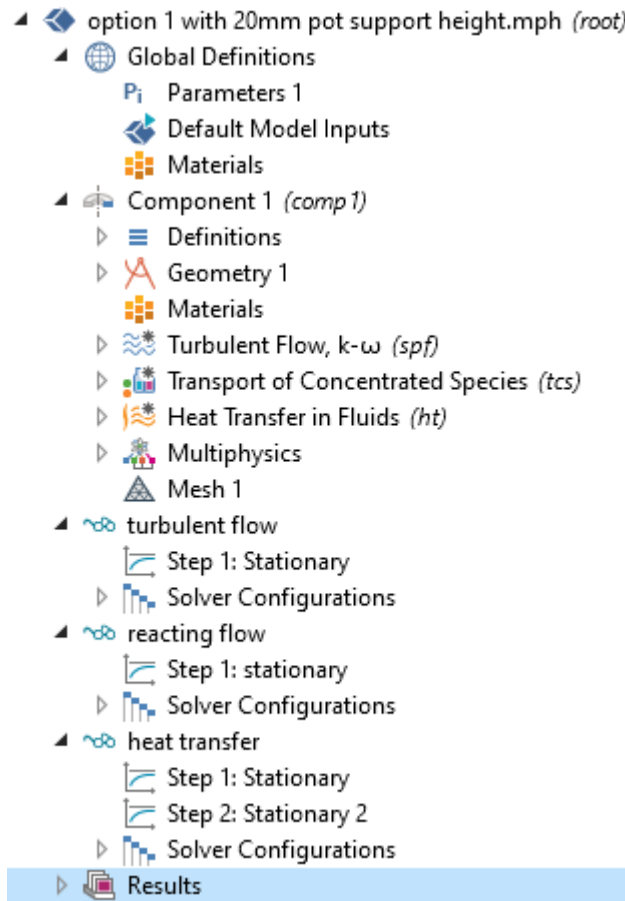


Figure 3.8 Screenshot of COMSOL model Structure

3.4. The stove performance analysis resulting from the simulation

To calculate the thermal efficiency of the developed stove, first, the heat fluxes to the pot bottom wall was calculated by using data from the simulation (Figure 5.9) and then integrate it over the pot bottom cross-sectional area. Then the resulted value ratio against the total heat input to the stove (Pundle et al, 2019).

Therefore, the thermal efficiency is equal to:

$$\eta_{thermal} = \eta_{gasification} * \eta_{convection} \quad (3.25)$$

$$\eta_{convection} = \frac{U_{pot}}{U_{input}} \quad (3.26)$$

Where:

U_{pot} - Heat transfer from the combustion chamber to the pot bottom, KJ

U_{input} - Total heat energy input, KJ

$$U_{pot} = \int_0^r q'' 2\pi r dr$$

(3.27)

Where:

q'' - Heat flux [taken from the simulation result], W/m^2

r –radius of the pot, m

3.5. The manufacturing process of forced draft microgasifier

By using data from the analytical design of the gasifier stove discussed in section 3.2, the sheet metal was cut at the circumference of the inner cylinder. Then the air inlet hole for primary and secondary air supply was drilled by using the drilling machine. Then the sheet metal was rolled to make it cylinder by using a rolling machine. Similarly, for the outer cylinder, the circumference of the outer cylinder was used to cut the sheet metal, and then the sheet metal was rolled. Then, the upper cover, handling, lower support, and pot support was manufactured. The clay used for insulation was manufactured by local potters. Then after, welding was used for merging individual parts to form the stove. Nuts and bolts are used to fasten the stove body with pot supports. Figure 3.9 shows the manufacturing processes (see Appendix D).



Figure 3.9 manufacturing processes

3.6. Testing of the performance of the Gasifier

The performance of the gasifier stove in this study could be analyzed based on thermal performance analysis. Thermal performance analysis is measured in terms of firepower, specific fuel consumption, and efficiency.

The performance of the developed gasifier stoves is established through the testing guidelines developed by the International Standards Organization ISO 19867-1:2018. ISO 19867-1:2018 guidelines provide a 4-tier system for cookstove performance; 1 for the lowest level performance and 4 being the highest and measured by using water boiling test protocol (ESA, 2018). The performance parameters examine, thermal efficiency, emission of CO and PM, and indoor air pollutions.

The Water Boiling Test is a relatively short and simple simulation of a common cooking procedure in which a standard quantity of water is used to simulate the cooking process. It is designed in such a way that, stoves made in different places and for the different cooking applications can be compared through standardized and replicate tests.

The WBT consists of three phases and the duration of each phase shall include a fuel-burning period and variable time needed for shutdown and it is approximately 30 minutes for each phase (ESA, 2018).

Phase 1: At the beginning first phase (high power test), the cookstove and the water in the cooking vessel shall be at ambient temperature and uses a pre-weighed bundle of wood or other fuel to boil a measured quantity of water in a standard pot. The remaining char shall be weighed at the end of the test.

Phase 2: At the beginning of the second phase (medium power test), the cookstove shall be at operating temperature and the water in the cooking vessel shall be at the ambient temperature. Similarly, in this phase, a pre-weighed bundle of fuel to boil a measured quantity of water in a standard pot is used. The remaining char shall be weighed before commencing phase 3.

Phase 3: At the beginning of phase three (low power test), the cookstove shall be at operating temperature after completion of phase two. The water in the cooking vessel shall be at the ambient temperature. Any char remaining shall be removed from the cookstove and weighed.

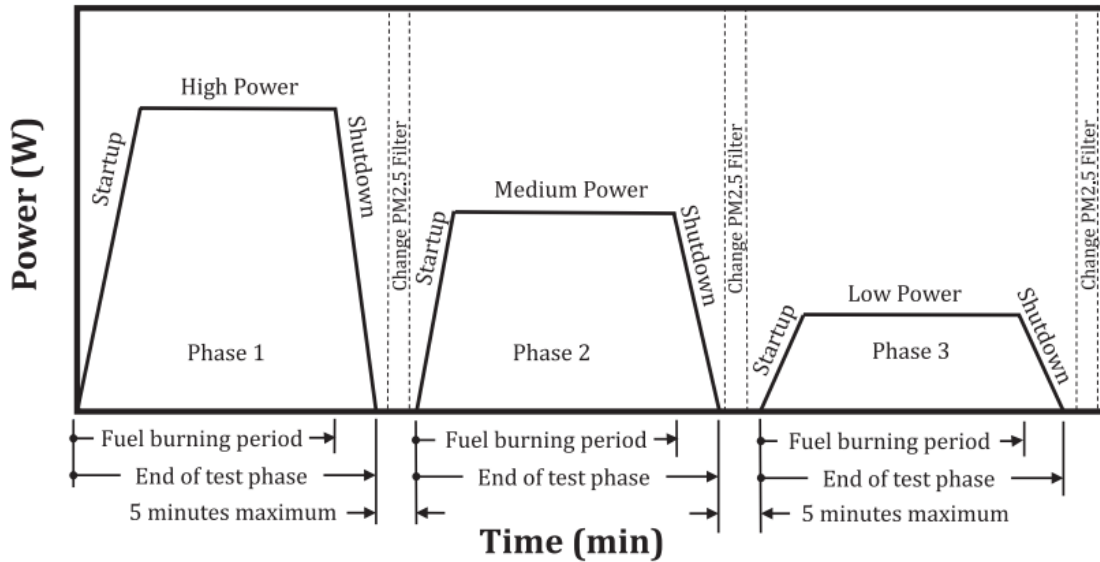


Figure 3.10 Diagram of the standard test sequence of cookstove with ranging cooking power (ESA, 2018)

This combination of tests measures some aspects of the stove’s performance at both high medium and low power outputs, which are associated with the stove’s ability to conserve fuel. However, rather than report a single number indicating the thermal efficiency of the stove, which is not necessarily a good predictor of stove performance, this test is designed to yield several quantitative outputs (Bailis et al, 2007). The outputs are the time to boil, burning rate, specific fuel consumption, firepower, and thermal efficiency.

3.7. Experimental set-up

Before starting the test the following experimental set-up should be fulfilled. A stainless steel pot with a capacity of 5 liters was used to conduct the cooking process. The suitable type of fuel shall be selected, moisture content of the biomass fuel shall be determined, the water inside the pot shall be weighed and the mass of water and initial water temperature shall be recorded, the temperature sensor (thermocouple) should be placed inside the pot using the holder and the tips of the sensor shall be located in the center of the volume of

the water in the cooking vessel and environmental meter displays the temperature on the screen. An infrared thermometer is used to measure the stove body temperature. The local boiling point of water shall be determined by heating water using any cookstove or heating device.

The experimental tests on the forced draft microgasifier were carried out during the duration starting from October 01/08/2020-05/08/2020 between 08:00 am to 05:00 pm. The station is located at Addis Ababa Institute of Technology, Addis Ababa University, Addis Ababa, Ethiopia where a longitude of 38.7 °E and latitude of 9.04 °N. Figure 3-11 shows the schematic and actual experimental set-up.

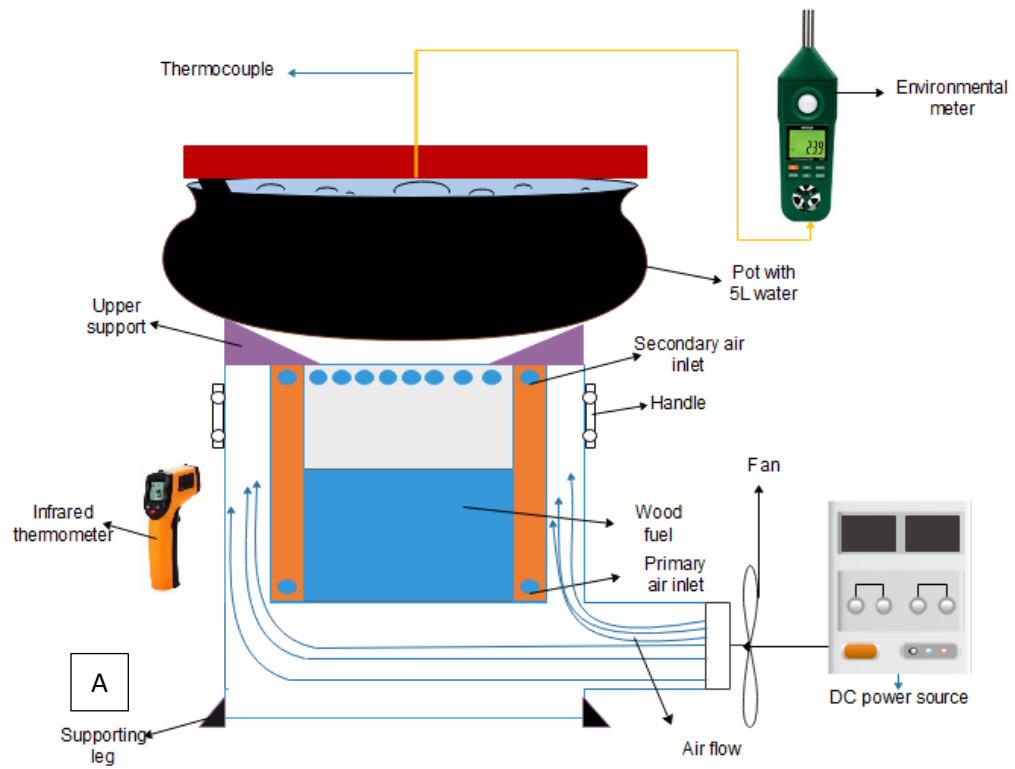


Figure 3.11 (a) schematic of the experimental setup (b) actual experimental set up of microgasifier stove

3.7.1. The procedure of Water Boiling Test

Once the experimental setup is over, the testing process was started. WBT testing procedures were the following steps: the fire shall be lit and the time shall be recorded (time start recorded when the match struck); the temperature of the water shall be recorded at least every one minute during the test phase; if the local boiling point is reached before 30 minutes, the time it reached the local boiling point shall be recorded; if the local boiling point reached at the end of 30 minutes, then the water temperature shall be recorded and the test is over when the water temperature drops to 5°C below the boiling point attained or five minutes elapse after the end of the 30 minutes. Also if at the end of 30 minutes, the local boiling point is not reached, the water temperature shall be recorded and the test shall be over after 5 minutes or when the temperature drops 5°C from the local boiling point. Once the testing procedure is over the fuel feeding shall be stopped and char shall remain in the cookstove and unburned cookstove shall be removed from the cookstove. The mass of the char remaining at the end of the test shall be recorded, if present. Upon the conclusion of the test, the water shall be weighted and recorded (ESA, 2018).

3.7.2. The stove performance analysis resulting from the experiment

Useful energy delivered calculation is the amount of energy transferred to the cooking pot and calculated using equation (3.28):

$$Q_i = C_p * W_1(T_2 - T_1) + (G_1 - G_2) \Psi \quad (3.28)$$

Where:

Q_i – The useful energy delivered, kJ

C_p – Specific heat capacity of water between 20 -100°C, $\frac{kJ}{kg \cdot K}$

G_1 – Initial mass of water in the cooking vessel, kg

G_2 – Final mass of water in the cooking vessel, kg

T_1 – Initial temperature of water in the cooking vessel, °C

T_2 – Final temperature of water in the cooking vessel, °C

Ψ – Latent heat of water vaporization at the local boiling point, $\frac{kJ}{kg}$

Another one is cooking power and shall be calculated by using equation (3.29):

$$P_c = \frac{Q_i}{(t_3 - t_1)} \quad (3.29)$$

Where:

P_c - cooking power, KW

t_3 - Final time at the end of a test phase, Sec

t_1 - Initial time at the end of a test phase, Sec

Thermal efficiency of the cookstove without considering energy for the remaining char shall be calculated by using equation (3.30):

$$\eta_{thermal_1} = \frac{Q_i}{BQ_{net.af}} \times 100\% \quad (3.30)$$

Where:

$\eta_{thermal_1}$ - Cooking thermal efficiency without energy credit for remaining char, %

$Q_{net.af}$ - The lower heating value of the fuel, $\frac{KJ}{Kg}$

B – The mass of the fuel used, Kg

The thermal efficiency of the cookstove with considering energy for the remaining char shall be calculated by using equation (3.31):

$$\eta_{thermal_2} = \frac{Q_i}{BQ_{net.af} - CQ_{net.af}} \times 100\% \quad (3.31)$$

Where:

$\eta_{thermal_2}$ - Cooking thermal efficiency with energy credit for remaining char, %

C – Mass of the remaining char, Kg

CHAPTER 4

ANALYTICAL ANALYSIS OF FORCED DRAFT MICROGASIFIER STOVE

4.1. Mode of Heat Transfer of The Forced draft microgasifier cookstove

In order to improve the thermal and combustion efficiency of cook stoves the heat transfer and heat losses should be assessed accurately. In order to increase the heat transfer to the pot bottom, heat losses from the stove should be minimized. In this study, by using thermodynamics concept integration with heat transfer, the thermal performance of the forced draft microgasifier stove is studied. Figure 4.1 below shows the different modes of heat transfer of the FDM stove which plays a great role in the stove performance.

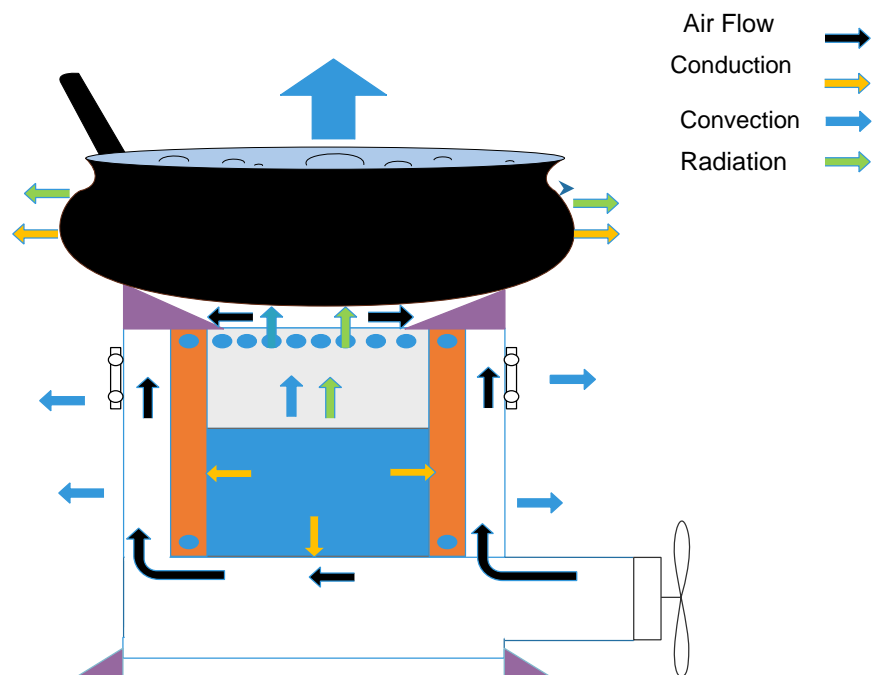


Figure 4.1 Schematic diagram of axis-symmetry of different mode of heat transfer

4.2. Heat Transfer and Energy Balance

To simplify the analysis, the stove divided into three different zones: fuel bed zone (zone where: drying, devolatilization, pyrolysis, char gasification and combustion takes place), flame zone (zone where gas combustion and pollutant formation takes place) and convective heat transfer zone. In order to determine the heat transfer and heat losses within each of the three different heat zones of the stove, energy balance method is used.

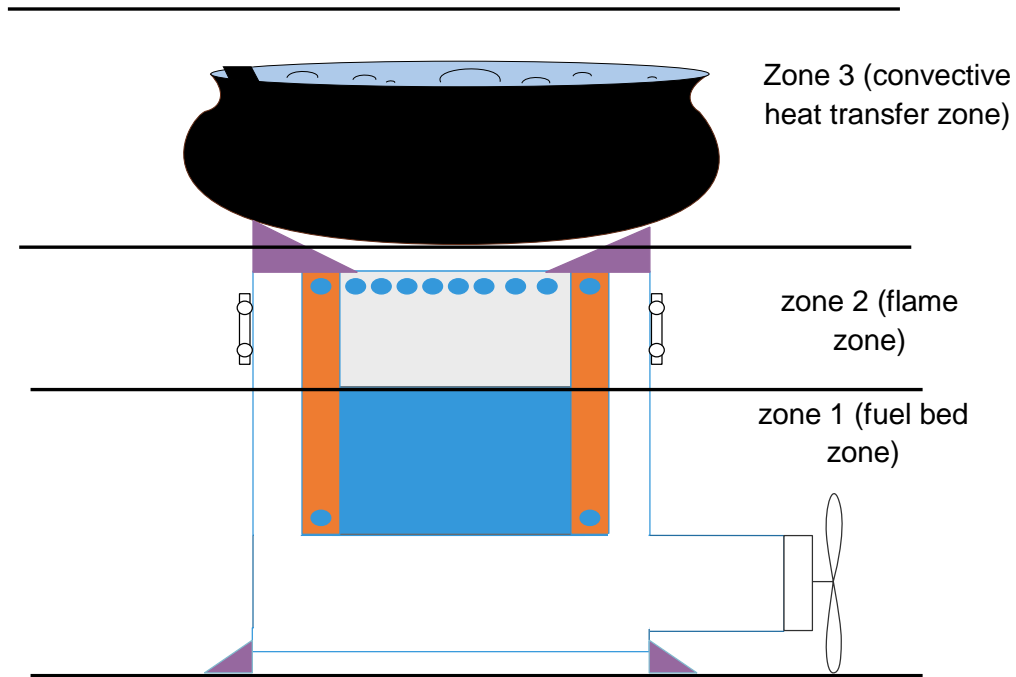


Figure 4.2 Axis-symmetry of different heat zones within FDM stove

Based on the result from the conducted test and data from the related literature, the following assumption was taken: the operation is steady state; the value of temperature and velocity used in each zone the mean value of temperature and velocity of that zone; zone 1 covers entire the bottom part of the stove; the radiation heat transfer mode is neglected.

4.2.1. Heat Transfer Analysis of Zone 1 (fuel bed zone)

Zone 1 is filled with solid wood fuel. In this region, fuel drying, pyrolysis, char gasification and combustion takes place. By using measured values of temperature from conducted test as well as assumed values of temperature based on different literatures, heat transfer analysis is conducted.

i. Heat loss to the grate (base plate)

The heat lost to the stove base plate is mainly by conduction and conduction heat loss to the stove base plate is calculated by using the following formula:

$$Q_{cond_loss} = \frac{T_{biomass} - T_{grate}}{R_t}; \text{ Where: } R_t = \frac{L}{K_{steel} * A}$$

Equation Chapter (Next) Section 1

(4.1)

Where:

Q_{cond_loss} - Conduction heat loss to the grate

$T_{biomass}$ - 650K [Mean temperature of zone 1]

T_{grate} - 500K [Grate temperature]

R_t - Thermal resistance

K_{steel} - Thermal conductivity of steel (material which the grate is made of)

As a result, $Q_{cond_loss} = 535.7W$

ii. Heat loss through the wall

The stove loss through the wall in zone 1 is combination of heat loss by conduction and convection. The heat loss through the wall is represented by the analog model of thermal resistance. In the case of natural convection, the radiative heat transfer coefficient value approximated equal to convective heat transfer coefficient. In the case of forced convection, the value of radiative heat transfer coefficient is much higher by magnitude than that of convective heat transfer coefficient. So that thermal radiation can be neglected (Lienhard IV & Lienhard V, 2004). In case of stove of metal combustion chamber and the chamber is covered by insulating material, only the insulation layer is considered. The analysis is performed as multiple layer material by using the sum of the resistance of each layer.

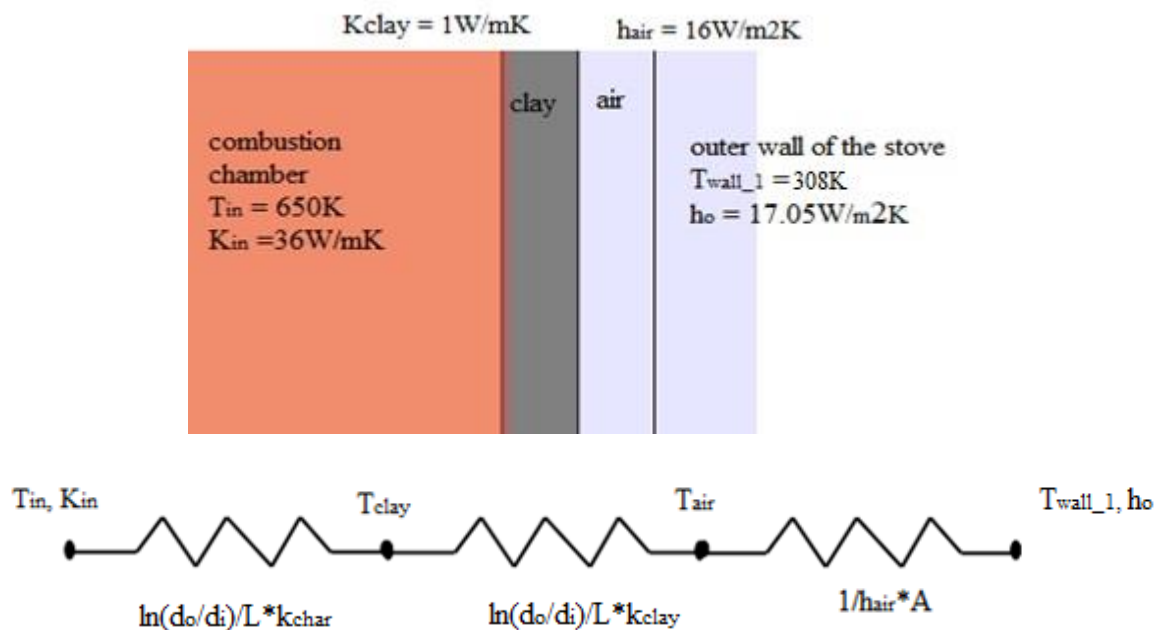


Figure 4.3 Schematic diagram of heat transfer in zone 1 with thermal resistance circuit

From the thermal circuit diagram, the heat loss can be calculated.

$$Q_{-1} = \frac{T_{in} - T_{wall_{-1}}}{\frac{\ln(d_o / d_i)}{L * K_{char}} + \frac{\ln(d_o / d_i)}{L * K_{clay}} + \frac{1}{h_{air} * A} + \frac{1}{h_o * A}} = 7.54W \quad (4.2)$$

Where:

Q_{-1} - Heat loss through stove side in zone 1

T_{in} - 650K [Mean Temperature inside zone 1 of the combustion chamber taken from (Chaurasia, 2018)]

$T_{wall_{-1}}$ - 308K [Outer stove body mean temperature in zone 1; measured during the test]

K_{char} - Thermal conductivity of biomass char (MacCarty & Bryden, 2016)

K_{clay} - Thermal conductivity of clay and the value was taken from (Incropera et al))

h_{air} - Convective heat transfer coefficient of air (calculated value and the detail analysis is discussed in Appendix A)

h_o - Convective heat transfer coefficient of ambient air (calculated value and the detail analysis is discussed in appendix A)

L - 0.1m [Length of the stove section where heat transfer takes place (zone 1)]

d_i - 200mm [diameter of the combustion chamber]

d_o - 260mm [outer diameter of the stove]

4.2.2. Heat Transfer Analysis of Zone 2 (flame zone)

Zone 2 is filled with pyrolyzed gases from zone 1. In this region, the pyrolyzed gas generated from drying and pyrolysis is combusted and also the pollutant is formed. By using measured values of temperature from conducted test as well as assumed values of temperature based on related literatures and simulation result, the heat transfer analysis is conducted.

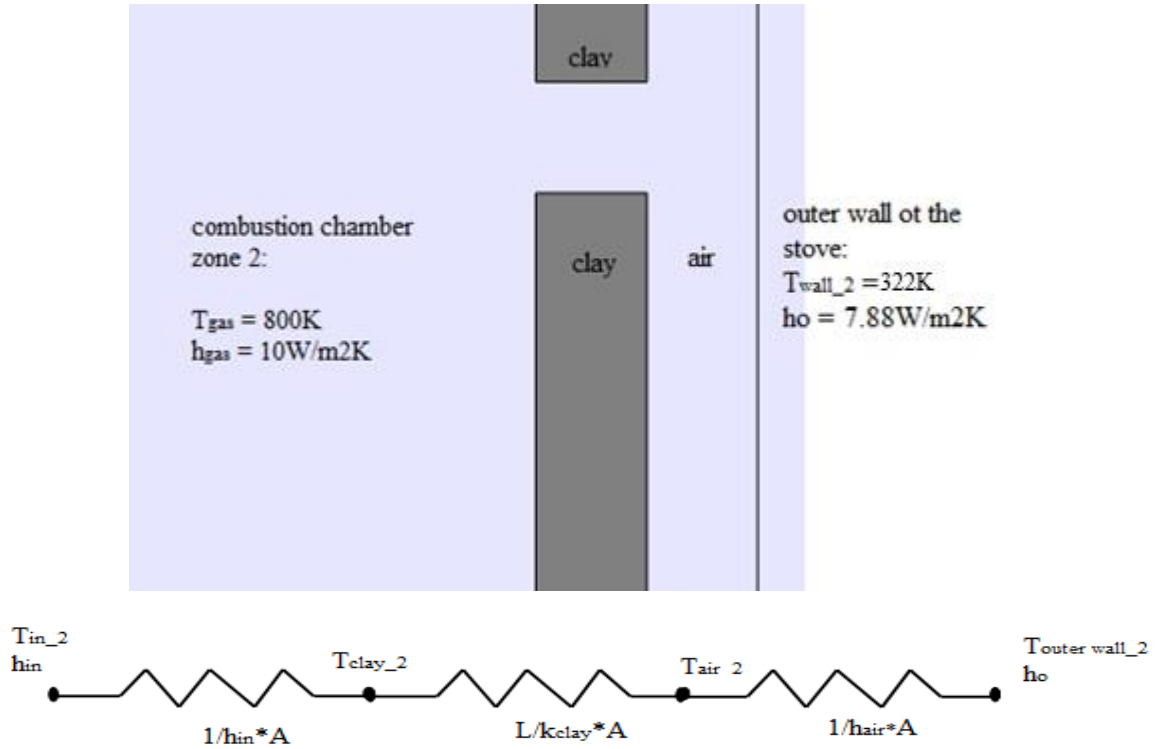


Figure 4.4 schematic diagram of heat transfer in zone 2 with thermal resistance circuit

Heat loss through the outer wall of the stove (zone 2)

Similar to zone 1, heat loss to the wall in this zone is the combination of conduction and convection heat transfer mode.

From the thermal circuit diagram, the heat loss can be calculated.

$$Q_{_2} = \frac{T_{gas_1} - T_{wall_2}}{\frac{1}{h_{gas_1} * A_1} + \frac{\ln(d_o / d_i)}{K_{clay_1} * L_1} + \frac{1}{h_{air} * A_1} + \frac{1}{h_{o_1} * A_1}} = 4.86W \quad (4.3)$$

Where:

$Q_{_2}$ - Heat loss through stove wall in zone 2

T_{gas_1} - 800K [Mean Temperature of gas of zone 2 of the combustion chamber; taken from previous work done by (Varunkumar et al, 2011)]

T_{wall_2} -323K [Outer stove outer wall mean temperature in zone 2 (measured during the test)]

h_{gas_1} - Convective heat transfer coefficient of gases resulted from pyrolysis of biomass (detailed calculation and the value is discussed in appendix A section)

K_{clay_1} - Thermal conductivity of clay and the value was taken from (Incropera et al))

h_{air_1} - Convective heat transfer coefficient of air (calculated value and the detail analysis is discussed in appendix A section)

h_o - Convective heat transfer coefficient of ambient air (calculated value and the detail analysis is discussed in appendix A section)

L – 0.1m [Length of the stove section where heat transfer takes place (zone 2)]

4.2.3. Heat Transfer Analysis of Zone 3 (convective heat transfer zone)

i. Pot bottom center

The pot bottom is treated as single cylindrical region above the combustion chamber exit and it is treated as a stagnation point of average heat transfer to the pot only with no losses.

$$Q_{pot_center} = h_{air_2} * A_{pot_bottom} * (T_{gas_2} - T_{pot_bottom}) + \phi \epsilon \sigma A_{pot_bottom} (T_{gas_2}^4 - T_{pot_bottom}^4) \quad (4.4)$$

Where:

Q_{pot_center} - Heat transferred to the pot bottom center

h_{air_2} - Convective heat transfer coefficient of zone 3

A_{pot_bottom} - Area between the stove and the pot

T_{gas_2} - 900K [The temperature of exit gas from the combustion chamber]

T_{pot_bottom} - 350K [Temperature of upper wall of the stove]

ϕ - Radiation heat transfer view factor

σ - Stefan-boltzman constant [$5.67 * 10^{-8} \text{W/m}^2 \text{K}^4$]

$A_{pot} = \pi r_{pot}^2 = 0.045 \text{m}^2$ - Area of pot bottom [diameter of pot is 240mm]

$T_{pot_bottom} = 350\text{K}$ [taken from the test conducted]

$\epsilon = 1$ [emissivity of char at temperature of around 1000K]

The view factor is independent of geometry and the material properties or the temperature. It is calculated by using equation (4.4):

$$\phi = \frac{1}{2} (s_{gas_2} - (s_{gas_2}^2 - 4(\frac{r_{chamber}}{r_{pot}})^2)^{\frac{1}{2}}) = 0.21 \quad (4.5)$$

Where:

$$s_{gas_2} = 1 + \left(\frac{1 + \left(\frac{r_{pot}}{L_{flame}} \right)^2}{\left(\frac{r_{chamber}}{L_{flame}} \right)^2} \right) = 3.505$$

r_{pot} - 0.12m [pot radius]

L_{flame} - 0.15m [length between char and pot bottom]

$r_{chamber}$ - 0.1m [radius of combustion chamber]

In order to calculate the heat transfer coefficient correlation the correlation from the literature is used (MacCarty & Bryden, 2016).

For entire pot bottom, the Nusselt number is calculated by using the following formula:

$$Nu = 0.5(1.65 Re^{0.5} + 2.733 Re^{0.59}); \quad Re = \frac{V * L}{\nu} = 492.2 \quad (4.6)$$

Where;

Nu – Nusselt number for entire pot bottom

V – Velocity of gas between stove and pot gap [estimated from simulation result]

ν - Kinematic viscosity of air at T_{gas_2} [taken from (Incropera et al)]

L – The gap between pot and the stove

Finally, convective heat transfer coefficient of zone 3 is calculated:

$$h_{air_2} = \frac{Nu * K_{air@T_{gas_2}}}{L} = 12.09 W/m^2K$$

Then, by substituting the values to equation 4.4 the heat transferred from char (inside of combustion chamber) to the pot center is calculated and it is equal to 642.74W

ii. Pot bottom above the stove body

Heat is transferred from the combustion chamber to the pot bottom through convection and radiation as well as from stove body to the pot bottom by conduction and convection.

$$Q_{pot_bottom} = h_{air_2} A_{pot} (T_{gas_2} - T_{pot_bottom}) + Q_{upper_wall} + \phi \epsilon \sigma A_{pot} (T_{gas_2}^4 - T_{pot_bottom}^4) \quad (4.7)$$

Thus,

$$Q_{upper_wall} = \frac{T_{gas_2} - T_{pot_bottom}}{\frac{L_{flame}}{K_{stove_wall} * A_{pot}} + \frac{1}{h_{air_2} * A_{pot}}} \quad (4.8)$$

Where:

Q_{pot_bottom} - Heat transfer to the pot bottom

Q_{upper_wall} - Heat transfer to the pot bottom by conduction

Q_{pot_bottom} - Heat transfer to the pot bottom

ϕ - Radiation heat transfer view factor

σ - Stefan-boltzman constant [$5.67 * 10^{-8} \text{W/m}^2 \text{K}^4$]

$A_{pot} = \pi r_{pot}^2 = 0.045 \text{m}^2$ - Area of pot bottom [diameter of pot is 240mm]

$T_{pot_bottom} = 350 \text{K}$ [taken from the test conducted]

ε - 0.72 [emissivity taken from (MacCarty & Bryden, 2016)]

L - 0.26 length of the flame [m]

The view factor from flame to the pot center was calculated as:

$$\phi = \frac{1}{2} [S_{flame_out} - [S_{flame_out}^2 - 4(\frac{R_{flame_in}}{R_{flame_out}})^2]^{\frac{1}{2}}] = 0.4$$

$$s_{flame_out} = 1 + \left(\frac{1 + (\frac{R_{flame_in}}{L_{flame}})^2}{(\frac{R_{flame_out}}{L_{flame}})^2} \right) = 1.5$$

Thus, by substituting the value to the equation 4.8, the total heat transfer from the upper part of the stove to the pot bottom is equal to 2219.601W

iii. Heat transfer analysis of pot side

At the pot sides, there is no heat transfer to the pot but there is heat loss from the pot to the ambient by convection and radiation. Radiation from the pot to the ambient is considered with view factor of 1 and the temperature used is average temperature of the stove body.

$$Q_{pot_side_loss} = h_{air_3} A_{pot} (T_{pot_side} - T_{amb}) + \phi \sigma A_{pot} (T_{pot_side}^4 - T_{amb}^4) \quad (4.9)$$

To calculate the convective heat transfer coefficient, since the pot is not shielded and it is forced convection, forced convection laminar heated plate concept is used. Therefore Nusselt number is calculated by using the formula developed by MacCarty & Bryden (2016):

$$Nu = 0.664\sqrt{Re} ; Re = \frac{V * L}{\nu} = 1434.03 \quad (4.10)$$

Where:

V – Velocity of air around pot side [assumed based on simulation result]

L – The pot height

ν - Kinematic viscosity of air

From the result obtained above, the convective heat transfer coefficient is equal to 56.16W/m²K. By substituting each value in equation above heat loss from the pot to ambient through the side of the pot is equal to 218.7W

Total energy balance and thermal efficiency

i. Energy balance

$$Energy_balance = U_{fuel} - U_{combustion} - Q_{total} \quad (4.11)$$

Where:

$$Q_{total} = (Q_{total})_{zone_1} + (Q_{total})_{zone_2} + (Q_{total})_{zone_3} = 2862.341W \quad (4.12)$$

$$U_{fuel} = \frac{LHV_{wood} * m_{fuel}}{t_{boiling}} = 7134.5W \quad (4.13)$$

$$U_{combustion} = \eta_{combustion} * U_{fuel} = 142.7W \quad [\text{by taking combustion efficiency } 98\%$$

(Varunkumar et al, 2011)]

Where:

U_{fuel} - Energy inside the fuel in W

$U_{combustion}$ - Combustion energy in W

Q_{total} - Total heat transfer of the stove in W

LHV_{wood} - Lower heating value of wood in Kg/KJ (eucalyptus wood)

m_{fuel} - Mass of fuel (in kg)

$t_{boiling}$ - Boiling time in second.

By substituting the value to the equation above the energy balance is equal to be 4,129.459W.

ii. Thermal efficiency

Thermal efficiency is calculated by dividing the total heat energy transferred to the pot by total energy if the fuel:

$$\eta = \frac{Q_{pot_bottom}}{Q_{fuel}} \times 100\% = 40.12\% \quad (4.14)$$

CHAPTER 5

RESULT AND DISCUSSION

5.1. Constructed Stove

The constructed biomass gasifier stove schematic diagram is shown in Figure 4.1. The biomass fired forced draft microgasifier developed consists of four main parts: fan, combustion chamber, combustion chamber insulator and external cylinder. Different parts of the stove could be attached together by bolts and nuts and welding mechanism. The stove consists of combustion chamber of the reactor, grate, air gap between inner and outer cylinder which used for secondary air inlet as well as used as an additional insulation, and fan used for adjusting and facilitating primary and secondary air inlet. The reaction chamber/combustion chamber of the stove is cylindrical mild steel having diameter of about 200mm and height of 260mm. in order to minimize heat losses insulation material added, clay with thickness of 20mm, cover the inside cylinder, and also the secondary air inlet airy gap was. All parts of the stove were constructed from locally available materials except the fan which is taken from malfunctioning desktop computer.

The stove works as top-lit up draft gasifier stove. The primary air enter into the reaction chamber through the primary air inlet which is found at the bottom part of the chamber of the stove and flows upward toward the center of combustion chamber and out in gas burner at the top. Producer gas is generated while the primary air pass through the hot combustion chamber filled with the fuel and leaves the chamber at the top. The speed of air flow is controlled speed controller integrated to the fan; mechanically also by opening the air entry and by closing the air entry the air speed was controlled. The detail manufacturing drawing is included in Appendix D.



Figure 5.1 The manufactured stove during operation

The air used for the gasification is supplied from the bottom with help of external fan; this is to facilitate and improve the combustion process which takes place inside the chamber. It takes a while up to five minute for producer gas to be produced. This is because of the ignition build up slowly. Once the gas gets ignited, the flow of the gas is continuous and smooth.

Table 5-1 Physical observation of the stove

No	Parameter	Properties of constructed stove
1	Smoke	Insignificant; except during ignition
2	Operation	Simple
3	Fuel type	Biomass; Eucalyptus
4	Manufacturing technique	Welding, Grinding, Drilling, Cutting, Rolling, painting
5	Manufacturing materials	Mild steel
6	Accessibility	Available
7	Friendly usable	Very good

5.2. Water Boiling Test Result

The performance of the forced draft microgasifier cookstove designed and manufactured in this study was evaluated by using the ISO 19687-1:2018 guidelines; and the performance parameter for the gasifier were discussed in table 5.2.

Table 5-2 Performance result of forced draft microgasifier cookstove

No	Test Parameter	High Power Test					Average
		Test – 1	Test - 2	Test – 3	Test - 4	Test – 5	
1	Time to boil (min)	30	30	30	30	30	30.0
2	Burning rate (g/min)	9	9	8	8	10	9
3	Specific fuel consumption (g/liter)	55	57	52	54	61	56
4	Thermal efficiency (%)	42	45	48	47	41	44.7
5	Fire power (Watts)	2,680	2,824	2564	2634	2999	2740

5.2.1. Temperature of water

The temperature of the water during the five tests was shown in the Figure 5.3. As shown in the figure, all tests took 30 minute in order to complete. The temperature of the water was recorded with 1 minute gap for 30 minute. From the recorded data it was observed that, the water temperature range kept between 15.6 to 90.6°C.

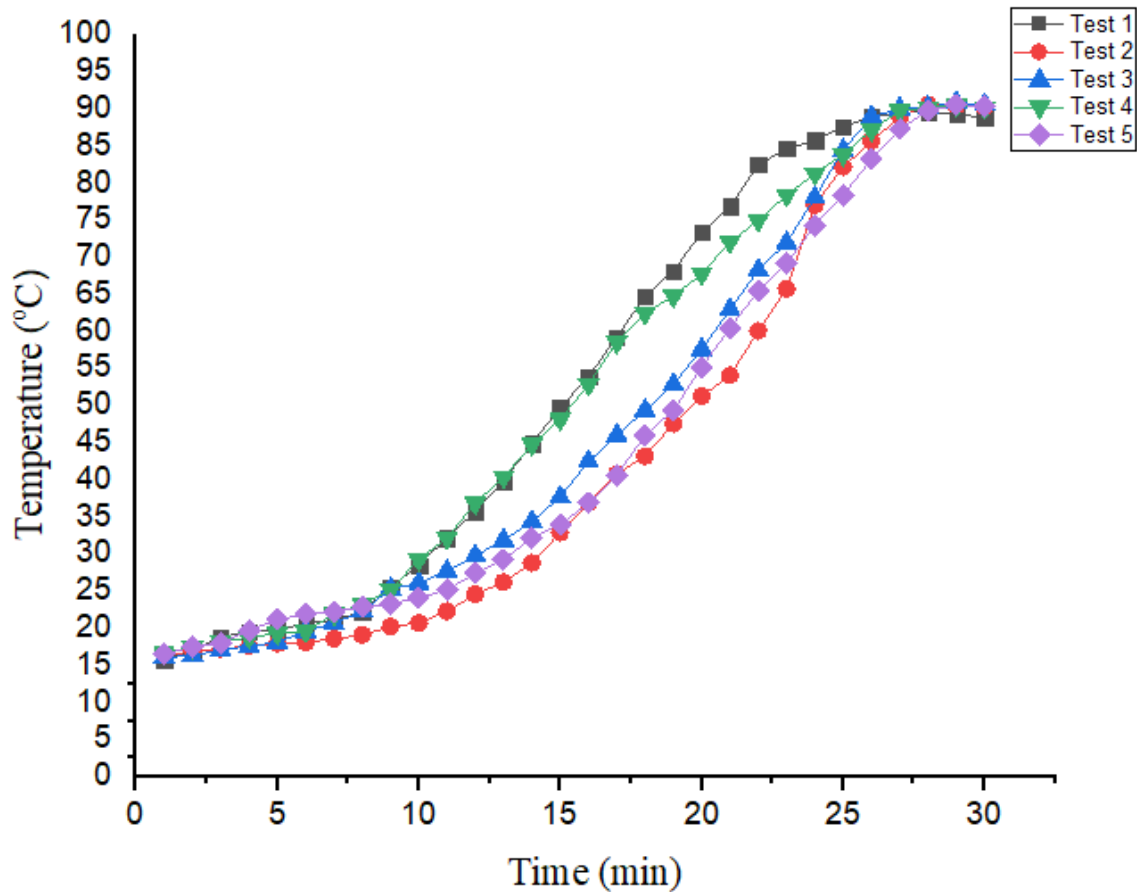


Figure 5.2 Water Temperature during WBT

5.2.2. Comparisons of different cookstoves

The average fuel required to bring 5 liter of water to boil was 730gram. There is no significant difference between the carried out tests. The amount of the ash remain after is almost negligible. The efficiency of the cookstove was determined by combustion efficiency as well as heat transfer rate to the pot bottom. The cookstove was performing at an average efficiency of 44.7%. And the average time required to boil five liter of water is 30minute. The result obtained in present study was compared with different related literatures (Table 5-3).

Table 5-3 comparisons of performance of various cookstoves

Component	Unit	Present study	Forced draft (Raman et al, 2014)	Forced draft (Raman et al, 2013)	Forced draft (Varunkumar et al, 2011)	Natural draft (Adem & Ambie, 2017)
Time to boil	Min	29.4	17.3			31.7
Fire power	Watt	2797	2535	7276		2644.7
SFC	g/liter	56	108.4	124.6		57
Thermal Efficiency	%	44.7	45	39.3	52	39.6

As seen in the table above, the thermal efficiency obtained in these studies is 44.7% which is lower than the other related literature which is 45 and 52%. This is because of in the case of both raman and varunkumar works, the commercialized stove with ceramic tile insulation was used. In the present study, the clay which is manufactured by traditional potters was used for the insulation of the combustion chamber.

5.3. CFD Analysis Result

In order to predict the performance of the developed microgasifier stove, heat and mass transfer, transport of chemical species and fluid flow simulation was studied according to setup discussed in previous chapter by using COMSOL Multiphysics. The results of the CFD analysis can be shown below with graphical display output.

5.3.1. Velocity Profile

The resulting velocity field of the gasifier stove is visualized in figure below. There is some asymmetry in the velocity profile but does not appear significant. Since we are interested in overall thermal behavior, a symmetric parabolic profile was taken to approximate the velocity profile and the simulations were performed.

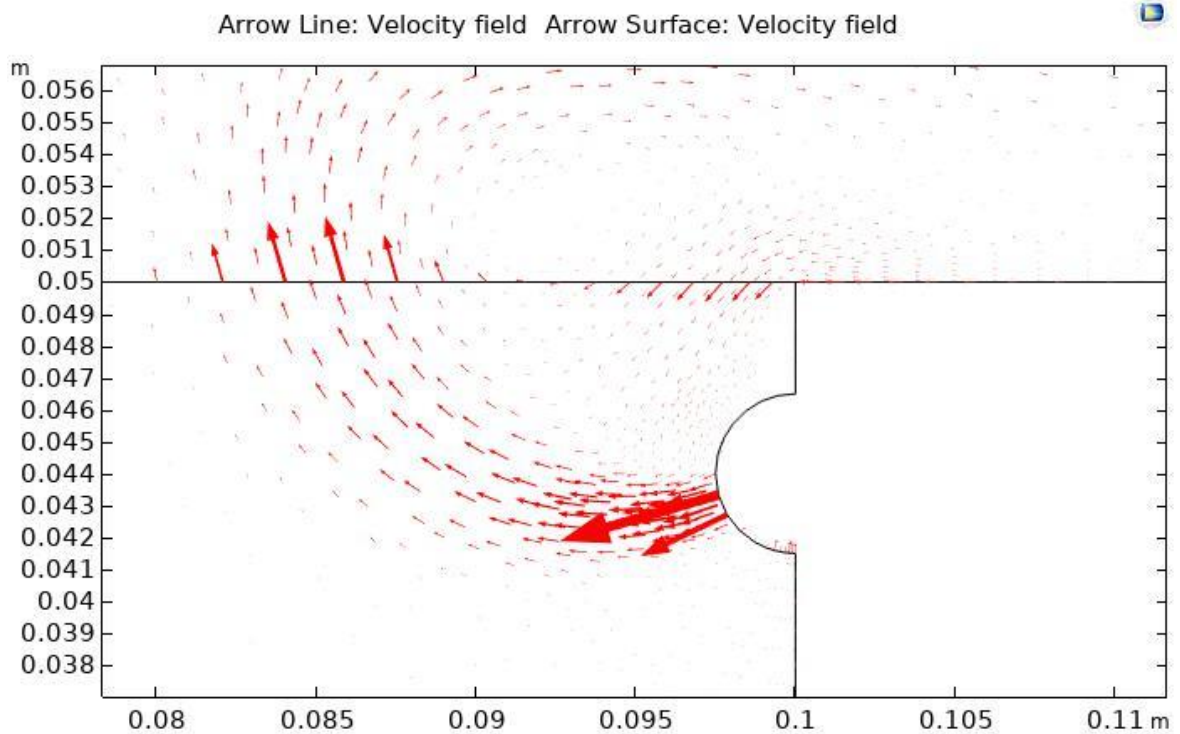
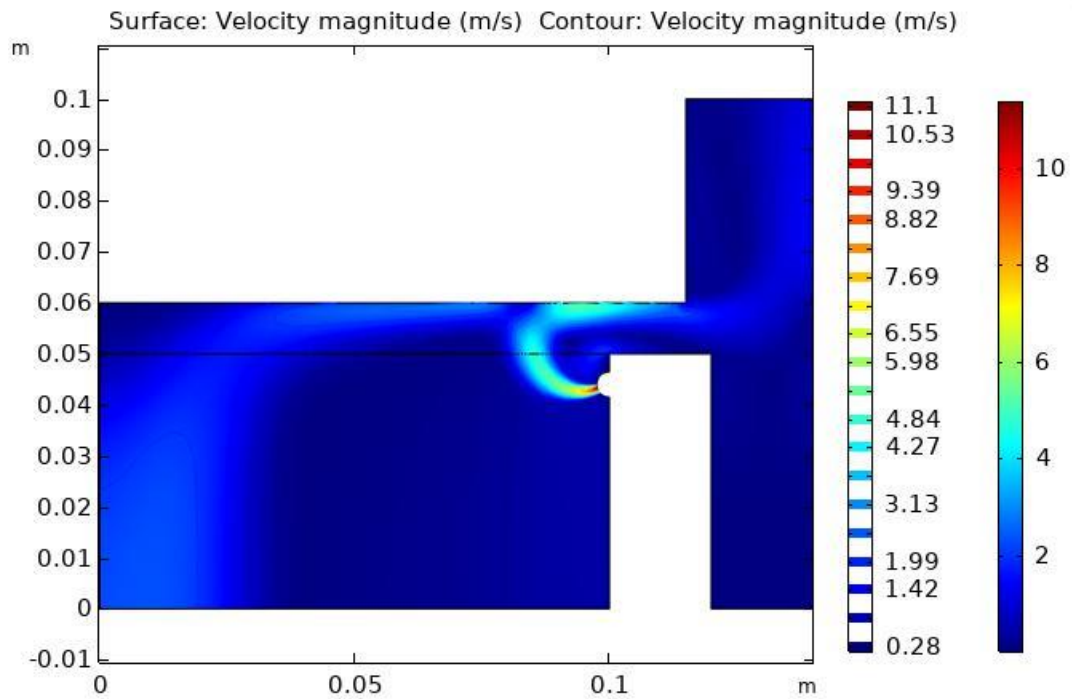


Figure 5.3 Velocity distribution

As seen in the figure, the velocity of the air flow was distributed uniformly inside the combustion chamber. At the exit of the secondary air inlet, air inlet collide with the producer gas at the upper top of the chamber. As seen in the picture, the jet is generated at the exit of the secondary air inlet and it penetrate to combustion chamber.

At the exit of the chamber, the air flow was influenced due to the presence of the surrounding air as seen in the picture.

5.3.2. Temperature Profile

As shown in the figure below, the temperature distribution in the stove varies from 900 K in the flame front to 300 K at the air inlet. Around the flame, there is a zone of cold air, which does not contribute to the combustion process but reduces the heat transfer process since they mixed with the burned gases.

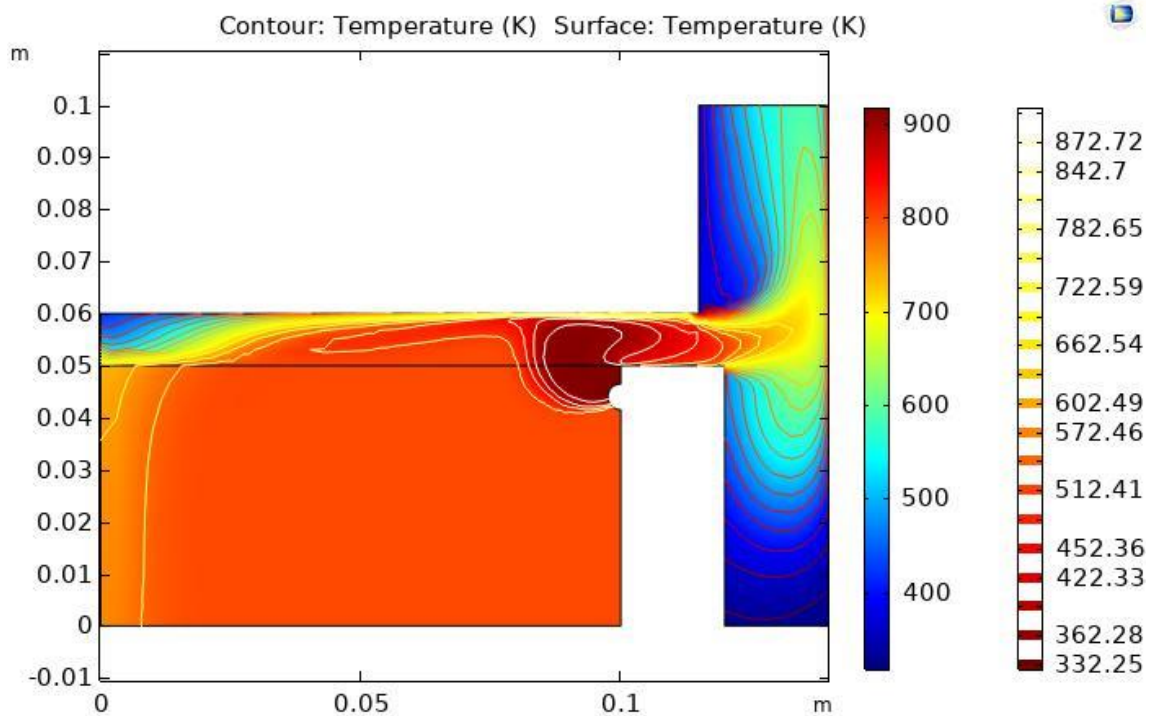


Figure 5.4 Temperature distribution

The temperature distribution inside the combustion chamber was due to uniform heat generation assumption inside the chamber. The combustion chamber was a circular chamber enclosed by the insulation clay. At the exits of the combustion chamber the temperature is the highest. High temperature is expected at the center of the combustion chamber at the center of the flame, not at the exit of the chamber. As a result, the temperature field is not a realistic approximation of the actual conditions.

5.3.3. Temperature profile of the top of the stove

The temperature profile of the top of the stove was shown in figure below and the data taken from the simulation was compared with the data taken during actual experiment.

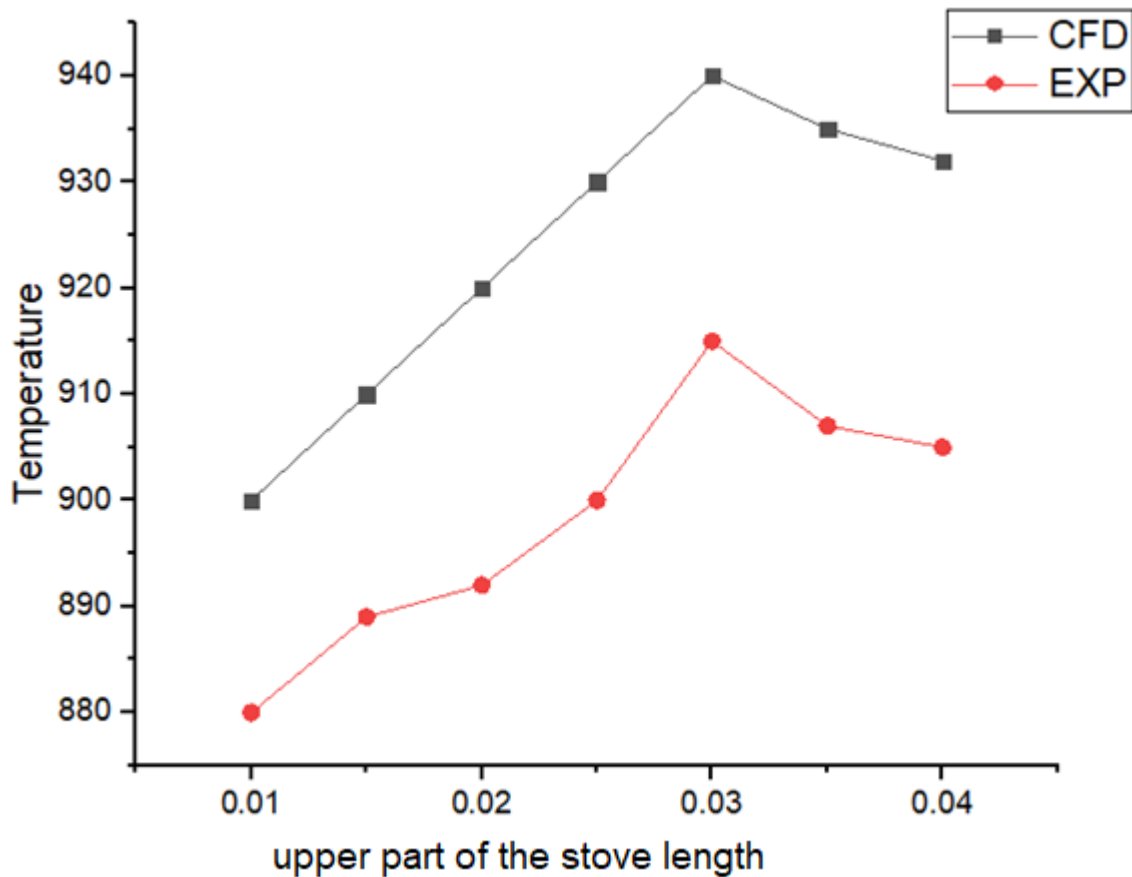


Figure 5.5 Comparison of temperature distribution at the top of the stove

As seen in the figure 5.5, the temperature of the top of the stove measured during experiment has lower value when compared to the data from the simulation and this is because of in case of actual experiment the the influence of surrounding air is significant compared to CFD as a result the maximum temperature is recorded at the center of the flame at the exit of secondary air section of the combustion chamber. Also different losses from the stove contribute to the reason of temperature value. But in case of CFD the system is assumed to be well insulated as well as constant heat generation assumption was used.

5.3.4. Effect of pot support height on thermal efficiency

The Thermal efficiency is estimated from the result of COMSOL Multiphysics based on reactive flow, heat and mass transfer and fluid flow by using equation (3.31).

To analyze the effect of pot support height to the thermal efficiency of the stove, in these study three different configurations were used. The configurations are:

- Configuration A: pot support height of 10mm
- Configuration B: pot support height of 20mm
- Configuration C: pot support height of 30mm

In order to understand the effect of the pot height on the thermal efficiency, the thermal efficiency of each configuration is calculated by using method discussed in previous chapter. Figure 5.5 below shows the wall heat flux, the height of pot support and heat transfer to the pot up to radius r as a function of radius of the pot.

In the case of configuration A, where the pot support 10mm, the heat flux transfer to the pot bottom was high. And also due to the height of the pot support was minimum the effect of surrounding air on the heat transfer process is minimum. Similarly, in case of configuration B, the height of pot support is 20mm and the affect of the surrounding air on the heat transfer process was minimum again in these configuration also. In case of configuration C, since the gap between pot and the stove's upper part was high compared to configuration A and configuration B, the surrounding air influence the process of heat transfer as shown in the figure 5.5.

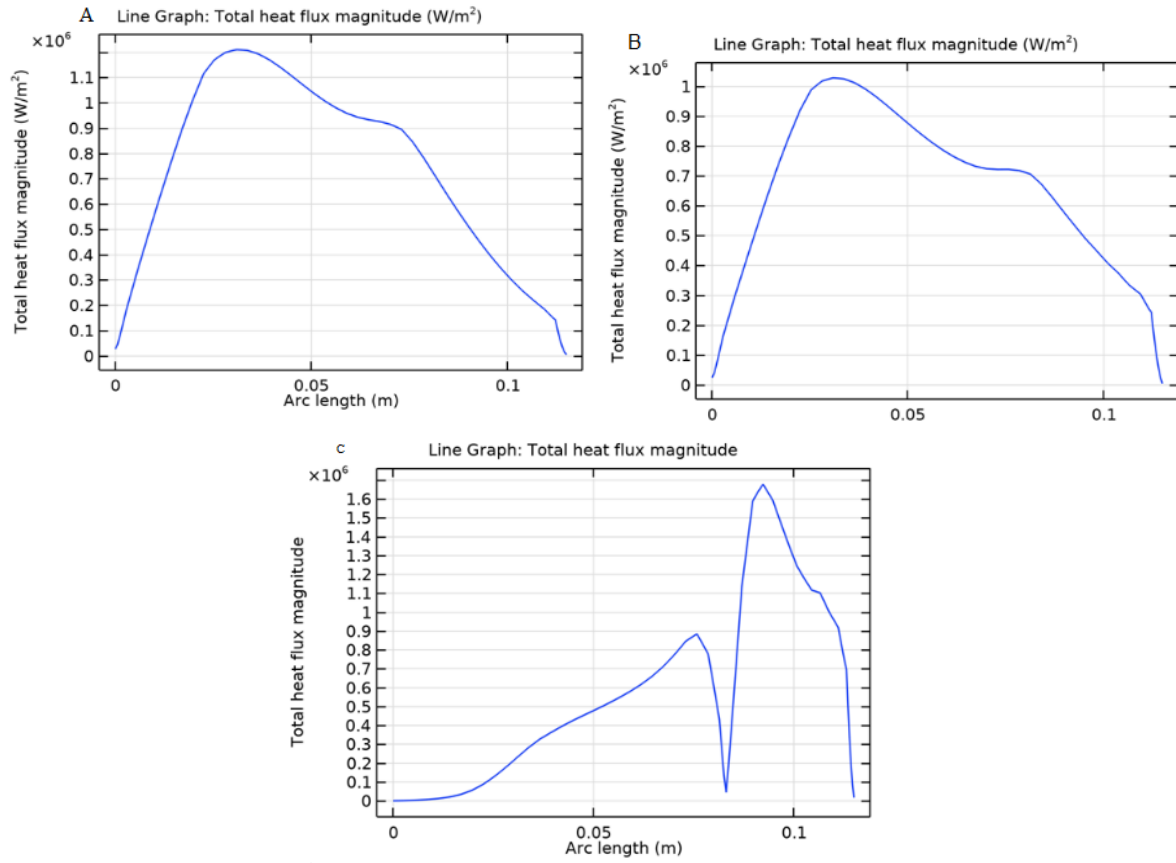


Figure 5.6 Convective heat flux of wall of pot bottom for A, B, and C configurations

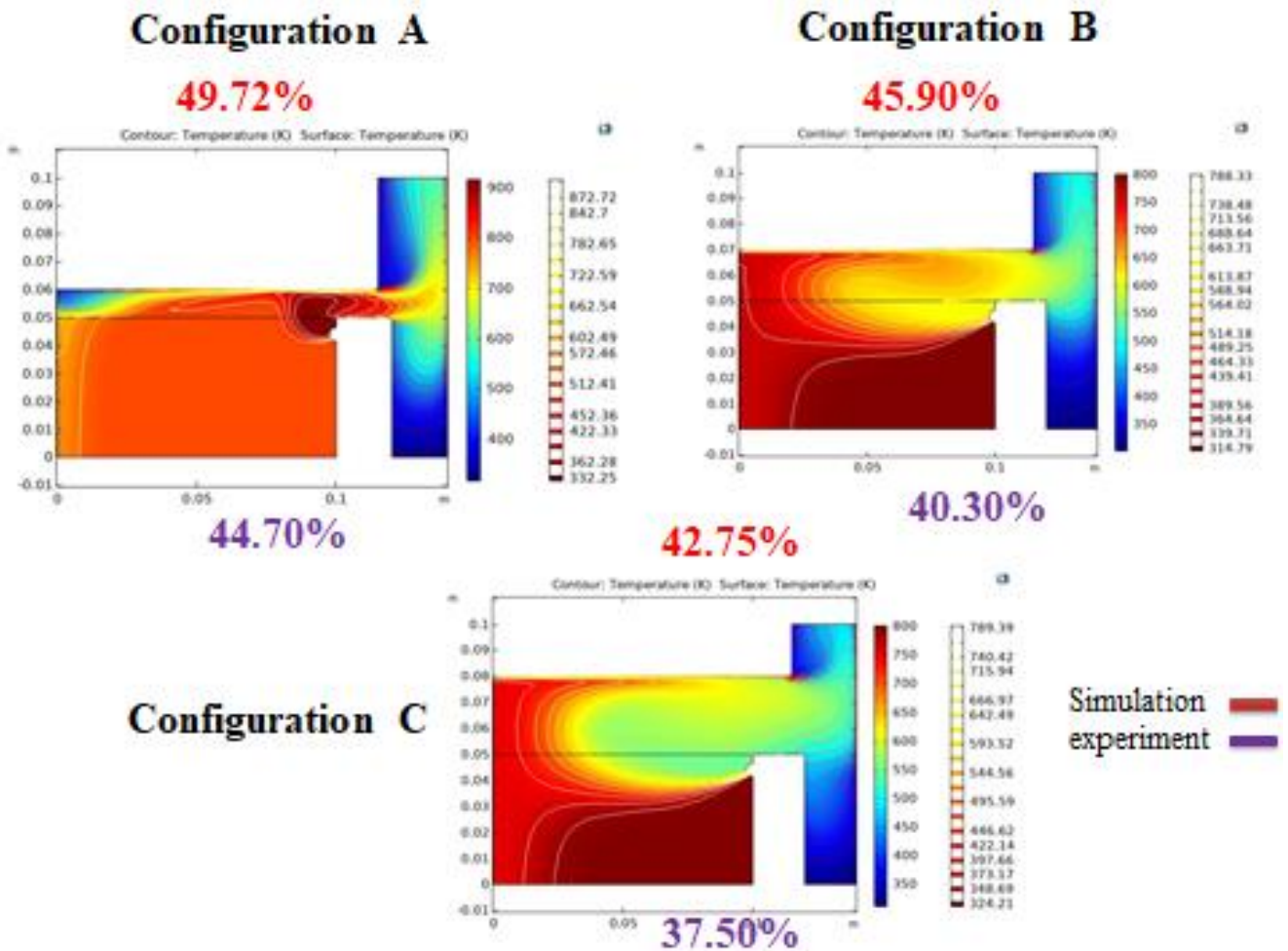


Figure 5.7 Thermal efficiency of three different pot support height

After, the heat flux magnitude is calculated by using equation (3.33), the thermal efficiency of the stove for configuration A, B, and C was computed by using equation (3.42). From the result it is shown that, configuration A has the highest thermal efficiency of 49.72% compared to 45.9% of configuration B and 42.75% of configuration C.

The experiment conducted on the developed forced draft microgasifier stove is used to calculate the thermal efficiency by using ISO 19867-1:2018. The thermal performance of the stove is compared with the predicted CFD simulation result for validation purpose.

By inserting different measured parameters to WBT 4.2.4 the average thermal efficiency obtained from experimental analysis is 44.7%, 40.3% and 37.5% for configuration A, B and C respectively.

The mismatch may arise is because in the case of simulation, the system is well insulated and unidentified losses is neglected. Also, during the simulation process also because the model in simulation is at steady-state, while the experimental procedures are not.

5.3.5. Manufacturing cost of the developed forced draft microgasifier cookstove

The developed forced draft microgasifier cookstove was made up of mild steel of 1.5mm thickness and assumed to be operated without any maintainance at least for three years. The production cost of the developed stove is discussed in the table below. These costs could be low when compared to the currently manufactured and distributed forced draft microgasifier cookstove. For wide dissemination of the developed microgasifier cookstove, awareness creation and its implication for alleviating the health related problems needed to be carried out through joint effort of different governmental organization and non governmental organization.

Table 5-4 Production cost of the developed forced draft microgasifier cookstove

No	Description	Quantity	Costs (Eth birr)
1	Mild steel sheet metal 1.85m X 0.5m X 0.0015m	1	700
2	Rectangular hollow section (RHS) 30mm X 92mm X 92mm	1	80
3	Wood for handle dia 20mm and 110mm length	2	10
4	Fan 92mm, 12V	1	100
5	Machining cost	1	250
6	Labour cost	1	500
7	Bolt with nut (for fastening fan to the stove)	4	20
8	Bolt with nut (for fastening pot support to the stove body)	3	20
			1680

The unit cost of the developed forced draft microgasifier is 1680Eth birr which is 42\$. The cost will reduce significantly in case of mass production of the stove. The cost of the current commercially available turbo stove was 55\$ as well as the cost of the forced draft microgasifier developed by raman was 50\$ (Bensaid et al, 2012; Raman et al, 2014).

CHAPTER 6

CONCLUSION AND RECOMMENDATION

6.1. Conclusion

Energy is the key that determines the progress, status, and well-being of the society of each country. And to show the progressive development of socio-economy of the each country, energy is explored, developed, distributed, and utilized efficiently and appropriately. Based on this fact, designing, simulating, manufacturing, and testing the performance have been discussed to develop the forced draft biomass microgasifier stove.

The analytical method was used for designing different parts of the gasifier and SOLIDWORK 2020 was used for modeling the geometric of the stove. The thermal performance of forced draft microgasifier stove has been implemented by using COMSOL Multiphysics and the result from the simulation is compared by using data from the conducted experiment. The simplified approach used for the simulation; is based on the 2D axis symmetry of the stove. CFD analysis is based on the combustion process fluid and heat transport in the stove. The fluid flow field shows that the producer gas rising from the combustion chamber is affected by the high momentum jet. The temperature flow inside the combustion chamber is based on the uniform heat generation assumption. The gasifier stove was manufactured from locally available materials, and ISO 19867-1:2018 guidelines were used for testing the performance of the developed stove.

Based on the result of this study the following conclusion was made:

- The temperature distribution inside the combustion chamber was due to uniform heat generation assumption.
- It found that, the developed forced draft gasifier stove operates at high thermal efficiency with lower pot support height. As the pot support height increase the efficiency of the stove decreases
- The stove is developed from locally available materials and stove emits significant smoke during operation.

- The test result gave a thermal efficiency of 44.7% and the specific fuel consumption of 56gram/liter.

6.2. Recommendation

To further improve the thermal efficiency and reduce further the emission released from the stove:

- The CFD simulation in this study was limited to only secondary combustion zone of the gasifier stove. The complex chemical kinetics which enables prediction of pollutant formation rate in detail based on the chemistry of biomass combustion process as well as description of the flow should be included. This is done by modeling the reactive flow starting with the basic biomass combustion reactions. A detail model needs high performance computers.
- The experimental test related to the emission should be carried out for the further implementation of the developed stove.

REFERENCES

Adem, Kamil Dino & Ambie, Demiss Alemu (2017) Performance and emission reduction potential of micro-gasifier improved through better design. *AIMS Energy*, 5(1), 63-76.

Adem, Kamil Dino; Ambie, Demiss Alemu; Maria, Puig Arnavat; Birk, Henriksen Ulrik; Jesper, Ahrenfeldt & Pape, Thomsen Tobias (2019) First injerabaking biomass gasifier stove to reduce indoor air pollution, and fuel use, *AIMS Energy*, 7(2), 227–245.

Adria, Oliver(CSCP) & Bethge, Jan (CSCP) (2013) *What users can save with energy-efficient cooking stoves and ovens*, 2013 Available online: http://www.bigee.net/media/filer_public/2014/03/17/appliance_residential_cookingstoves_user_savings_20140220_8.pdf [Accessed Date 28.11.2019].

Alam, Md; Hossain, Mondal; Elizabeth, Bryan; Claudia, Ringler; Dawit, Mekonnen & Mark, Rosegrant (2018) Ethiopian energy status and demand scenarios: Prospects to improve energy efficiency and mitigate GHG emissions. *sciencedirect*, energy 149, 161-172.

Alexis, Belinio T. (2005) *RICE HUSK GAS STOVE HANDBOOK*. (20.12.2019. Iloilo City, Philippines. Available online: http://bioenergylists.org/stovesdoc/Belonio/Belonio_gasifier.pdf.

Arnavat, Maria Puig (2011) *Performance Modeling and Validation of Biomass Gasifiers for Trigeneration Plant*(PhD Thesis) UNIVERSITAT ROVIRA I VIRGILI

Asranna, Anoop (2015) *Computational Modeling of a Biomass Microgasifier Cookstove*(MSc Thesis Thesis) Delft University of Technology.

Bailis, Rob ; Ogle, Damon ; MacCarty, Nordica ; Still, Dean ; Smith, Kirk R. & Edwards, Rufus (2007) *water boiling test*, 2007 Available online: https://energypedia.info/images/3/38/Wbt_version_3.0_jan2007.pdf [Accessed Date 15.12.2019].

Beiliecki, C & Wingenbach, G (2014) Rethinking improved cook stove diffusion programs: a case study of social perceptions and cooking choice in rural Guatemala, *energy policy* 8, 66-350.

Bensaid, Samir; Brignone, Mauro; Ziggiotti, Alessandro & Specchia, Stefania (2012) High efficiency Thermo-Electric power generator. *International journal of hydrogen energy*, 37(2), 1385-1398.

Beyene, Abebe D. & Koch, Steven F. (2013) Clean fuel-saving technology adoption in urban Ethiopia. *ENEECO Energy Economics*, 36, 605-613.

Bhattacharya, S. C & Leon, M. Augustus (2005) *prospect of biomass gasifiers for cooking application in asia*, 2005 Available online: <http://www.armchairpatriot.com/HardCorePrepper/Gasifier%20stove%20for%20cooking.pdf>
[Accessed Date [29.10.2019].

biofuelsacademy.org Available online: <http://www.enggcyclopedia.com/2012/01/types-gasifier/>
[Accessed Date.

Chaplin, CR (1983) Wood Burning Stoves: Material selection and thermal shock testing fired ceramic bodies, *Proc Indian Acad Sci (Eng Sci)* 6(1), 47-58.

Chaurasia, Ashish (2018) Modeling of downdraft gasification process: Studies on particle geometries in thermally thick regime. *Sciencedirect*, energy 142, 991-1009.

COMSOL (2018) *CFD Module's user manual*. (10.01.2020. Available online: www.comsol.com/cfd_user_manual.

Daniel, Ayantu (2016) "*Geometrical Optimization of Biomass Cook Stove for Efficient Utilization of Energy*" (In case of Tikikil Stove)(MSc thesis Thesis) Addis Ababa University.

De La Hoz, Keily C; Perez, J. F. & Arrieta, E. L. C. (2017) Design of a top-lit up-draft micro-gasifier biomass cookstove by thermodynamic analysis and fluent modeling. *Int. J. Renew. Energy Res. International Journal of Renewable Energy Research*, 7(4), 2172-2187.

De Lepeleire, Guido; Krishna Prasad, K.; Verhaart, P. & Visser, P. (1981) *A woodstove compendium*, Eindhoven: Technische Hogeschool Eindhoven.

De, Wan A; Green, K; Li, X & Hayden, D (2013) using social marketing tools to increase fuel-efficient stove adoption for the conservation of goldensnub-nosed monkey, , *conserv evid* 6, 10-32.

Deng, Mengsi ; Li, Pengchao; Shan, Ming & Yang, Xudong (2019) Characterizing dynamic relationships between burning rate and pollutant emission rates in a forced-draft gasifier stove consuming biomass pellet fuels. *sciencedirect*, environmental pollution 255, 113338.

ESA (2018) *2018: Clean cookstoves and clean cooking solutions*. Ethiopia: Ethiopian Standards Agency.

Febriansyah, Hermawan ; Setiawan, Ahmad Agus; Suryopratomo, Kutut & Setiawan, Agus (2014) Gama Stove: Biomass Stove for Palm Kernel Shells in Indonesia. *Sciencedirect*, Energy Procedia 47, 123-132.

Fikadu, Mamuye; Bekele, Lemma & Teshale, Woldeamanuel (2018) Emissions and fuel use performance of two improved stoves and determinants of their adoption in Dodola, southeastern Ethiopia. *sciencedirect*, sustainable environment research 28, 32-38.

Gambarotta, Agostino; Morini, Mirko & Zubani, Andrea (2018) A non-stoichiometric equilibrium model for the simulation of the biomass gasification process. *Sciencedirect*, applied energy 227.

Gao, Xiaoyan; Xu, Fei; Bao, Fubing; Tu, Chengxu ; Zhang, Yaning ; Wang, Yingying ; Yang, Yang & Li, Bingxi (2019) Simulation and optimization of rice husk gasification using intrinsic reaction rate based CFD model. *sciencedirect*, renewable energy 139, 611-620.

Gashie, Workeneh (2005) *Factors Controlling Households Energy Use: Implication for the Conservation of the Environment*. MSc Thesis) Addis Ababa University.

GIZ (2009) *GIZ_Manual_for_Production_of_Tikiki_Amharic*. Available online: https://energypedia.info/images/8/83/GIZ_Manual_for_Production_of_Tikiki_Amharic.pdf.

GIZ (2013) *Sustainable Utilization of Natural Resources for Improved Food Security: Energy, 2013* Available online: https://energypedia.info/wiki/File:Cookstove_-_Mirt_Stove_User_Manual.pdf?page=23 [Accessed Date [20.10.2019].

Gonzalez-Vazquez, M.P; García, R ; Gil, M.V ; Pevida, C & Rubiera, F (2018) Unconventional biomass fuels for steam gasification: Kinetic analysis and effect of ash composition on reactivity. *Sciencedirect*, energy155, 426-437.

GTZ (2007) *East Africa: Overview of Regional Energy Resources*. Available online: https://energypedia.info/wiki/Ethiopia:_Best_Practice_Case_Studies.

Incropera; DeWitt; Bergman & Lavine *Fundamental of Heat and Mass Transfer, six Edition*.

Jacob, NG (2013) promotion and use of improved cook stove in the conservation of biomass resources and biomass briquettes from solid waste in gambia, *science technology* 9, 17-26.

Keily De La Hoz, C.; Perez, J. F. & Arrieta, E. L. C. (2017) Design of a top-lit up-draft micro-gasifier biomass cookstove by thermodynamic analysis and fluent modeling. *Int. J. Renew. Energy Res. International Journal of Renewable Energy Research*, 7(4), 2172-2187.

Kshirsagara, Milind P & Kalamkar, Vilas R (2014) A comprehensive review on biomass cookstoves and a systematic approach for modern cookstove design. *sciencedirect, renewable and sustainable energy review*30 580-603.

Kumar, Manjor; Kumar, Sachin & Tyagi, S.K (2013) Design, development and technical advancement in biomass cookstoves: A review. *ScienceDirect, Renewable and Sustainable Energy Reviews* 26, 265-285.

Kumar, Umesh & Paul, Manosh C (2019) CFD modelling of biomass gasification with a volatile break-up approach. *Sciencedirect, chemical engineering science* 195, 413-422.

Li, Xiyan & Yin, Chungen (2019) A Drying for thermally large biomass particle pyrolysis. *Sciencedirect, Energy Procedia* 158, 1294-1302.

Lienhard IV, John H. & Lienhard V, John H. (2004) *Heat Transfer Textbook*. UK: PHLOGISTON PRESS CAMBRIDGE MASSACHUSETTS.

Luo, Hao; Lu, Zhimin; Jensen, Peter Arendt; Glarborg, Peter ; Lin, Weigang; Dam-Johansen, Kim & Wu, Hao (2020) Experimental and modelling study on the influence of wood type, density, water content, and temperature on wood devolatilization. *Sciencedirect, fuel* 260, 116410.

MacCarty, Nordica ; Ogle, Damon; Still, Dean ; Bond, Tami & Roden, Christoph (2008) A laboratory comparison of the global warming impact of five major types of biomass cooking stoves. *ScienceDirect, Energy for Sustainable Development* 12(2), 56-65.

MacCarty, Nordica A. & Bryden, Kenneth M. (2016) A generalized heat-transfer model for shielded-fire household cookstoves. *sciencedirect, Energy for Sustainable Development* 33(96-107).

Mal, Risha; Prasad, Rajendra; Vijay, Virendra Kumar; Environment, Ieee th International Conference on & Electrical, Engineering (2015) Design and testing of thermoelectric generator embedded clean forced draft biomass cookstove, 95-100.

Masera, O; Edward, R; Arnez, CA; Berrueta, V; Johnson, N & Bracho, LR (2007) Impact of patsari improved cook stove on indoor air quality in michoachan mexico, energy sustain dev 11, 45-56.

Murugan, P.C. & Sekhar, S. Joseph (2017) Species – Transport CFD model for the gasification of rice husk (*Oryza Sativa*) using downdraft gasifier. *Sciencedirect*, computers and electronics in agriculture 139, 33-40.

Park, Hoon Chae & Choi, Hang Seok (2019) Fast pyrolysis of biomass in a spouted bed reactor: Hydrodynamics, heat transfer and chemical reaction. *Sciencedirect*, renewable energy 143, 1268-1284.

Patra, Tapas Kumar & Sheth, Pratik N. (2015) Biomass gasification models for downdraft gasifier: A state-of-the-art review. *Sciencedirect*, renewable and sustainable energy reviews 50, 583-593.

Patrick, ; Wamalwa; Nyaanga, David; Owino, George (2017) Development of an Experimental Biomass Micro gasifier Cook Stove. *IOSR Journal of Mechanical and Civil Engineering (IOSR-JMCE)*, Volume 14(Issue 5 Ver. V (Sep. - Oct. 2017),), PP 06-10.

Pundle, Anamol ; Sullivan, Benjamin ; Means, Paul ; Posner, Jonathan D. & Kramlich, John C. (2019) Predicting and analyzing the performance of biomass-burning natural draft rocket cookstoves using computational fluid dynamics *Sciencedirect*, biomass and bioenergy 131, 105402.

Raman, P.; Murali, J.; Sakthivadivel, D. & Vigneswaran, V. S. (2013) Performance evaluation of three types of forced draft cook stoves using fuel wood and coconut shell. *JBB Biomass and Bioenergy*, 49, 333-340.

Raman, P.; Ram, N. K. & Gupta, R. (2014) Development, design and performance analysis of a forced draft clean combustion cookstove powered by a thermo electric generator with multi-utility options. *Energy.*, 69, 813-825.

Ravi, M.R ; Kohli, Sangeeta & Ray, Anjan (2002) Use of CFD simulation as a design tool for biomass stoves. *Sciencedirect*, energy for sustainable development VI No.2.

Reed, T. B & Larson, Ronal (1996a) A WOOD-GAS STOVE FOR DEVELOPING COUNTRIES *Developments in Thermochemical Biomass Conversion*. Banff, Canada, , 20-24 may, 1996.

Reed, T. B.; Anselmo, E. & Kirchef, K. (2001) Testing & Modeling the Wood-Gas Turbo Stove, 693-704.

Reed, T.B & Das, A (1988) Handbook of Biomass Downdraft Gasifier Engine Systems *solar energy research institute*

Reed, T_ B. & A, Das. (1988) *Handbook of Biomass Downdraft Gasifier Engine Systems* Available online: <https://www.nrel.gov/docs/legosti/old/3022.pdf>.

Reed, TB & Larson, R. (1996b) A wood-gas stove for developing countries., *Developments in thermochemical biomass conversion*. 1996 May 20–24,. Blackie Academic Press; .

Robert, B. Williams & Kaffka, Stephen (2015) *biomass gasification - DRAFT*.public interest energy research.

Roth, Christa (2011a) *micro gasification: cooking with gas from biomass*, 2011a Available online: https://energypedia.info/images/f/f6/Micro_Gasification_Cooking_with_gas_from_biomass.pdf [Accessed Date [25.10.2019].

Roth, Christa (2011b) Micro gasification: cooking with gas from biomass. *GIZ HERA Poverty-oriented Basic Energy Service*.

Safarian, Sahar; Unnpórrsson, Rúnar & Richter, Christiaan (2019) A review of biomass gasification modelling. *RSER Renewable and Sustainable Energy Reviews*, 110, 378-391.

Sansaniwal, S.K; Rosen, M.A & Tyagi, S.K (2017) Global challenges in the sustainable development of biomass gasification: An overview. *sciencedirect*, renewable and sustainable energy reviews 80, 23-43.

Series, WP (2016) *Fuel Flexible Energy Generation solid, liquid and gaseous fuels, number 91*. UK: Woodhead Publishing is an imprint of Elsevier.

Sharma, Avdhesh Kr. (2008) Equilibrium modeling of global reduction reactions for a downdraft (biomass) gasifier. *Sciencedirect*, energy conversion and management 49, 832-842.

Shiferaw, Yohannes (2011) *Design Performance Evaluation of Biomass Gasifier Stove*. (Msc. Thesis) Addis Ababa University.

SNV, Ethiopia (2018) *Review of Policies and Strategies Related to the Clean Cooking Sector in Ethiopia*. Available online: https://snv.org/cms/sites/default/files/explore/download/eth-seccs-review_of_policies_and_strategies_final_report.pdf.

Still, D ; MacCarty, N; Ogle, D; Bond, T & Bryden, M (2011) *Test results of cook stove performance*, 2011 Available online: http://s40e865f7155facb.jimcontent.com/download/version/1442346443/module/5632981862/name/Test-Results-Cookstove-Performance_1.pdf [Accessed Date 5.12.2019].

Sutar, kailasnath B; Kohlin, Sangeeta & Ravi, M.R (2017) Design, development and testing of small downdraft gasifiers for domestic cookstoves. *Sciencedirect*, Energy 124, 447-460.

Sutar, Kailasnath B; Kohlin, Sangeeta; Ravi, M.R & Ray, Anjan (2015) Biomass cookstoves: A review of technical aspects. *sciencedirect*, renewable and sustainable energy review 41, 1128-1166.

Varunkumar, S; Rajan, N.K.S & Mukunda, H.S (2011) Experimental and computational studies on a gasifier based stove. *sciencedirect*, energy conversion and management 53, 135-141.

Wanga, Xuebin; Niu, Ben ; Deng, Shuanghui; Liu, Yuanyi & Tan, Houzhang (2014) Optimization study on air distribution of an actual agriculture up-draft biomass gasification stove. *sciencedirect*, energy procedia 61, 2335-2338.

WBA (2016) *Clean and Efficient Bioenergy Cookstoves*, 2016 Available online: <https://worldbioenergy.org/uploads/Factsheet%20-%20Cookstoves.pdf> [Accessed Date 1.11.2019].

White, M. Frank (2001) *Fluid Mechanics, 4th edition*. University of Rhode Island.

Woodring, J. H. & Reed, J. C. (1996) Radiographic manifestations of lobar atelectasis. *J Thorac Imaging*, 11(2), 109-44.

Yu, Jia & Smith, Joseph D (2018) Validation and application of a kinetic model for biomass gasification simulation and optimization in updraft gasifiers. *sciencedirect*, chemical engineering & processing: process intensification 125, 214-226.

Yuntenwi, Ernestine AT; MacCarty, Nordica; Still, Dean & Ertel, Jürgen (2008) Laboratory study of the effects of moisture content on heat transfer and combustion efficiency of three biomass cook stoves. *Energy for Sustainable Development*, 12(2), 66-77.

APPENDIX A

Analytical Calculations

Calculation of finding convective heat transfer coefficient analytically

I. Calculation of determining convective heat transfer coefficient of inlet air and ambient air of zone 1.

First, let's calculate for inlet air

Known values;

$$V_{m_a} = 5\text{m/s [Mean velocity]}$$

$$L = 0.04\text{m [length at which heat transfer process takes place]}$$

$$A = 0.004\text{m [area exposed to heat transfer]}$$

$$\nu = 35.32 \times 10^{-6} \text{m}^2/\text{s [kinematic viscosity of air at 480K]}$$

Next, to identify whether the flow is laminar or turbulent, Reynolds number has to be calculated.

$$Re = \frac{V * L}{\nu} = 2831.26 \text{ [since } 2831.26 > 2300; \text{ the flow is turbulent.]}$$

Next, for turbulent flow, Nusselt number is calculated by using the following formula;

$$Nu = 1.86 \left(\frac{Re * Pr}{\frac{D}{L}} \right)^{\frac{1}{3}} \left(\frac{\mu}{\mu_s} \right)^{0.14} = 8.28 \text{ [Pr}_{@480K_air} = 0.6838 \text{ taken from (Incropera et al)}]$$

By substituting the values to the following formula we can calculate convective heat transfer coefficient of inlet air:

$$h_{air} = \frac{Nu_{D_@480K} * K_{air@480K}}{L} = 16\text{W/m}^2\text{K} \quad [K_{air@480K} = 0.0391\text{W/m}^*\text{K taken from}$$

(Incropera et al)]

For outside air of stove wall around zone 1, convective heat transfer coefficient can be calculated by using air property at mean wall temperature of zone 1 which is equal to 308K.

$$\therefore h = 9.15\text{W/m}^2\text{K}$$

II. Calculation of determining convective heat transfer coefficient of pyrolyzed gases, inlet air and ambient air of zone 2.

First, let's calculate for pyrolyzed gases:

Known values (by taking assumption of treating the pyrolyzed gas property similar to air):

$$V = 0.5\text{m/s [mean velocity]}$$

$$L = 0.04\text{m [length at which heat transfer process takes place]}$$

$$A = \Pi \frac{(d_o^2 - d_i^2)}{4} = 0.55\text{m}^2 \text{ [Area exposed to heat transfer]}$$

$$\nu = 84.93 \times 10^{-6} \text{m}^2/\text{s [kinematic viscosity of air at 800K]}$$

$$\text{Pr} = 0.709 \text{ [prandtl number, taken from (Incropera et al)]}$$

Next, to identify whether the flow is laminar or turbulent, Reynolds number has to be calculated.

$$\text{Re} = \frac{V * L}{\nu} = 235.49 \text{ [since } 235.49 > 2300; \text{ the flow is laminar.]}$$

Next, for fully developed laminar flow, Nusselt number is calculated by using the following formula;

$$\text{Nu} = 1.86 \left(\frac{\text{Re} * \text{Pr}}{D / L} \right)^{\frac{1}{3}} \left(\frac{\mu}{\mu_s} \right)^{0.14} \quad \text{Where: } D = d_o - d_i$$

Therefore; $\text{Nu} = 8.13$

By substituting the values to the following formula we can calculate convective heat transfer coefficient of inlet air:

$$h_{air} = \frac{\text{Nu}_{D @ 800K} * K_{air @ 800K}}{L} = 11.6 \text{W} / \text{m}^2 \text{K} \quad [\text{K}_{air @ 800K} = 0.0573 \text{W/m}^2 \text{K taken from}$$

(Incropera et al)]

Next, for secondary air inlet of zone 2

To identify whether the flow is laminar or turbulent, Reynolds number has to be calculated:

$$\text{Re} = \frac{V_{m-a} * L}{\nu} = 2354.9$$

As a result, since $2354.9 > 2300$; therefore the flow is turbulent

Next, for fully developed turbulent flow, the Nusselts number can be calculated by using the following formula:

$$Nu = 1.86 \left(\frac{Re * Pr}{D / L} \right)^{\frac{1}{3}} \left(\frac{\mu}{\mu_s} \right)^{0.14} = 11.2$$

Finally convective heat transfer coefficient of inlet air at zone 2 is calculated as:

$$h_{air} = \frac{Nu_{D_@500K} * K_{air@500K}}{L} = 15.2 W / m^2 K$$

For outside air of stove wall around zone 2, convective heat transfer coefficient can be calculated by using air property at mean wall temperature of zone 2 which is equal to 323K.

$$\therefore h = 7.88 W/m^2K$$

APPENDIX B

Water Boiling Test Excel Sheet (for 20mm pot support height)

B.1 Input Parameter of the WBT Excel Sheet of Test 1

WATER BOILING TEST - VERSION 4.2.4 - TEST #1

DATA AND CALCULATION FORM (for one to four pots)*

Shaded cells and arrows require user input; unshaded cells automatically display outputs

Qualitative data

Name(s) of Tester(s)	Samuel Kelbesa
Test Number	Test 1
Date	11/06/2020: morning
Location	Addis Ababa University - AAIT Workshop
Stove type/model	Forced Draft Microgasifier
Type of fuel	Eacalyptus camaldunelsis red river gum red gum

gray: efficiency
blue: emissions
pink: error, missing input

Initial Test Conditions

Data	value	units	label	Data	value	units	label
Air temperature	22.0	°C		Dry weight of Pot # 1 (grams)	427	g	P1
Wind conditions	Moderate wind			Dry weight of Pot # 2 (grams)		g	P2
Fuel dimensions	25X30X35			Dry weight of Pot # 3 (grams)		g	P3
Fuel moisture content (wet basis)	12%	%	MC	Dry weight of Pot # 4 (grams)		g	P4
Gross calorific value (dry fuel)	20,160	kJ/kg	HHV	Weight of container for char (grams)	312	g	k
Net calorific value (dry fuel)	18,840	kJ/kg	LHV	Local boiling point	90.0	°C	T _b
Effective calorific value				Background concentrations: CO ₂		ppm	CO _{2,b}
(accounting for fuel moisture)	16,274	kJ/kg	EHV	CO		ppm	CO _b
Char calorific value	29,500	kJ/kg		PM		ug/m3	PM _b

TEST #1 Test 1		COLD START HIGH POWER			
Measurements	Units	Start		Finish: when Pot #1 boils	
		data	label	data	label
Time (in 24 hour form)	hr:min	2:25	t _{ci}	2:49	t _{cf}
Weight of fuel	g	1669.8	f _{ci}	813.8	f _{cf}
Water temperature, Pot # 1	°C	19.2	T1 _{ci}	90.4	T1 _{cf}
Water temperature, Pot # 2	°C		T2 _{ci}		T2 _{cf}
Water temperature, Pot # 3	°C		T3 _{ci}		T3 _{cf}
Water temperature, Pot # 4	°C		T4 _{ci}		T4 _{cf}
Weight of Pot # 1 with water	g	5426.5	P1 _{ci}	5177	P1 _{cf}
Weight of Pot # 2 with water	g		P2 _{ci}		P2 _{cf}
Weight of Pot # 3 with water	g		P3 _{ci}		P3 _{cf}
Weight of Pot # 4 with water	g		P4 _{ci}		P4 _{cf}
Fire-starting materials (if any)	--	20			
Weight of charcoal+container	g			612	c _c
Average CO ₂	ppm				CO _{2,c}
Average CO	ppm				CO _c
Average PM	ug/m3				PM _c
Average Duct Temperature	°C				T _{cd}
Total CO ₂ (if available)	g				m _{CO_{2,c}}
Total CO (if available)	g				m _{CO,c}
Total PM (if available)	g				m _{PM,c}

B.2 Input Parameter of the WBT Excel Sheet of Test 2

WATER BOILING TEST - VERSION 4.2.4 - TEST #2

DATA AND CALCULATION FORM (for one to four pots)*

Shaded cells and arrows require user input; unshaded cells automatically display outputs

Qualitative data

Name(s) of Tester(s)	Samuel Kelbesa
Test Number	Test 2
Date	11/06/2020: Afternoon
Location	Addis Ababa University - AAJT Workshop
Stove type/model	Forced Draft Microgasifier
Type of fuel	Eacalyptus camaldunelsis red river gum red gum

gray: efficiency
blue: emissions
pink: error, missing input

Initial Test Conditions

Data	value	units	label	Data	value	units	label
Air temperature	21.4	°C		Dry weight of Pot # 1 (grams)	427	g	P1
Wind conditions	Moderate wind			Dry weight of Pot # 2 (grams)		g	P2
Fuel dimensions	30X30X35			Dry weight of Pot # 3 (grams)		g	P3
Fuel moisture content (wet basis)	13%	%	MC	Dry weight of Pot # 4 (grams)		g	P4
Gross calorific value (dry fuel)	20,160	kJ/kg	HHV	Weight of container for char (grams)	312	g	K
Net calorific value (dry fuel)	18,840	kJ/kg	LHV	Local boiling point	90.0	°C	T _b
Effective calorific value (accounting for fuel moisture)	16,017	kJ/kg	EHV	Background concentrations: CO2		ppm	CO2,b
Char calorific value	29,500	kJ/kg		CO		ppm	CO,b
				PM		ug/m3	PM,b

TEST #2 Test 2		COLD START HIGH POWER			
Measurements	Units	Start		Finish: when Pot #1 boils	
		data	label	data	label
Time (in 24 hour form)	hr:min	2:59	t _{ci}	3:28	t _{cf}
Weight of fuel	g	1960.2	f _{ci}	900.7	f _{cf}
Water temperature, Pot # 1	°C	19.5	T1 _{ci}	90.1	T1 _{cf}
Water temperature, Pot # 2	°C		T2 _{ci}		T2 _{cf}
Water temperature, Pot # 3	°C		T3 _{ci}		T3 _{cf}
Water temperature, Pot # 4	°C		T4 _{ci}		T4 _{cf}
Weight of Pot # 1 with water	g	5425.7	P1 _{ci}	5140.4	P1 _{cf}
Weight of Pot # 2 with water	g		P2 _{ci}		P2 _{cf}
Weight of Pot # 3 with water	g		P3 _{ci}		P3 _{cf}
Weight of Pot # 4 with water	g		P4 _{ci}		P4 _{cf}
Fire-starting materials (if any)	--	20			
Weight of charcoal+container	g			710	c _c
Average CO2	ppm				CO2 _c
Average CO	ppm				CO _c
Average PM	ug/m3				PM _c
Average Duct Temperature	°C				T _{cd}
Total CO2 (if available)	g				m _{CO2,c}
Total CO (if available)	g				m _{CO,c}
Total PM (if available)	g				m _{PM,c}

B.3 Input Parameter of the WBT Excel Sheet of Test 3

WATER BOILING TEST - VERSION 4.2.4 - TEST #3

DATA AND CALCULATION FORM (for one to four pots)*

Shaded cells and arrows require user input; unshaded cells automatically display outputs

Qualitative data

Name(s) of Tester(s) _____
 Test Number _____
 Date _____
 Location _____
 Stove type/model Forced Draft Microgasifier _____
 Type of fuel _____

gray: efficiency
 blue: emissions
 pink: error, missing input

Initial Test Conditions

Data	value	units	label	Data	value	units	label
Air temperature	20.2	°C		Dry weight of Pot # 1 (grams)	427	g	P1
Wind conditions	No wind			Dry weight of Pot # 2 (grams)		g	P2
Fuel dimensions	22X30X43			Dry weight of Pot # 3 (grams)		g	P3
Fuel moisture content (wet basis)	11%	%	MC	Dry weight of Pot # 4 (grams)		g	P4
Gross calorific value (dry fuel)	20,160	kJ/kg	HHV	Weight of container for char (grams)	312	g	k
Net calorific value (dry fuel)	18,840	kJ/kg	LHV	Local boiling point	90.0	°C	T _b
Effective calorific value (accounting for fuel moisture)	16,495	kJ/kg	EHV	Background concentrations: CO ₂		ppm	CO _{2,b}
Char calorific value	29,500	kJ/kg		CO		ppm	CO _b
				PM		ug/m3	PM _b

TEST #3		COLD START HIGH POWER			
Measurements	Units	Start		Finish: when Pot #1 boils	
		data	label	data	label
Time (in 24 hour form)	hr:min	9:46	t _{ci}	10:16	t _{cf}
Weight of fuel	g	2272.3	f _{ci}	1112.7	f _{cf}
Water temperature, Pot # 1	°C	17.6	T1 _{ci}	90.5	T1 _{cf}
Water temperature, Pot # 2	°C		T2 _{ci}		T2 _{cf}
Water temperature, Pot # 3	°C		T3 _{ci}		T3 _{cf}
Water temperature, Pot # 4	°C		T4 _{ci}		T4 _{cf}
Weight of Pot # 1 with water	g	5426.5	P1 _{ci}	5154	P1 _{cf}
Weight of Pot # 2 with water	g		P2 _{ci}		P2 _{cf}
Weight of Pot # 3 with water	g		P3 _{ci}		P3 _{cf}
Weight of Pot # 4 with water	g		P4 _{ci}		P4 _{cf}
Fire-starting materials (if any)	—	20			
Weight of charcoal+container	g			789	c _c
Average CO ₂	ppm				CO _{2,c}
Average CO	ppm				CO _c
Average PM	ug/m3				PM _c
Average Duct Temperature	°C				T _{cd}
Total CO ₂ (if available)	g				m _{CO_{2,c}}
Total CO (if available)	g				m _{CO,c}
Total PM (if available)	g				m _{PM,c}

B.4 Input Parameter of the WBT Excel Sheet of Test 4

WATER BOILING TEST - VERSION 4.2.4 - TEST #4

DATA AND CALCULATION FORM (for one to four pots)*

Shaded cells and arrows require user input; unshaded cells automatically display outputs

Qualitative data

Name(s) of Tester(s)	
Test Number	
Date	
Location	Addis Ababa University - AAIT Workshop
Stove type/model	Forced Draft Microgasifier
Type of fuel	

gray: efficiency
blue: emissions
pink: error, missing input

Initial Test Conditions

Data	value	units	label	Data	value	units	label
Air temperature	18.1	°C		Dry weight of Pot # 1 (grams)	332	g	P1
Wind conditions	(Select from list)			Dry weight of Pot # 2 (grams)		g	P2
Fuel dimensions	20X20X20			Dry weight of Pot # 3 (grams)		g	P3
Fuel moisture content (wet basis)	13%	%	MC	Dry weight of Pot # 4 (grams)		g	P4
Gross calorific value (dry fuel)	20,160	kJ/kg	HHV	Weight of container for char (grams)	423	g	k
Net calorific value (dry fuel)	18,840	kJ/kg	LHV	Local boiling point	90.0	°C	T _b
Effective calorific value				Background concentrations: CO2		ppm	CO2,b
(accounting for fuel moisture)	16,058	kJ/kg	EHV	CO		ppm	CO,b
Char calorific value	29,500	kJ/kg		PM		ug/m3	PM,b

TEST #4		COLD START HIGH POWER			
Measurements	Units	Start		Finish: when Pot #1 boils	
		data	label	data	label
		Time (in 24 hour form)	hr:min	5:19	t _{ci}
Weight of fuel	g	1722.5	f _{ci}	1050	f _{cf}
Water temperature, Pot # 1	°C	16.1	T1 _{ci}	90.9	T1 _{cf}
Water temperature, Pot # 2	°C		T2 _{ci}		T2 _{cf}
Water temperature, Pot # 3	°C		T3 _{ci}		T3 _{cf}
Water temperature, Pot # 4	°C		T4 _{ci}		T4 _{cf}
Weight of Pot # 1 with water	g	5331.7	P1 _{ci}	4933	P1 _{cf}
Weight of Pot # 2 with water	g		P2 _{ci}		P2 _{cf}
Weight of Pot # 3 with water	g		P3 _{ci}		P3 _{cf}
Weight of Pot # 4 with water	g		P4 _{ci}		P4 _{cf}
Fire-starting materials (if any)	--				
Weight of charcoal+container	g			580	c _c
Average CO2	ppm				CO2 _c
Average CO	ppm				CO _c
Average PM	ug/m3				PM _c
Average Duct Temperature	°C				T _{cd}
Total CO2 (if available)	g				m _{CO2,c}
Total CO (if available)	g				m _{CO,c}
Total PM (if available)	g				m _{PM,c}

B.5 Input Parameter of the WBT Excel Sheet of Test 5

WATER BOILING TEST - VERSION 4.2.4 - TEST #5

DATA AND CALCULATION FORM (for one to four pots)*

Shaded cells and arrows require user input; unshaded cells automatically display outputs

Qualitative data

Name(s) of Tester(s)	
Test Number	
Date	
Location	Addis Ababa University - AAIT Workshop
Stove type/model	Forced Draft Microgasifier
Type of fuel	

gray: efficiency
blue: emissions
pink: error, missing input

Initial Test Conditions

Data	value	units	label	Data	value	units	label
Air temperature	20.3	°C		Dry weight of Pot # 1 (grams)	325	g	P1
Wind conditions	No wind			Dry weight of Pot # 2 (grams)		g	P2
Fuel dimensions	30X30X30			Dry weight of Pot # 3 (grams)		g	P3
Fuel moisture content (wet basis)	10%	%	MC	Dry weight of Pot # 4 (grams)		g	P4
Gross calorific value (dry fuel)	20,160	kJ/kg	HHV	Weight of container for char (grams)	418	g	k
Net calorific value (dry fuel)	18,840	kJ/kg	LHV	Local boiling point	90.0	°C	T _b
Effective calorific value				Background concentrations: CO2		ppm	CO2,b
(accounting for fuel moisture)	16,701	kJ/kg	EHV	CO		ppm	CO,b
Char calorific value	29,500	kJ/kg		PM		ug/m3	PM,b

TEST #5		COLD START HIGH POWER			
Measurements	Units	Start		Finish: when Pot #1 boils	
		data	label	data	label
Time (in 24 hour form)	hr:min	2:27	t _{ci}	3:57	t _{cf}
Weight of fuel	g	2287	f _{ci}	1287	f _{cf}
Water temperature, Pot # 1	°C	16.9	T1 _{ci}	90.6	T1 _{cf}
Water temperature, Pot # 2	°C		T2 _{ci}		T2 _{cf}
Water temperature, Pot # 3	°C		T3 _{ci}		T3 _{cf}
Water temperature, Pot # 4	°C		T4 _{ci}		T4 _{cf}
Weight of Pot # 1 with water	g	5325	P1 _{ci}	4990	P1 _{cf}
Weight of Pot # 2 with water	g		P2 _{ci}		P2 _{cf}
Weight of Pot # 3 with water	g		P3 _{ci}		P3 _{cf}
Weight of Pot # 4 with water	g		P4 _{ci}		P4 _{cf}
Fire-starting materials (if any)	--	10			
Weight of charcoal+container	g			785	c _c
Average CO2	ppm				CO2 _c
Average CO	ppm				CO _c
Average PM	ug/m3				PM _c
Average Duct Temperature	°C				T _{cd}
Total CO2 (if available)	g				m _{CO2,c}
Total CO (if available)	g				m _{CO,c}
Total PM (if available)	g				m _{PM,c}

B.6 Result From Water Boiling Test

WATER BOILING TEST - VERSION 4.2.4

TEST

All cells are linked to data worksheets, no entries are required

Stove type/model Forced Draft Microgasifier
 Location Addis Ababa University - AAIT Workshop
 Fuel description Eucalyptus Camaldulensis (Red River Gum, Red Gum)
 Wind conditions #REF!
 Ambient temperature #REF!

1. HIGH POWER TEST (COLD START)

units	Test 1	Test 2	Test 3	Test 4	Test 5	Test 6	Test 7	Test 8	Test 9	Test 10	Average	St Dev	COV
Time to boil Pot # 1	min	24	29	30	30	90	-	-	-	-	40.6	-	
Temp-corrected time to boil Pot # 1	min	25	31	31	30	92	-	-	-	-	42	-	
Burning rate	g/min	11	10	9	11	3					9		
Thermal efficiency	%	40%	41%	42%	40%	39%					0.4049104		
Specific fuel consumption	g/liter	57	59	56	70	66					62		
Temp-corrected specific consumption	g/liter	60	63	58	71	68					64		
Temp-corrected specific energy cons.	kJ/liter	1,128	1,180	1,102	1,341	1,282					1206		
Firepower	watts	3,532	3,009	2,813	3,418	1,088					2772.0025		

2. HIGH POWER TEST (HOT START)

units	Test 1	Test 2	Test 3	Test 4	Test 5	Test 6	Test 7	Test 8	Test 9	Test 10	Average	St Dev	COV
Time to boil Pot # 1	min	-	-	-	-	-	-	-	-	-			
Temp-corrected time to boil Pot # 1	min	-	-	-	-	-	-	-	-	-			
Burning rate	g/min												
Thermal efficiency	%												
Specific fuel consumption	g/liter												
Temp-corrected specific consumption	g/liter												
Temp-corrected specific energy cons.	kJ/liter												
Firepower	watts												

3. LOW POWER (SIMMER)

units	Test 1	Test 2	Test 3	Test 4	Test 5	Test 6	Test 7	Test 8	Test 9	Test 10	Average	St Dev	COV
Burning rate	g/min												
Thermal efficiency	%												
Specific fuel consumption	g/liter	(2,247)	(2,607)	(2,897)	(2,740)	(3,782)							
Temp-corrected specific energy cons.	kJ/liter	(42,331)	(49,109)	(54,573)	(51,614)	(71,254)							
Firepower	watts												
Turn down ratio	-												

BENCHMARK VALUES (for 5L)

	Test 1	Test 2	Test 3	Test 4	Test 5	Test 6	Test 7	Test 8	Test 9	Test 10	Average	St Dev	COV
Fuel Use Benchmark Value	g	(10,935)	(12,720)	(14,191)	(13,342)	(18,570)							
Energy Use Benchmark Value	kJ	#####	#####	#####	#####	#####							
Carbon Monoxide Benchmark Value	g												
Particulate Matter Benchmark Value	g												

IWA PERFORMANCE METRICS

units	Test 1	Test 2	Test 3	Test 4	Test 5	Test 6	Test 7	Test 8	Test 9	Test 10	Average	St Dev	COV
High Power Thermal Efficiency	%	40.4%	40.5%	42.3%	40.1%	39.1%					0.4049104		
Low Power Specific Fuel Consumption	MJ/(min-L)												
High Power CO	g/MJ												
Low Power CO	g/(min-L)												
High Power PM	mg/MJ												
Low Power PM	mg/(min-L)												
Indoor CO Emissions	g/min												
Indoor PM Emissions	mg/min												

IWA PERFORMANCE TIERS

	Tier
High Power Thermal Efficiency	3
Low Power Specific Fuel Consumption	NA
High Power CO	NA
Low Power CO	NA
High Power PM	NA
Low Power PM	NA
Indoor CO Emissions	NA
Indoor PM Emissions	NA

APPENDIX C

COMSOL Design Parameter

Table C.1 COMSOL Multiphysics design parameters based on the procedure adapted from
(COMSOL, 2018; Klayborworn & Pakdee, 2019)

Name	Expression	Unit	Value	Description
D _i	5	[mm]	0.005 m	secondary air inlet hole diameter
P _l	D _i *4	[m]	0.02 m	secondary air inlet hole length
U _{jet}	5	[m/s]	5 m/s	secondary air inlet velocity
U _{cf}	0.7	[m/s]	0.7 m/s	gas velocity
T ₀	900	[K]	900 K	gas temperature
x _{0_CO}	0.3	-	0.3	Inlet volume fraction CO
x _{0_O2}	0	-	0	Inlet volume fraction O2
x _{0_CO2}	0	-	0	Inlet volume fraction CO2
x _{0_H2}	0.2	-	0.2	Inlet volume fraction H2
x _{0_H2O}	0	-	0	Inlet volume fraction H2O
x _{0_N2}	0.5	-	0.5	Inlet volume fraction N2
wcf_O2	0.21	-	0.21	mass fraction O2 of secondary air
mu_mix	0.00001	[Pa*s]	1E-5 Pa·s	Dynamic viscosity, mixture
k_mix	0.1	[W/m/K]	0.1 W/(m·K)	Thermal conductivity, mixture
M_CO	28	[g/mol]	28g/mol	Molar mass CO
M_O2	32	[g/mol]	32g/mol	Molar mass O2
M_CO2	44	[g/mol]	44g/mol	Molar mass CO2
M_H2	2	[g/mol]	2g/mol	Molar mass H2
M_H2O	18	[g/mol]	18g/mol	Molar mass H2O
M_N2	28	[g/mol]	28g/mol	Molar mass N2
dH_CO	-26.42	[kcal/mol]	-26.42kcal/mol	Standard enthalpy of formation CO
dH_CO2	-94.061	[kcal/mol]	-94.061kcal/mol	Standard enthalpy of formation CO2
dH_H2	0	[kcal/mol]	0	Standard enthalpy of formation H2
dH_H2O	-57.8	[kcal/mol]	-57.8kcal/mol	Standard enthalpy of formation H2O
dH_N2	0	[kcal/mol]	0	Standard enthalpy of formation N2
dH_O2	0	[kcal/mol]		Standard enthalpy of formation O2

APPENDIX D
Manufacturing Drawing

4

A

3

2

1

F

F

E

E

D

D

C

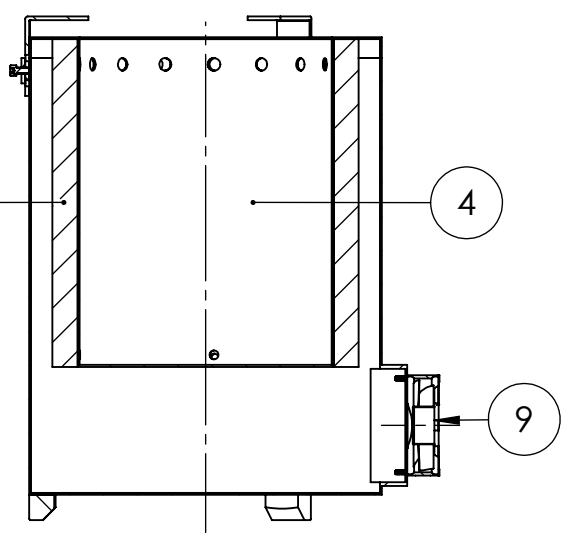
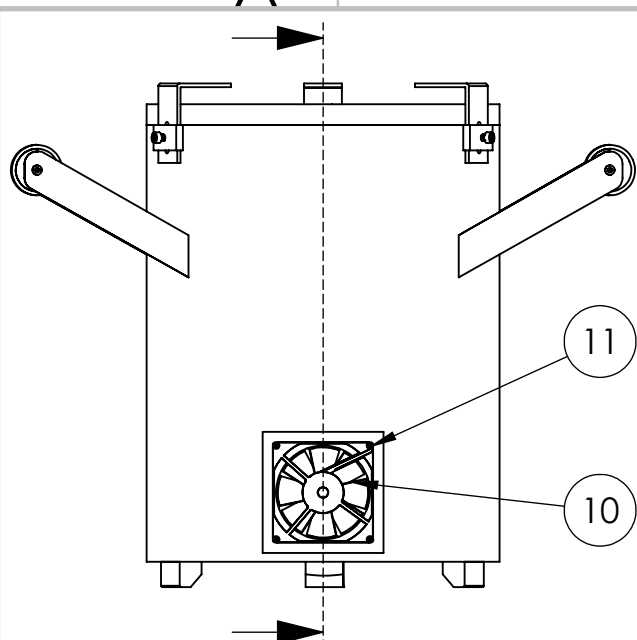
C

B

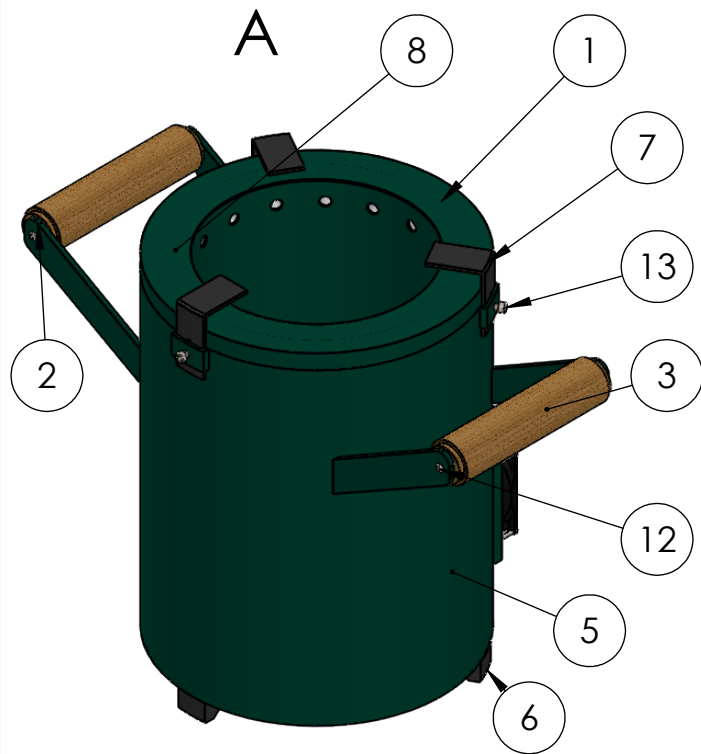
B

A

A



SECTION A-A



ITEM NO.	PART NUMBER	QTY.
1	Ckay insulator	1
2	Handling_S&W_05	2
3	Handling_S&W_05.1	2
4	Inner_cylinder	1
5	Outer_cylinder	1
6	Support_Leg	1
7	Top_Support	3
8	Upper_Cover	1
9	Housing	1
10	Propeller	1
11	B18.3.5M - 3 x 0.5 x 35 Socket FCHS -- 18S	4
12	B18.3.4M - 4 x 0.7 x 16 SBHCS --N	4
13	B18.3.1M - 5 x 0.8 x 10 Hex SHCS -- 10SHX	4

DESIGNED BY: Samuel Kelbesa
DATE: March 2020

CHECKED BY: Kamil D. Adem(PhD)
DATE: March 2020

DRAWN BY: Samuel Kelbesa
DATE: March 2020

ADDIS ABABA UNIVERSITY
ADDIS ABABA INSTITUTE OF TECHNOLOGY
SMiE THERMAL ENGINEERING

Assembly of FDM

SIZE A4 all DIMENSION is in mm
SCALE:1:4 MATERIAL: WEIGHT:

DRAWING NO. FDM001/2020

SHEET 1

QTY:1

4

3

2

1

4

3

2

1

F

F

E

E

D

D

C

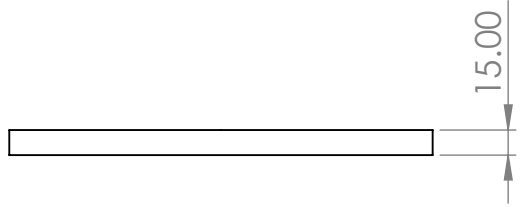
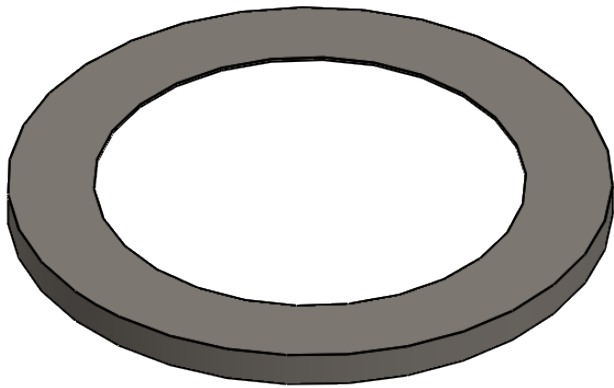
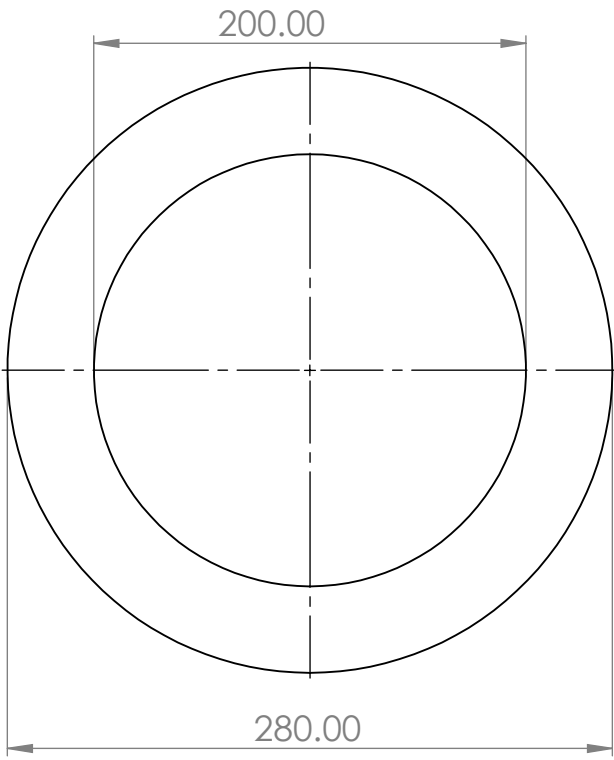
C

B

B

A

A



DESIGNED BY: Samuel Kelbesa
DATE: March 2020

CHECKED BY: Kamil D. Adem(PhD)
DATE: March 2020

DRAWN BY: Samuel Kelbesa
DATE: March 2020

ADDIS ABABA UNIVERSITY
ADDIS ABABA INSTITUTE OF TECHNOLOGY
SMiE THERMAL ENGINEERING

Upper_Cover

SIZE A4		all DIMENSION is in mm
SCALE:1:4	MATERIAL:	WEIGHT:

DRAWING NO. FDM005/2020

SHEET 5

QTY:1

H
G
F
E
D
C
B
A

4

3

2

1

90

4

3

2

1

F

F

E

E

D

D

C

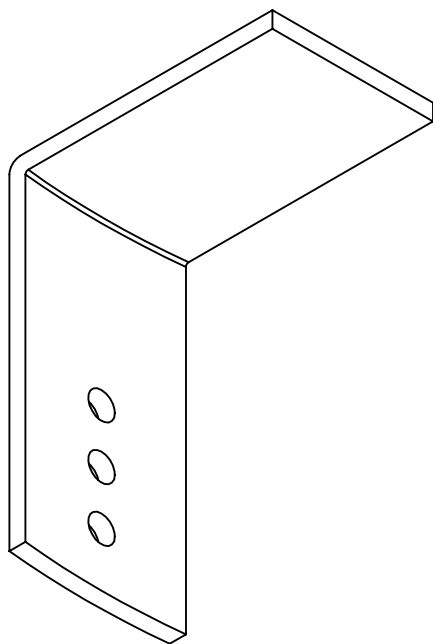
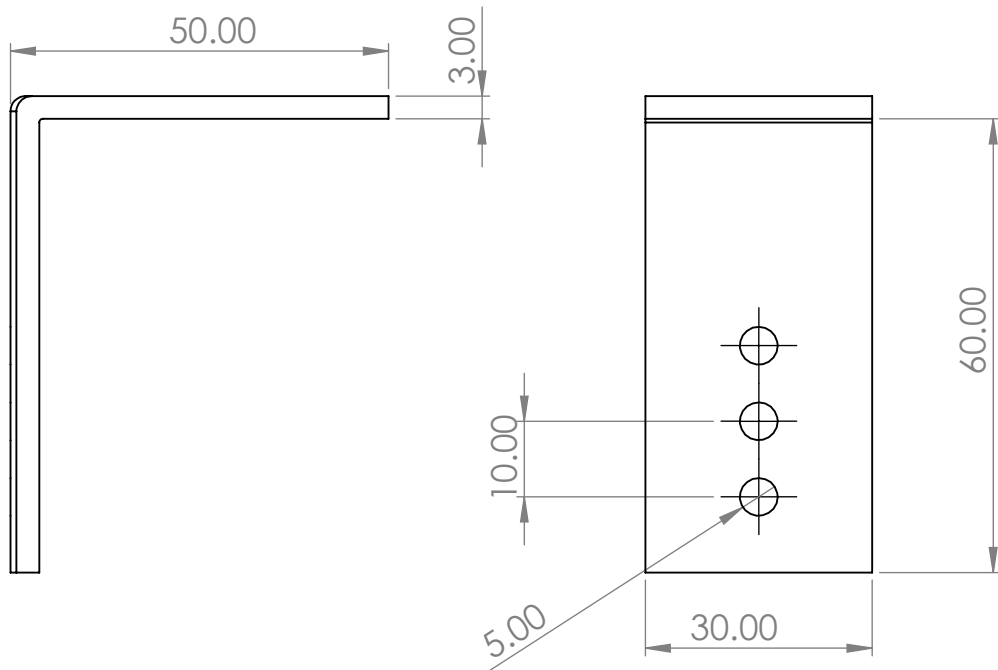
C

B

B

A

A



DESIGNED BY: Samuel Kelbesa
 DATE: March 2020

CHECKED BY: Kamil D. Adem(PhD)
 DATE: March 2020

DRAWN BY: Samuel Kelbesa
 DATE: March 2020

SIZE A4
 SCALE:1:4 MATERIAL: WEIGHT:

ADDIS ABABA UNIVERSITY
ADDIS ABABA INSTITUTE OF TECHNOLOGY
SMiE THERMAL ENGINEERING

Top_Support

DRAWING NO. FDM009/2020 SHEET 9 QTY:1

H
G
F
E
D
C
B
A

4

3

2

1

4

3

2

1

F

F

E

E

D

D

C

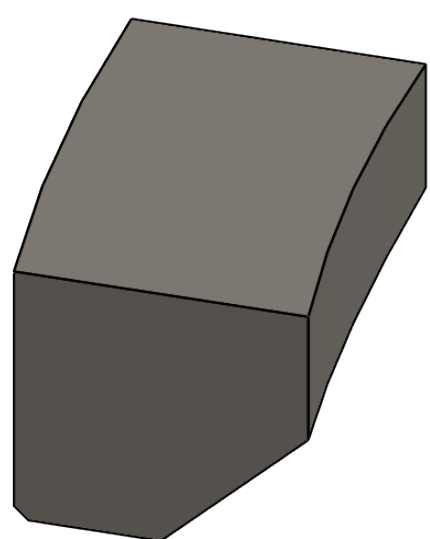
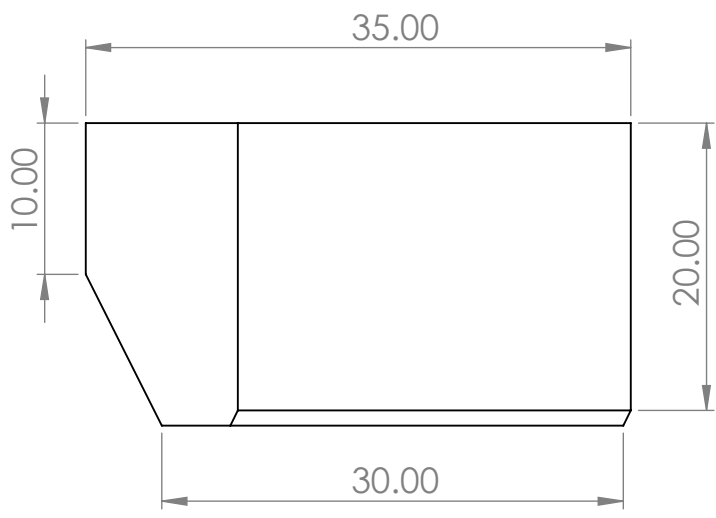
C


B

B

A

A



DESIGNED BY: Samuel Kelbesa DATE: March 2020		ADDIS ABABA UNIVERSITY ADDIS ABABA INSTITUTE OF TECHNOLOGY SMiE THERMAL ENGINEERING		
CHECKED BY: Kamil D. Adem(PhD) DATE: March 2020				H
DRAWN BY: Samuel Kelbesa DATE: March 2020		Supporting_Leg		G
SIZE A4		all DIMENSION is in mm	DRAWING NO. FDM008/2020	F
SCALE:1:0.5	MATERIAL:	WEIGHT:	SHEET 8	E
			QTY:1	D
				C
				B
				A

4

3

2

1

4

3

2

1

F

F

E

E

D

D

C

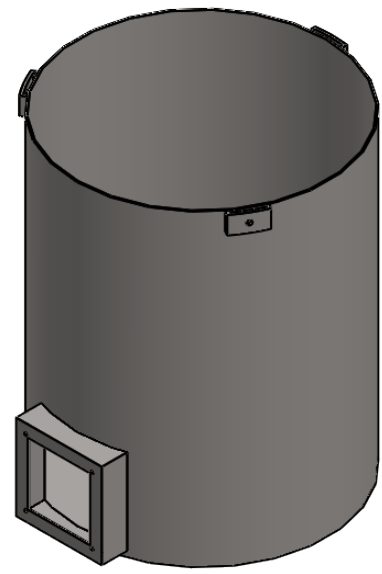
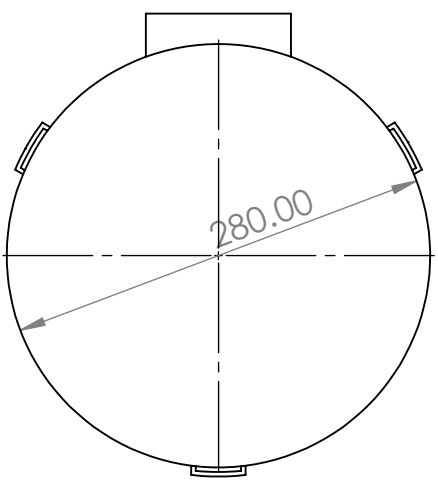
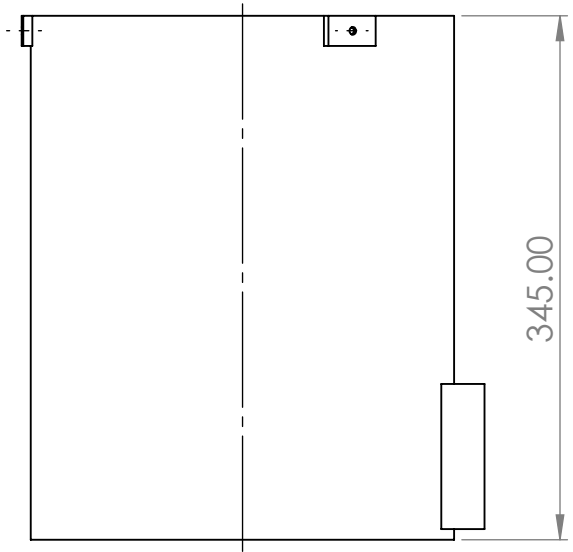
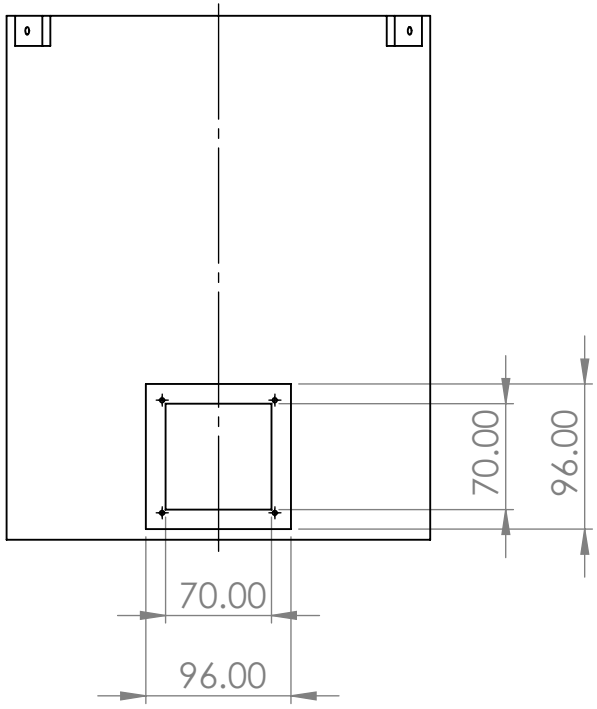
C

B

B

A

A



DESIGNED BY: Samuel Kelbesa
DATE: March 2020

CHECKED BY: Kamil D. Adem(PhD)
DATE: March 2020

DRAWN BY: Samuel Kelbesa
DATE: March 2020

SIZE A4
SCALE:1:4 MATERIAL: WEIGHT:

ADDIS ABABA UNIVERSITY
ADDIS ABABA INSTITUTE OF TECHNOLOGY
SMiE THERMAL ENGINEERING

Outer_Cylinder

DRAWING NO. FDM002/2020

SHEET 2

QTY:1

H
G
F
E
D
C
B
A

4

3

2

1

4

3

2

1

F

F

E

E

D

D

C

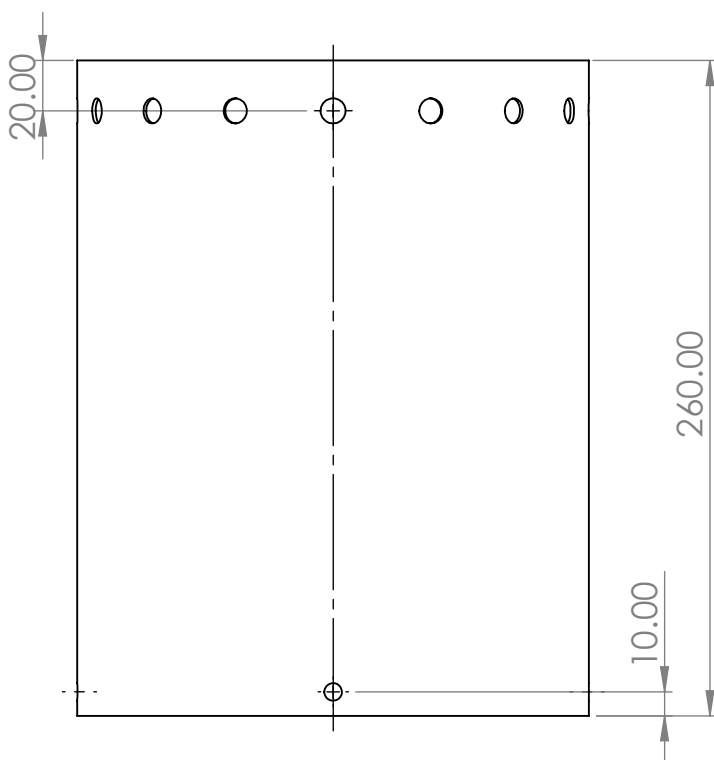
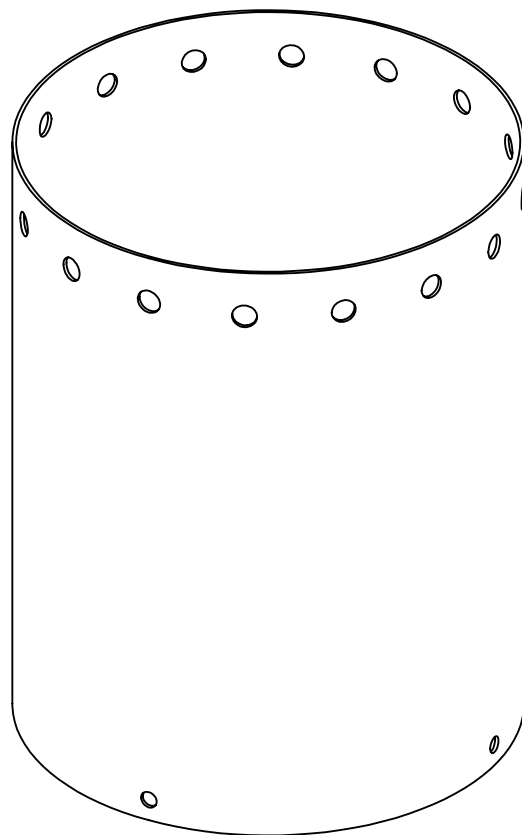
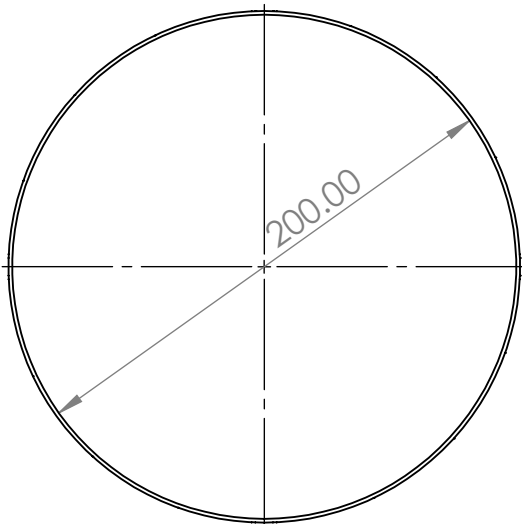
C

B

B

A

A




DESIGNED BY: Samuel Kelbesa
 DATE: March 2020

CHECKED BY: Kamil D. Adem(PhD)
 DATE: March 2020

DRAWN BY: Samuel Kelbesa
 DATE: March 2020

ADDIS ABABA UNIVERSITY
ADDIS ABABA INSTITUTE OF TECHNOLOGY
SMiE THERMAL ENGINEERING

Inner_Cylinder

SIZE A4		all DIMENSION is in mm
SCALE:1:4	MATERIAL:	WEIGHT:

DRAWING NO. FDM003/2020

SHEET3

QTY:1

H
G
F
E
D
C
B
A

4

3

2

1

4

3

2

1

F

F

E

E

D

D

C

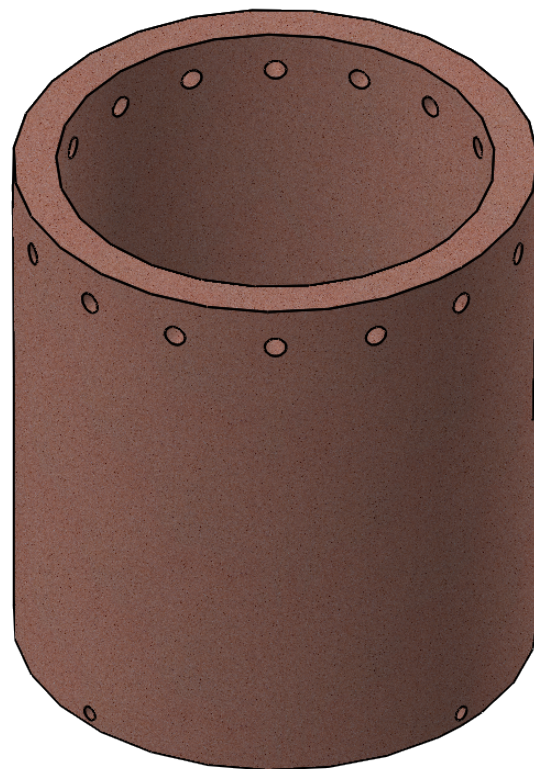
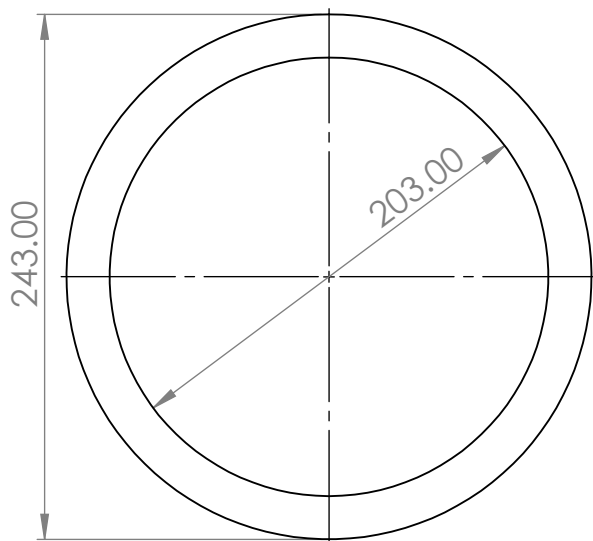
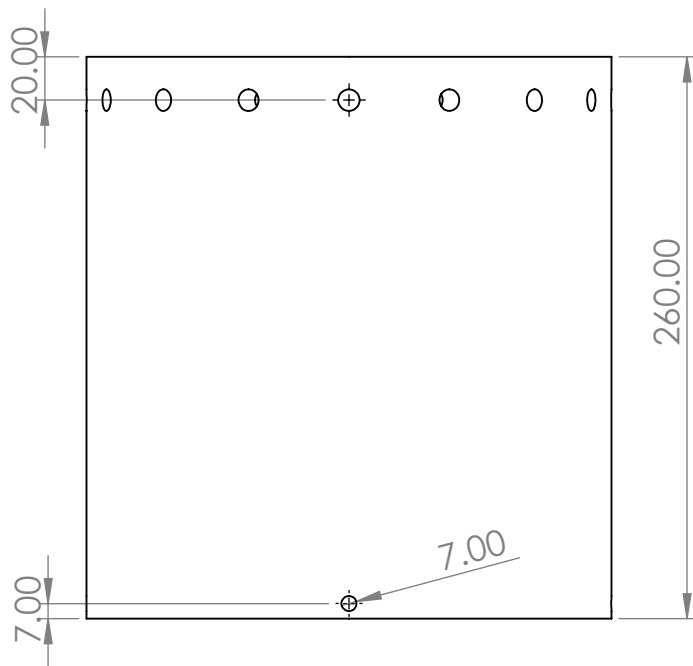
C

B

B

A

A



DESIGNED BY: Samuel Kelbesa
DATE: March 2020

CHECKED BY: Kamil D. Adem(PhD)
DATE: March 2020

DRAWN BY: Samuel Kelbesa
DATE: March 2020

SIZE A4		all DIMENSION is in mm
SCALE:1:4	MATERIAL:	WEIGHT:

ADDIS ABABA UNIVERSITY
ADDIS ABABA INSTITUTE OF TECHNOLOGY
SMiE THERMAL ENGINEERING

Insulator_Clay

DRAWING NO. FDM004/2020

SHEET 4

QTY:1

H
G
F
E
D
C
B
A

4

3

2

1

4

3

2

1

F

F

E

E

D

D

C

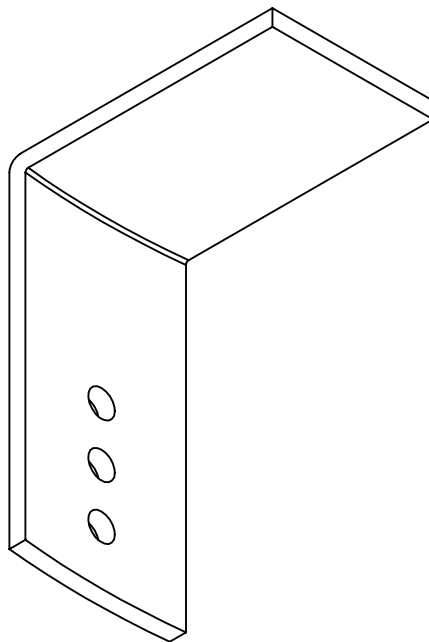
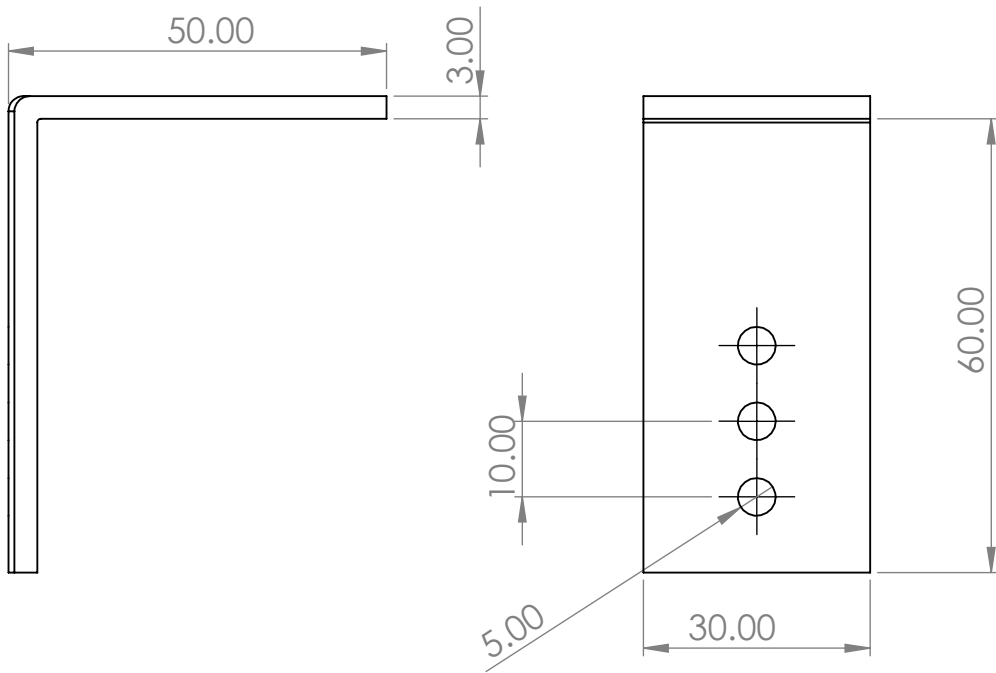
C

B

B

A

A



DESIGNED BY: Samuel Kelbesa
 DATE: March 2020

CHECKED BY: Kamil D. Adem(PhD)
 DATE: March 2020

DRAWN BY: Samuel Kelbesa
 DATE: March 2020

SIZE A4
 SCALE:1:4 MATERIAL: WEIGHT:

ADDIS ABABA UNIVERSITY
ADDIS ABABA INSTITUTE OF TECHNOLOGY
SMiE THERMAL ENGINEERING

Top_Support

DRAWING NO. FDM009/2020

SHEET 9

QTY:1

H
G
F
E
D
C
B
A

4

3

2

1

96





